IMPLEMENTING GROUND SOURCE HEAT PUMP

AND GROUND LOOP HEAT EXCHANGER

MODELS IN THE ENERGYPLUS

SIMULATION ENVIRONMENT

By

MURUGAPPAN ARUNACHALAM

Bachelor of Engineering

Annamalai University

Chidambaram, India

1998

IMPLEMENTING GROUND SOURCE HEAT PUMP

AND GROUND LOOP HEAT EXCHANGER

MODELS IN THE ENERGYPLUS

SIMULATION ENVIRONMENT

By

MURUGAPPAN ARUNACHALAM

Bachelor of Engineering
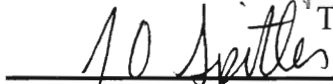
Annamalai University

Chidambaram, India

1998

Submitted to the Faculty of the
Graduate College of the
Oklahoma State University
in partial fulfillment of
the requirements for
the Degree of
MASTER OF SCIENCE
December, 2002

IMPLEMENTING GROUND SOURCE HEAT PUMP

AND GROUND LOOP HEAT EXCHANGER

MODELS IN THE ENERGYPLUS

SIMULATION ENVIRONMENT

Thesis Approved:

_____
Thesis Adviser

_____

_____
Dean of the Graduate College

ACKNOWLEDGMENTS

I would like to express my sincere appreciation to my advisor Dr. Daniel E. Fisher, for his continued and unrelenting support through out this project. Thanks for the faith and confidence you had in me. Thanks for the patience you showed towards me during my dark hours. Again I express my gratitude for all your guidance and leadership.

I would like to extend my thankfulness to my advisory committee members Dr. Jeffrey D. Spitler and Dr. Afshin J. Ghajar, who offered their guidance, support and constructive criticism, which helped in improving this work to this level.

I wish to thank Dr. Simon J. Rees for sharing his expertise in the Energy Simulation, which helped me to improve the quality of the work in many ways. Your mental acumen to solve problems helped in finishing this work sooner than it could have taken!

I would also like to thank all my colleagues Chanvit Chantrasrisalai, David Eldridge, Kim Tacheol, Hui Jin, Xiaobing Liu for their suggestion and ideas, which helped a long way towards improving the quality of this work.

Last but the not least, I like to thank my father Arunachalam, my mother Meenal, my brother Kannappan and my little niece Umachu for their unfathomable love and support during my stay away form home.

TABLE OF CONTENTS

LIST OF TABLES

.

LIST OF FIGURES

1. Introduction

The global energy crisis has led to the development of a number of new low energy systems for building heating and cooling. One such system is the ground source heat pump. These water to water or water to air heat pumps are ground coupled on the source side of the cycle. If designed correctly, the ground coupling can, for certain climates, improve both heating and cooling efficiencies.

1.1. Objective

The aim of this work was to implement water-to-water Ground Source Heat Pump component models in EnergyPlus Crawley et al. (1997), which is a new building energy simulation program currently under development by the US Department of Energy. The EnergyPlus program is discussed in Chapter 2. Implementation of these models in EnergyPlus will allow evaluation of ground source heat pumps in a full building/system simulation.

The ground source heat pump system were implemented in EnergyPlus as two separate components: the water to water heat pump model developed Jin and Spitler (2002) and the ground loop heat exchanger model developed by Yavuzturk and Spitler (1999). The EnergyPlus water-to-water heat pump model and the EnergyPlus ground loop heat exchanger model are discussed in Chapters 3 and 4 respectively.

There are two further objectives related to the implementation of the water-to-water heat pump model. First, a sensitivity analysis on the heat pump model was

performed to determine the relative sensitivity of different parameters to the output of the model. Second, the heat pump model was enhanced to give a more accurate estimation of the power consumption for cyclic operation. Both the sensitivity analysis and cyclic operation are discussed in Chapter 3.

The major focus for the ground loop heat exchanger model was to extend the model developed by Yavuzturk and Spitler (1999) to handle variable short time steps and to develop a suitable aggregation algorithm for the short time step part of the model. A second objective was to validate the enhanced model against an analytical solution. These topics are discussed in Chapter 4.

The final objective of this investigation was to implement the models in EnergyPlus in a way that would be useful for both design and analysis. This required modification of the simulation environment to support multi-year simulations and full integration with existing EnergyPlus systems. A case study based on a building located southwest of Stillwater, Oklahoma was developed to demonstrate the capabilities of the simulation. Various ground source heat pump system models were attached to the building model. Each simulation was run with weather for Tulsa, Oklahoma and Anchorage, Alaska. The case studies are discussed in Chapter 5.

1.2. Overview of the Simulation Environment.

EnergyPlus is a building energy simulation program created as a merger of DOE-2 (LBNL, 1980) and BLAST (BSO 1991). It uses an integrated solution technique (simultaneous loads and systems), which solves the most serious deficiency of the

2

BLAST and DOE–2 sequential simulations, Crawley et al. (1997). Sequential simulation of the zone and system models leads to inaccurate space temperature predication due to the lack of feedback from the HVAC module to the zone load calculations. Predicting the space temperature accurately is crucial to energy efficient system engineering. System size, plant size, occupant comfort and occupant health all depend on space temperatures. The integrated solution technique is an important requirement for ground source heat pump system simulation. Both the ground loop heat exchanger and the water-to-water heat pump need to be sized properly to make it a viable alternative for conventional systems. The EnergyPlus integrated solution technique properly accounts for all interactions between models and makes EnergyPlus a prime candidate for analyzing low energy system performance. Energy Plus was made highly modular for the following reasons: easy to implement new modules, data access between modules can be controlled easily, easy to maintain the program, new changes to a module (model) can be implemented with out affecting the other sections of the program. Figure 1.1 shows the structure of the EnergyPlus simulation engine. It consists of different modules called "Managers". The top-level manager is the simulation manager, which controls the overall simulation and the interaction between the systems for every time-step which could range from sub-hourly levels to user selected time-step during the simulation period which could be anywhere from a design day to several years. At the next level are the Heat and Mass Balance Manager (Heat and mass balance simulation) and HVAC Manager (building systems simulation). These are self-contained modules themselves and in turn control their part of the simulation in the program and interact with each other through well-defined interfaces in the program. The Heat Balance Manager simulates the zone

side and passes its output to the HVAC manger, which handles its own simulation using the input from the zone side. Any unmet load for that time-step is reflected in the following time-step as increase or decrease zone space temperature. The input files are text-based and object-oriented. This eases interface development by the third party developers. Chapter 2 describes the EnergyPlus environment in such a detailed way needed for the implementation of the models in study.
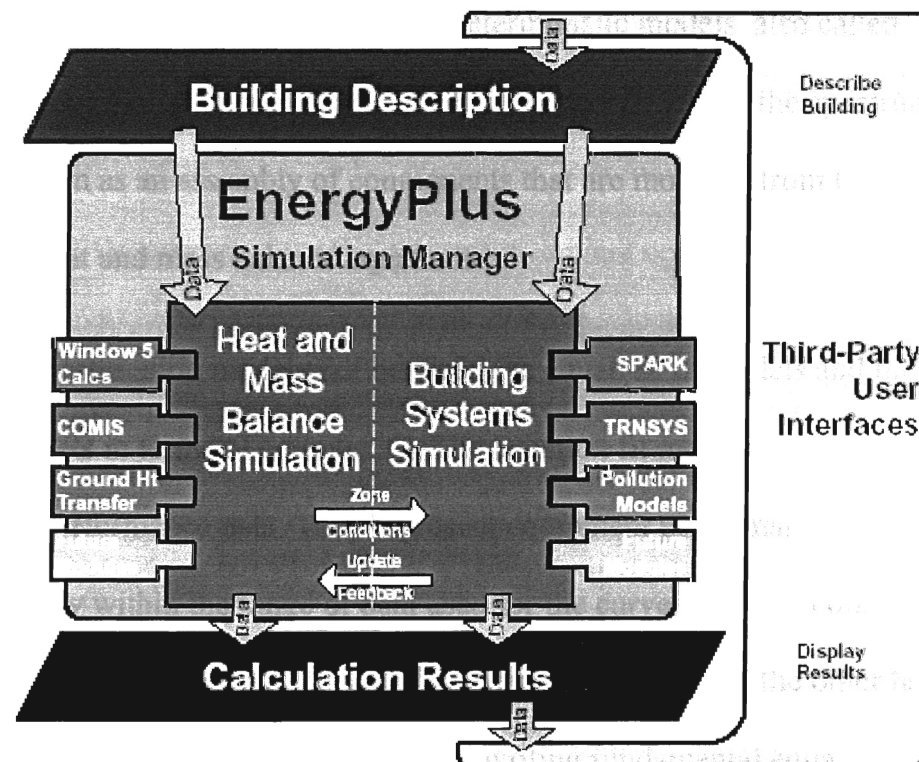
Figure 1.1 *Overall EnergyPlus structure, Crawley et al. (1997).*

1.3. Overview of the Parameter Estimation Water-to-Water Heat Pump Model

Since EnergyPlus is a modular building energy analysis program, it supports the implementation of different types of component models. Hamilton and Miller (1990) classified these models as equation fit models (also called "functional fit" or "curve fit" models), deterministic models. Equation fit models treat the system as black box and fits one or more equation to represent the system. Deterministic models, also called "first principle" models by Hamilton and Miller, are at the opposite end of the spectrum; they represent the system as an assembly of components that are modeled from the basic thermodynamic heat and mass balance equations.

Parameter estimation models fall between the equation fit models and the deterministic models in terms of complexity. The equation fit models are basically curve fits of published performance data. They represent equipment performance with reasonable accuracy within the range of data used for the curve fit, but become unrealistic when extrapolated beyond the catalog data. Deterministic models, on the other hand, are very detailed. They are modeled meticulously by writing fundamental equations to describe the basic thermal process and their interactions in every component of the system. Although these models behave well in simulation programs, they require data that are not readily available in the manufacturers' catalogs. They need internal data, which must be estimated through field experiments. This type of model also often requires a lot of computation time. The parameter estimation model is a hybrid of equation fit and deterministic models. It alleviates the problems encountered in the other

two types of models. Parameter estimation models can be extrapolated beyond the catalog data; yet, they are based on data available from the manufacturers' catalogs. These models are based on fundamental equations applied to individual components like deterministic models. Unlike deterministic models, the model parameters are estimated using the manufacturers catalog data rather than laboratory experimental data. These parameters are estimated using a multi-variable optimization algorithm. Once the parameters are estimated, the model can be used in any multi-component energy simulation program. The choice of the optimization algorithm is critical in these types of models. A wrong choice could lead to catastrophic results. For example, the optimization could end up at a local rather than a global minimum. This would make the model unpredictable in the simulation, since the parameters are not optimized. However, there is no rule of thumb to choose an optimization method for the problem at hand. To some extent, it is done with experience gained by using the various optimization techniques.

There are many heat pump models found in the literature. Most of them are either equation fit models or deterministic model. Both of them have their own limitations: the deterministic models require data beyond what is available in the manufactures catalog and for the equation fit models, the range over which they could represent the physical model is restricted to the range of data provided in the catalog.

1.3.1. Review of Existing Models.

Jin (2002) presents a detailed and comprehensive review of existing models. A summary of selected models as reviewed by Jin (2002) is presented in the following paragraphs.

Allen and Hamilton (1983) developed a chiller model using regression to curve fit the manufacturer's catalog data. The chiller was modeled as a single unit. The model does not account for the individual component operations, the equations used to model does not involve the internal temperature or pressure of the refrigerant. All the equations involve only external variables, which are readily available from manufacturer's catalog data. The final model consisted of five equations and nine coefficients, which are to be fit using the catalog data.

Hamilton and Miller (1990) developed a modified version of the Allen and Hamilton (1983) model. They modeled individual components using the internal variables in the equations. This has the benefit of modeling new systems by assembling the basic components. The disadvantage of this model is that not all the data required are freely available in the manufacturers' catalogs.

Stoecker and Jones (1982) approached the problem with the idea that if the characteristics of the individual components are known the overall system performance can be estimated. They modeled the individual components of a vapor compression cycle system like the reciprocating compressor, condenser and evaporator using polynomial equations with unknown coefficients which are fit using the manufacturers catalog data. This model has the same drawback as the Hamilton and Miller (1990) model in that it also relies on some internal parameters, which are not guaranteed to be available in the manufacturers' catalogs.

Stefanuk et al (1992) developed one of the most detailed deterministic models. They use the basic laws of conservation of mass and energy to model each component of

the chiller. Each component is modeled in its basic form. Though deterministic models are supposed to be more accurate this model has errors as high as $\pm10\%$ for a few points The authors attributed the error to the over prediction of the heat exchanger heat transfer coefficients which were known only to within $\pm20\%$.

Bourdouxhe, et al (1994) employed a deterministic approach to model the performance of a chiller. They used a two-step approach. First they modeled the compressor with the following assumptions: isentropic compression, isobaric aspiration of the refrigerant into cylinders, no pressure drops and the discharge. The compressor model consisted of four parameters, which were identified using experiments. Once the compressor was modeled, the whole chiller was considered and the two heat exchangers, the condenser and the evaporator were modeled. They were modeled using the classical approach with heat transfer coefficients as the parameter, which is estimated by an exhaustive search method. The objective of which is to find the optimal values of the heat transfer coefficients by minimizing the error between published and estimated power consumption and cooling capacity.

Gordon and Ng (1994) developed a reciprocating compressor model that is supposed to be useful for diagnostic purposes. Their model does not predict the cooling capacity of the chiller; instead, the cooling capacity is required as an input to the model, and it predict the COP of the chiller. The model has three parameters, which are to be fitted with the catalog data. The model predicts the COP of the chiller, but there is no information about the method used to estimate cooling performance, power consumption or heat rejection.

There are numerous other models available in the open literature. However, all of them fall into the two broad categories as explained before- the equation fit models and the deterministic models. A more exhaustive survey of the models can be found in Jin (2002).

The parameter estimation heat pump model implemented in EnergyPlus is based on a model developed by Jin and Spitler (2002). They modeled the heat pump as four components: compressor, evaporator, condenser and the expansion device. Each component was modeled with some governing equations using the laws of thermodynamics. Each component model included unknown parameters, which are to be estimated using the manufacturers' catalog data. The parameter estimation is done using a multivariable search, which minimizes the error between the estimated and the published cooling performance, power consumption and heat rejection. This model is explained in depth in Chapter 3.

1.4. Ground Loop Heat Exchanger Model

Ground source heat pumps are potential alternatives to conventional heating and cooling systems for both residential and commercial buildings due to their high-energy efficiency. These system offers many benefits like lower operating cost, eco-friendliness and a lower life cycle cost all of which offset the high initial installation cost of these type of systems on a commercial basis. These systems take advantage of the fact that the temperature of the ground remains constant over the year and can be used to extract or reject heat from the system depending on the season. As ground source heat pump systems have developed, numerous types of ground-coupled heat exchanger

configurations are in vogue. Vertical ground loop heat exchangers are commonly used in commercial applications.

Vertical ground loop heat exchanger consists of a borehole into which has pipes inserted in a U-loop as shown in Figure 1.2. This type of ground-coupled heat exchanger is popular due to ease of installation and the small land area required for installation. Multiple boreholes, whose length normally varies from 40 and 150 m, are typically connected in parallel to form a borehole field. Figure 1.2 shows a single vertical ground loop heat exchanger in a U-tube configuration.
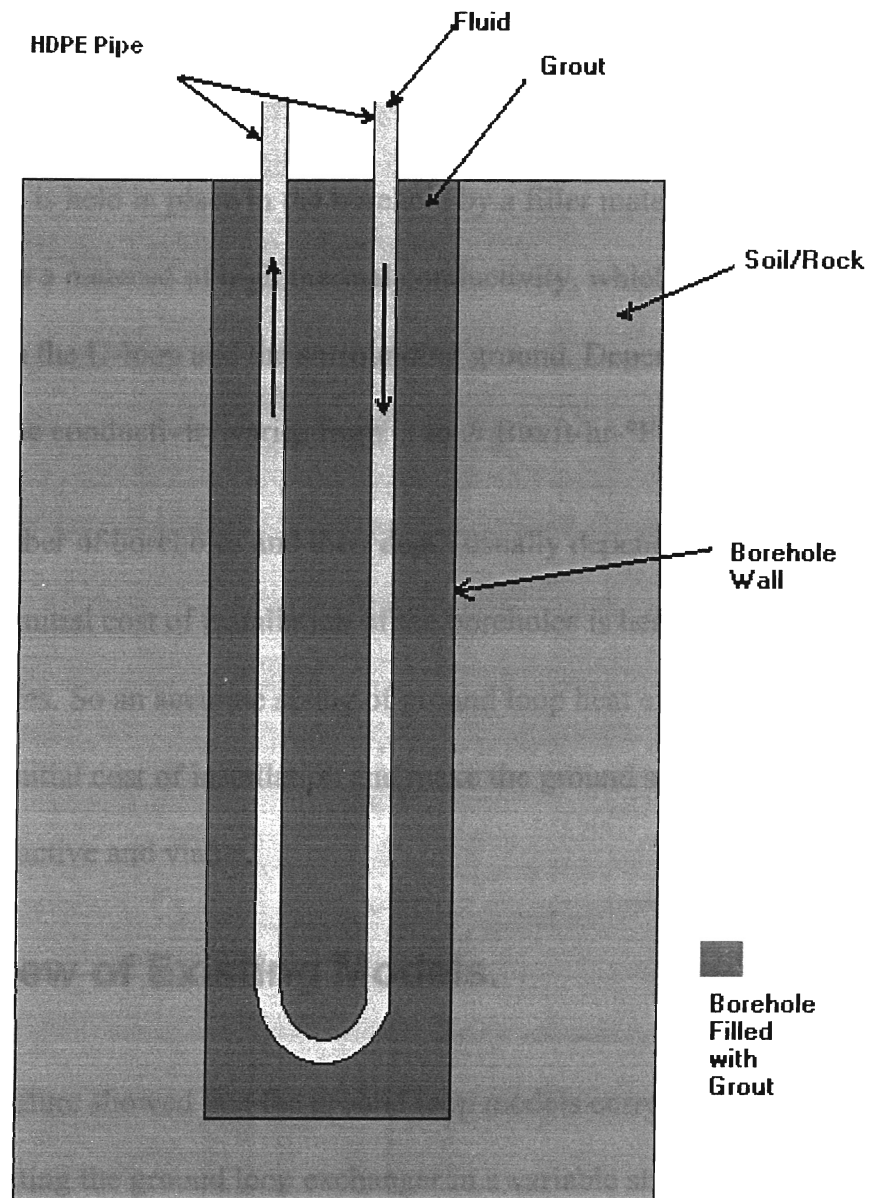
Figure 1.2 *Ground Loop Heat Exchanger with a U bend Pipe.*

The vertical ground loop heat exchanger consists of cylindrical holes (that vary in depth and diameter based on the application) drilled in the ground. "Borehole" as used in this thesis refers to the vertical hole with the pipe, grout and the surrounding rock or soil.

The pipe is made of high-density polyethylene (HDPE), because of its favorable physical and chemical properties. Pipe diameter typically ranges from ¾" to 1 ½". The

pipe is inserted inside the borehole as U loop, which consists of two straight pipe lengths connected by a "U-bend" at the bottom.

The tube is held in place in the borehole by a filler material, usually called "grout". Grout is a material of high thermal conductivity, which enhances the heat transfer between the U-loop and the surrounding ground. Depending on the grout material used, the conductivity varies from .3 to .9 Btu/ft-hr-°F or .173-.52 W/m-°K.

The number of boreholes and their depth usually depends on the soil's thermal properties. The initial cost of installation of the boreholes is heavily influenced by the depth of boreholes. So an accurate sizing of ground loop heat exchanger is required. This can reduce the initial cost of installation and make the ground source heat pump system option more attractive and viable.

1.4.1. Review of Existing Models.

The literature showed that the ground loop models currently available are not capable of modeling the ground loop exchanger in a variable short time step simulation with the required accuracy.

Currently available models in the literature can be categorized into two groups as analytical models and numerical models. The analytical models are either based on the Kelvin's (1882) line source approximation or Carslaw and Jaeger's (1947) cylindrical source approximation. The models described in the following paragraphs are summarized from a comprehensive review of the literature presented by Yavuzturk (1999).

Ingersoll (1948, 1954) used Kelvin's line source approximation to model ground loop heat exchangers. Kelvin's line source approximation assumes that an infinitely long heat source or sink with constant heat rate is turned on at time zero. Ingersoll gives the following equation to represent the temperature,

$$T - T_0 = \frac{Q'}{2\pi k} \int_x^\infty \frac{e^{-\beta^2}}{\beta} d\beta = \frac{Q'}{2\pi k} I(X) \qquad (1.1)$$

Where

$$X = \frac{r}{2\sqrt{\alpha t}} \qquad (1.2)$$

T = Temperature of ground at any selected distance from the line source in [°F or °C]

(Selecting a distance that is equal to the pipe radius represents the pipe surface temperature.)

T_o = Initial temperature of the ground in [°F or °C]

Q' = Heat transfer rate over the source in [BTU/(ft-hr) or W/m]

r = Distance from center line of pipe in [ft or m],

k = Thermal conductivity of the ground formation in [BTU/(ft-hr-°F or W/(m-°C)]

α = Thermal diffusivity of the ground formation defined to be $k/\rho c$,

ρ = Density of the ground formation in [lb/ft^3 or kg/m^3]

t = Time since the start of the operation in [hr]

β = Integration variable $= \dfrac{r}{2\sqrt{\alpha(t - t')}}$

The values of I(X) can be found in Ingersoll et al (1954).

Though this solution is exact for a true line source, Ingersoll suggested that this solution as given in equation 1.1 can be used for small pipes in the range of 2 inches or less. He also proposed a dimensionless term $\alpha t/r^2$ which must be greater than 20 to maintain an error that is small enough for practical applications.

Hart and Couvillion (1986) also use line source theory, but they argue that Kelvin's line source theory falsely predicts the temperature distribution of the ground once the line source is turned on, since Kelvin didn't consider any far field radius r_∞ beyond which the ground temperature remains at the undisturbed temperature. They modeled the ground loop heat exchanger taking into account an undisturbed far field temperature with the far field radius defined as:

$$r_\infty = 4\sqrt{\alpha t} \qquad (1.3)$$

and the temperature as

$$T - T_0 = \frac{Q'}{4\pi k} \int_y^\infty \frac{e^{-\lambda}}{\lambda} d\lambda \qquad\qquad (1.4)$$

where

$$y = \frac{r^2}{4\alpha t} \qquad\qquad (1.5)$$

The solution to the integral equation in (1.4) can be obtained from integral tables. The solution to the integral has a power series in its solution. The authors suggest using two terms of the series as long as $r_\infty / R \geq 3$ where R is the pipe radius. If the ratio is less than 3 they recommend using more terms in the series for better accuracy. Since this approach assumes that the heat transfer occurs between the ground formation and the line source of radius r_∞, the entire region beyond this radius is assumed to be at the undisturbed far field temperature. The value of the far field radius depends on time and the thermal diffusivity of the ground. In multiple borehole configurations after the time when there is thermal interaction between boreholes, the superposition technique is used to estimate the ground temperature.

Kavanaugh (1985) based his model on the Carslaw and Jaeger (1947) cylindrical source approximation. The model assumes a single isolated pipe surrounded by an infinite solid medium with constant thermo-physical properties. It also assumes that the heat transfer is purely through the mode of conduction and ground water movement; the thermal interaction between adjacent boreholes is neglected. The solution to the cylindrical problem is obtained from Carslaw and Jaeger (1947). Kavanaugh tested the

model in two test sites and provides the experimental data. According to him, the model works well if care is taken when choosing the property values for the ground and initial water temperatures are not required immediately after startup. Since Kavanaugh assumes a single U-tube pipe, some error is introduced in the solution.

The above models are based on analytical solutions. In practice, these methods cannot account for leg-to-leg thermal short-circuiting effects and pipe wall and contact resistances. These design considerations are insignificant to the long term performance of the ground loop, but may affect the short-term responses of the borehole which is measured in terms of hours or weeks. The numerical models try to model the complex phenomenon occurring around the borehole, but Yavuzturk (1999) claims that they are computationally inefficient. There are however, a number of models based on the numerical approach.

Eskilson (1987) developed non-dimensional temperature response factors (called g-functions) to estimate the temperature of the multiple borehole ground loop heat exchangers. The response factors are estimated using both numerical and analytical models. The numerical model consists of the two-dimensional explicit finite difference model of a single borehole in radial and axial directions. The borehole has a finite length and diameter; the pipe (U-tube) and grout's resistances are neglected in the numerical model. This model is then simulated to determine the response to a unit step function pulse. Using the response from a single borehole a spatial superposition of a pre-defined configuration of boreholes is performed to determine the response of borehole configuration to the unit step function pulse. Finally when these responses of borehole outer wall temperature vs time are non-dimensionalized, the resulting dimensionless

16

temperature vs dimensionless time curve is the *g*-function. Once the response to a step function is known, the response to any heat extraction/injection step can be determined by decomposing the heat extraction/injection into a series of unit step functions. Then by using the response factors (*g*-functions) to each unit step functions can be superposed to determine the overall response.

Hellstrom (1989, 1991) developed a model for vertical ground heat exchanger stores. These are densely packed ground loop heat exchangers used for seasonal thermal energy storage. Hellstrom divided the ground formation region into two separate regions and called one the local region, which is the volume that immediately surrounds the single borehole. The other region is the bulk of the heat store volume and the far field called as global problem. Using these the models he represented the initial ground formation as superposition of three separate parts: a global temperature difference, a temperature difference from the local solution immediately around the individual borehole and the temperature difference from the local steady-flux part. The model is a hybrid model, which uses the numerical method for the local and global problems and uses the analytical solution to superimpose the solution from steady flux part. His model is not suitable for short time responses of the ground.

Thornton et al. (1997) used Hellstrom's approach to model the ground loop heat exchanger. The model was developed as a detailed component model, which was implemented in TRNSYS (Klein, et al. 1996). They tested this model against experimental data from a family housing unit by adjusting the far-field temperature and ground thermal properties. The model was able to match the measured data accurately.

Mei and Emerson (1985) developed a model for a horizontal ground loop heat exchanger, which is good for modeling the effects of frozen ground formation and pipes. Their model was based on the numerical solution of three one-dimensional, partial differential equations using a finite difference approach. The three one-dimensional conduction equations were applied; one along the radial direction of the pipe, one to the frozen ground formation and one to the far-field region. These one-dimensional equations were coupled into one single partial differential equation resulting in a fourth quasi two-dimensional equation. The model used different time steps for different parts. It used a smaller time-step for the pipe wall and frozen ground and a significantly larger time-step for the unfrozen far-field region. The study had an experimental verification of their model based on a 448-day simulation period.

Yavuzturk and Spitler (1999) modeled the ground loop heat exchanger to account for short time step variation using response factors. They developed short time-step response factors using a transient, two-dimensional, implicit finite volume model on a polar grid, then adjusted the short time-step g-functions to match the long time-step g-functions developed by Eskilson (1987). Their g-function model is discussed in detail in Chapter 4 and is the basis of the g-function model implemented in EnergyPlus.

Chapter 2. The EnergyPlus Simulation Environment

Currently available building energy simulation programs are more than two decades old and were written in relatively unstructured and currently outdated programming languages. These programs have become very expensive to maintain and extend. In addition, they each had limitations and shortcomings that provided impetus for development of a new building energy simulation program. The new program would not only address these limitations, but would also provide a simulation environment that would be easy to maintain and extend.

EnergyPlus (Crawley et al., 1997) is a new simulation engine written in Fortran 90 and based on best of the features of BLAST (BSO 1991) and DOE-2 (LBNL 1980). EnergyPlus includes many innovative new features such as: variable time step, user configurable modular systems, integrated system/zone simulations and input and output data structures customized to assist third party module and interface development. EnergyPlus is highly modularized; this enables easy implementation of new components and allows developers to extend the capabilities of existing components and link to existing programs. A high degree of data encapsulation is maintained to facilitate third party module development and guard against unintentional corruption of data by unrelated modules.

The overall program structure of EnergyPlus is shown in Figure 2.1. The top-level manager routine manages the overall simulation. The HVAC block is divided into a number of simulation blocks or modules. Currently EnergyPlus has individual modules

for air systems, zone equipment, the plant supply side, plant demand side, condenser supply and the condenser demand side. The implementation of ground loop heat exchanger and water-to-water heat pump involves understanding of plant and condenser loop managers and their simulation.

```
Energy Plus
    ➢ Process the Input
    ➢ Manage Simulation
        ➢ Get Weather Data
        ➢ Calculate Heat
            ➢ Calculate Surface Heat
              Balance
            ➢ Calculate Air heat
                ➢ Simulate
```
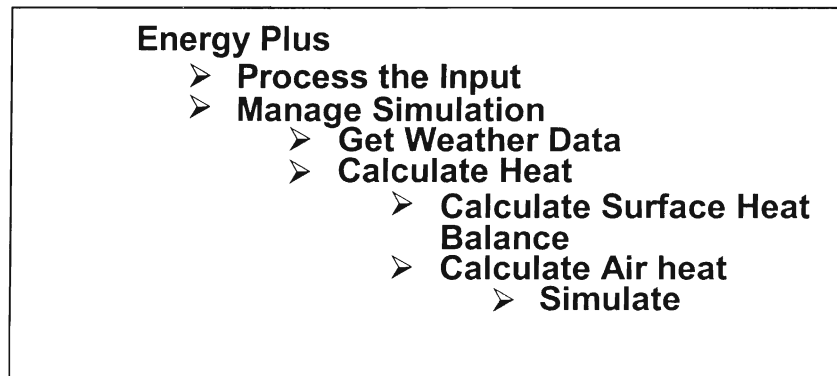
Figure 2.1 *Hierarchy of some higher level managers in EnergyPlus.*

2.1. The Plant and Condenser Loop Simulations

The HVAC simulation environment in EnergyPlus is a hybrid implementation of the two popular environments: system based and component based. EnergyPlus uses the best features of the two techniques.

The characteristics of the system based approach is mimicked by an abstract representation of the duct or piping systems as a "fluid loop" Fisher et al. (1999). The characteristic of a component-based system is represented by defining components, which are connected to the fluid loop. This offers the advantage of a flexible environment that allows development of a wide range of new sub-systems by connecting different existing components.

20

Two fluid loops define the HVAC simulation in EnergyPlus – a primary loop or the "plant" loop for equipment such as boilers, chillers, thermal storage or heat pumps and a secondary loop or the "condenser" loop for heat rejection equipments such as cooling towers, condenser or ground loop heat exchangers (Figure 2.2). The components are connected to the loops by defining explicit nodes at the connections. These nodes are data structures that hold information about the state variables and set point values for that location. This modular approach allows the users to add any plant equipment or combination of such equipments to form a subsystem, which are interconnected at the nodes. The order and type in which the components are specified in the loop determines the system type. As explained earlier the connection between the various loops and the loop equipment are defined using nodes, which are in turn defined in the input file. Each loop – plant and condenser are controlled by a set of loop managers, which handle initialization, convergence checks and loop operation and control functions. The lower level loop managers are controlled by a higher lever manger, which successively calls the individual loop managers until the entire system has converged. This type of communication is governed by a manager-interface protocol as discussed by Fisher et al. (1999).
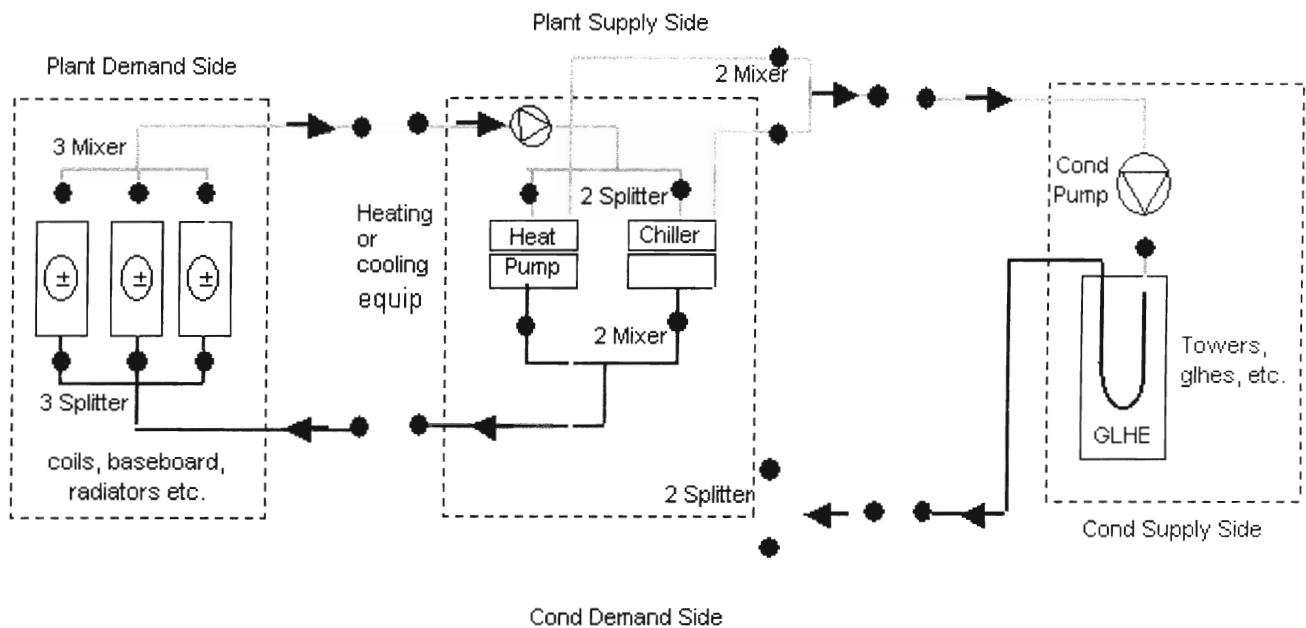
Figure 2.2 *Plant loop with demand and supply sides.*

2.2. Equipment Operation

Once the system is defined, an operation scheme must be specified for EnergyPlus to simulate the equipment. The operation scheme for a fluid loop (chilled water or hot water etc.) is specified using a unique identifier followed by a list of control schemes for different operating schedules. The operation of equipment based on the two operation schemes in EnergyPlus are given below:

1. **Load Range Based Operation** specifies a load range in which a specified list of plant equipment will operate. This operation scheme will only run equipment to meet the fluid loop demand. A water-to-water heat pump would typically be operated using a load range based scheme.

22

2. **Uncontrolled Operation:** specifies a list of equipment that will operate whenever the fluid loop pump is operating. Environmental heat exchangers, such as ground loop heat exchangers would typically be uncontrolled.

2.3. Implementing the Geothermal Systems in EnergyPlus

In order to implement the parameter estimation ground source heat pump model and the ground loop heat exchanger models in EnergyPlus, two significant enhancements to the simulation environment were required. The fluid routines were enhanced and multi-year simulation capabilities were implemented as discussed in the following sections.

2.3.1. Fluid Properties

The parameter estimation heat pump models require reliable fluid property routines in order to support reasonable extrapolation of the model beyond the available catalog data Jin (2002). The EnergyPlus fluid property routines were well suited to meet this requirement. However, they required extension and enhancement in order to meet all the property requirements of the parameter based models.

The properties at any state point in the range specified in the input file can be obtained through the fluid property functions. These functions retrieve the property data from the loaded arrays for the requested temperature, pressure or quality. To estimate the

requested fluid property at the intermediate points a double interpolation between temperature and pressure or quality, which surround the point is performed. In order to allow the parameter estimation models to converge, it is essential that the fluid property routines default to reasonable values when the simulation pushes the limits of non-physical conditions. The EnergyPlus error handling protocol was relaxed to accommodate this requirement. In addition, several new property routines were written as required by the parameter estimation heat pump model.

The EnergyPlus fluid property routines are based on a 'table look-up' approach, where tables of fluid properties are stored with the simulation input files. EnergyPlus fluid property routines were written as data organizers, instead of a set of embedded calculations. This ensured flexibility when adding new fluids, as there is no code change required. New fluid property data can be added without making any modifications to the code. It is enough to make the necessary changes in the respective section of the input file. This is described in the Guide for Module Developers, EnergyPlus (2002).

2.3.2. Multi-year Simulation

Though the EnergyPlus simulation environment was flexible enough to support multi-year simulation, until the geothermal models were implemented, there was no demand for these simulation capabilities. The currently available models in EnergyPlus do not require simulation in excess of one year for complete analysis. As explained before, geothermal system analysis requires a longer period of simulation (more than 10 years) for life cycle cost and design analysis. Therefore extending the EnergyPlus environment to run multi-year simulations was very critical.

Multi-year enhancement required several significant changes to the EnergyPlus weather manager and a new object for the Input specification. The weather manager was modified to read the same annual weather file repeatedly for every year of the multi-year simulation. The only change required to the simulation input was the addition of a single numeric field containing the number of years in the simulation.

2.4. Summary

This chapter introduced the EnergyPlus environment and explained the features of EnergyPlus important to the implementation of the geothermal models. The EnergyPlus simulation environment is well suited for the implementation of ground source heat pump models and ground loop heat exchangers. The simulation accounts for interactions between component models by means of the fluid loops. Multi-year simulation capabilities and enhanced fluid property routines were added to EnergyPlus in order to support ground source heat pump system analysis and parameter estimation based component models.

Following, Chapters 3 and 4 explain the parameter estimation based heat pump model and the variable short time-step vertical ground heat exchanger model respectively.

Chapter 3. Implementing the Heat Pump Model

The water-to-water heat pump system introduced in Chapter 1 is dealt with in detail in the following sections. This system was modeled by Jin and Spitler (2002) using the parameter estimation technique. Developing these, types of models require only published data, which is readily available in manufacturers' catalogs. No additional experimental data is needed. Jin and Spitler (2002) demonstrated that these models exhibit better fidelity to the catalog data than the equation fit models. Parameter estimation models also have the benefit of allowing extrapolation beyond the catalog data without a catastrophic failure of the model.

The research objective discussed in this chapter was to implement Jin and Spitler model in the EnergyPlus environment and test the model's sensitivity to estimated parameters and inputs, before implementing it. The method of influence coefficients was employed to analyze the sensitivity of the model. Influence coefficients (i.c.) are defined as "partial derivatives of one variable with respect to another variable in a system" Spitler et al. (1989).

$$\text{Influence Coefficient} = \frac{\partial(\text{Result})}{\partial(\text{Parameter})} \qquad (3.1)$$

Influence coefficients are useful in quantifying the effect of a model input on a simulation result. Spitler et al. gives four types of influence coefficients: dimensional type-1, non-dimensional type-1, dimensional type-2 and non-dimensional type-2. All these types are fundamentally the same; the difference lies in the non-dimensionalization

of the influence coefficients. Non-dimensional influence coefficients are particularly useful in comparing the significance of various model parameters. In this study, we are interested in dimensional type-2 i.c. and non-dimensional type-2 i.c. In dimensional type-2 i.c. the numerator alone is non-dimensionalized. This type can be particularly useful when the magnitude of the estimated error in the input parameter is varying. This type of i.c. is given by equation 3.2. Non-dimensional type-2 influence coefficients, where both numerator and denominator are non-dimensionalized is shown in equation 3.3

$$\frac{\partial R^*}{\partial P} \approx \frac{\Delta R^*}{\Delta P} = \frac{(R_{bc} - R_{\Delta})/R_{bc}}{(P_{bc} - P_{\Delta})} \tag{3.2}$$

$$\frac{\partial R^*}{\partial P^*} \approx \frac{\Delta R^*}{\Delta P^*} = \frac{(R_{bc} - R_{\Delta})/R_{bc}}{(P_{bc} - P_{\Delta})/P_{bc}} \tag{3.3}$$

Where,

P = Parameter

R = Result

* = non-dimensionality

bc = base-case

Δ = value for the perturbed case

These influence coefficients are useful in predicting which of the model input parameters influences the model output the most. These can be used to quantify which estimated parameter in the model is critical for the model's stability. This result can be very helpful in refining the model developed by the parameter estimation technique. The influence coefficients were also used to identify the dominant model inputs that affect the output of the model, which would prove to be useful in implementing the model in any simulation environment. Finally, this analysis provided insight into the model's behavior in the simulation.

3.1. Description of the model

The EnergyPlus model implemented during this investigation is based on the parameter estimation model of the water-to-water heat pump developed by Jin and Spitler (2002). This section gives an outline of the water-to-water model developed by Jin and Spitler. The heat pump model has four major components the compressor, the evaporator, the condenser and the expansion valve, which affect the system thermodynamics. These components are discussed in the following sections.

3.1.1. Compressor Model

Several assumptions were made in modeling the compressor. The thermodynamic cycle used in modeling the compressor was an approximation of a real compressor cycle. The compression and expansion coefficients were assumed to be constant isentropic. The pressure drops at the suction and discharge were assumed isenthalpic. The pressure drops across the suction and discharge valves were accounted for in the model using the results

from a study by Popovic and Shapiro (1995). They found that including the pressure drop

gave better accuracy. With these assumptions the mass flow rate of the refrigerant is

given as

$$\dot{m}_r = \frac{PD}{v_{suc}}\left[1+C-C\left(\frac{P_{dis}}{P_{suc}}\right)^{1/\gamma}\right] \tag{3.4}$$

Where,

$\dot{m}_r$ = refrigerant mass flow rate, Kg/s or lbm/hr

PD = piston displacement, m^3/s or CFM

v_{suc} = specific volume at suction state, m^3/kg or ft^3/lbm

C = clearance factor

P_{suc} = discharge pressure, Pa or psia

P_{suc} = suction pressure, Pa or psia

γ = isentropic exponent

The work done by the compressor is given by

$$\dot{W}_t = \frac{\gamma}{\gamma-1}\dot{m}_r P_{suc} v_{suc}\left[\left(\frac{P_{dis}}{P_{suc}}\right)^{\frac{\gamma-1}{\gamma}}-1\right] \tag{3.5}$$

Where,

$\dot{W}_t$ = theoretical power, W or Btu/hr

The actual power input is modeled using a simple linear relation given by

$$\dot{W} = \eta \dot{W}_t + \dot{W}_{loss} \qquad (3.6)$$

Where,

$\dot{W}$ = compressor power input, W or Btu/hr

η = mechanical efficiency of the compressor

$\dot{W}_{loss}$ = constant part of the electromechanical losses, W or Btu/hr

Based on the model from Bourdouxhe et al. (1994) the refrigerant that gets superheated at the inlet of the compressor is also modeled.

3.1.2. Evaporator and Condenser Models

The evaporator and condenser were modeled as counter flow heat exchangers. The model however, is valid for any flow configuration. Since pressure drop in the pipes were neglected, the phase change is assumed to occur at a constant temperature. Both condenser and evaporator were modeled based on the above assumptions with the effectiveness-NTU (number of transfer units) method.

$$\varepsilon = 1 - e^{-NTU} \qquad (3.7)$$

$$NTU = \frac{UA}{\dot{m}_w Cp_w} \tag{3.8}$$

Where,

ε = effectiveness of the heat exchanger

NTU = number of transfer units

UA = heat transfer coefficient, W/K or Btu/(hr-°F)

$\dot{m}_w$ = mass flow rate of water, Kg/s or lbm/hr

Cp_w = specific heat of water, J/(kg-K) or Btu/(lbm-°F)

3.1.3. Expansion Device

Though the expansion device is not modeled explicitly, the mass flow rate equation in the compressor and a constant degree of superheat takes care of this component in the parameter estimation model. This is, however, valid only for a thermostatic expansion valve, which is generally used by heat pump manufacturers in North America.

Once all the components were modeled, the following parameters were identified in modeling the heat pump: PD piston displacement, C clearance factor, ΔP pressure drop at suction and discharge, W_{loss} electro mechanical power losses, ΔT_{sh} Super heat the inlet

of the compressor, η the electro-mechanical efficiency of the compressor, UAL the heat transfer coefficient of the load side heat exchanger and UAS the heat transfer coefficient of the source side heat exchanger.

Both the heating and cooling mode have the same set of parameters and the same strategy is used to estimate the parameter values for each mode. However there exists a small difference; for a heat pump in cooling mode, the evaporator is the load side and in heating mode, the evaporator is the source side. The parameters are obtained using manufacturers' catalog data, by minimizing the error between the model's predicted compressor power and heating capacity (or cooling capacity) with that of the catalog's compressor power and heating capacity (or cooling capacity). A multi-variable optimization technique like Nelder Mead Simplex algorithm, with a multi-start random sampling strategy, to ensure a global minimum, is used to minimize the error between the model's prediction and the catalog data.

3.2. Model input parameters

The block diagram of the model is shown in Figure 3.1. It shows the model parameters for both cooling mode and heating mode. A simple thermostatic signal was employed to differentiate between the two modes, which was one of the inputs and the other inputs were inlet water temperature and mass flow rate on the source and load sides. The algorithm used to estimate the outlet conditions and the required compressor power, were similar to the one used in parameter estimation. However, a simple modification was made to accommodate the unknown values of heat transfer rates in the model implementation. These values were known from the manufacturer's catalog data in the

parameter estimation step. These unknown heat transfer rates in the model implementation were solved simultaneously using successive substitution. Thus, the model predicts conditions at the evaporator and condenser outlets and the required compressor power for the inlet condition.

Inputs

T_{wiL} $\dot{m}_{wiL}$ T_{wiS} $\dot{m}_{wiS}$ S

Heating Mode Parameters
$(UA)_S$
$(UA)_L$
PD
C
ΔP
ΔT_{sh}
W_{loss}
η
Phi
Plo

Parameter Estimation Based Water-to-Water Heat Pump Model

$(UA)_S$
$(UA)_L$
PD
C
ΔP
ΔT_{sh}
W_{loss}
η
Phi
Plo
Cooling Mode Parameters

T_{woL} $\dot{m}_{woL}$ T_{woS} $\dot{m}_{woS}$ W F
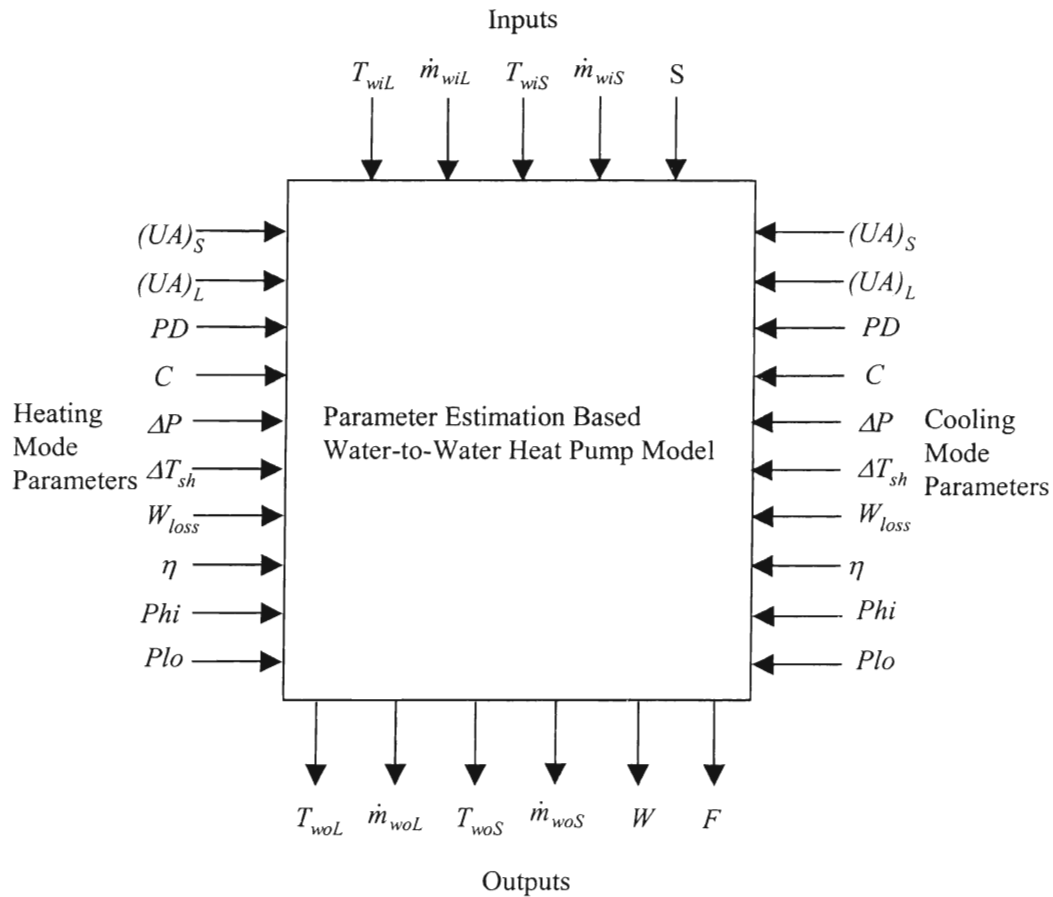
Outputs

Figure 3.1 *Block Diagram of the model parameters input and outputs (Jin 2002).*

3.3. Sensitivity Analysis

The sensitivity analysis carried out on different aspects of the heat pump model is discussed in this section. The sensitivity analysis was used to evaluate two different aspects of the model: sensitivity of the model to its estimated parameters and the

33

sensitivity of the model to its inputs. The results obtained are presented along with the conclusions for both analyses.

3.3.1. Sensitivity to model's estimated parameters

The parameter estimation models are developed by adjusting the parameter values in order to minimize the error between the model results and the catalog data. The sensitivity of the model outputs to the changes in the estimated parameters is therefore an important characteristic of the model. In view of this, a sensitivity analysis was carried out on all eight parameters of the water-to-water heat pump model. The influence of each of the parameters was studied based on three different results: the root mean square error based on the deviation of the model's heating capacity, rate of heat extraction and compressor power from published data as given in equation 3.9.

$$\frac{\partial RMS^*}{\partial EP^*} \approx \frac{\Delta RMS^*}{\Delta EP^*} = \frac{(RMS_{bc} - RMS_\Delta)/RMS_{bc}}{(EP_{bc} - EP_\Delta)/EP_{bc}} \tag{3.9}$$

Where,

EP = Estimated Parameters (piston displacement, clearance factor etc.)

RMS = Root mean square error between the manufacturer's catalog data and the estimated heating capacity, heat extraction or compressor power.

* = non-dimensionality

bc = base-case

Δ = value for the perturbed case

The test was carried out on a water-to-water heat pump selected randomly from an arbitrarily chosen manufacturer. The chosen heat pump was a small residential unit, with a nominal heating capacity of 7 KW. The tests were carried for the heating performance; however, a similar test could be carried out for cooling performance of the model.

The influence coefficients obtained are shown in Table 3.1. Figure 3.1 shows the comparisons of the non-dimensional type-2 influence coefficients based on heating capacity, heat extraction rate and compressor power. The parameters that decide the refrigerant mass flow rate have a significant influence on the model performance. Piston displacement, the clearance factor and the pressure drop are all critical to the determination of the heat pump's mass flow rate. The other parameters, which had some influence on the heat pump model, were the mechanical efficiency of the compressor and the constant part of electro-mechanical loss in the compressor and the heat transfer coefficient of the load and source side heat exchangers. The sensitivity analysis showed that the compressor model has a significant influence on the overall performance of the model.

Table 3-1 *Non-Dimensional influence coefficients type-2, for the water-to-water heat pump model developed by parameter estimation model.*

Simulation Parameter	Base Case Value	Non-Dimensional i.c. type 2 Based on Heating Capacity	Non-Dimensional i.c. type 2 Based on Rate of Heat Extraction	Non-Dimensional i.c. type 2 Based on Compressor Power
Piston Displacement	0.00162 [m³/s]	16.86	14.84	12.80
Clearance Factor	0.07	3.18	2.39	1.49
UA Load Side	1.98[KW/K]	0.07	0.11	0.14
UA Source Side	1.53[KW/K]	5.01	4.47	0.61
WLOSS	0.52[KW]	1.52	0.022	2.23
ETA	1.44	4.22	0.025	8.32
Pressure Drop	99.3[Pa]	1.14	3.18	0.46
Super Heat	9.8[°C]	0.19	0.27	0.017
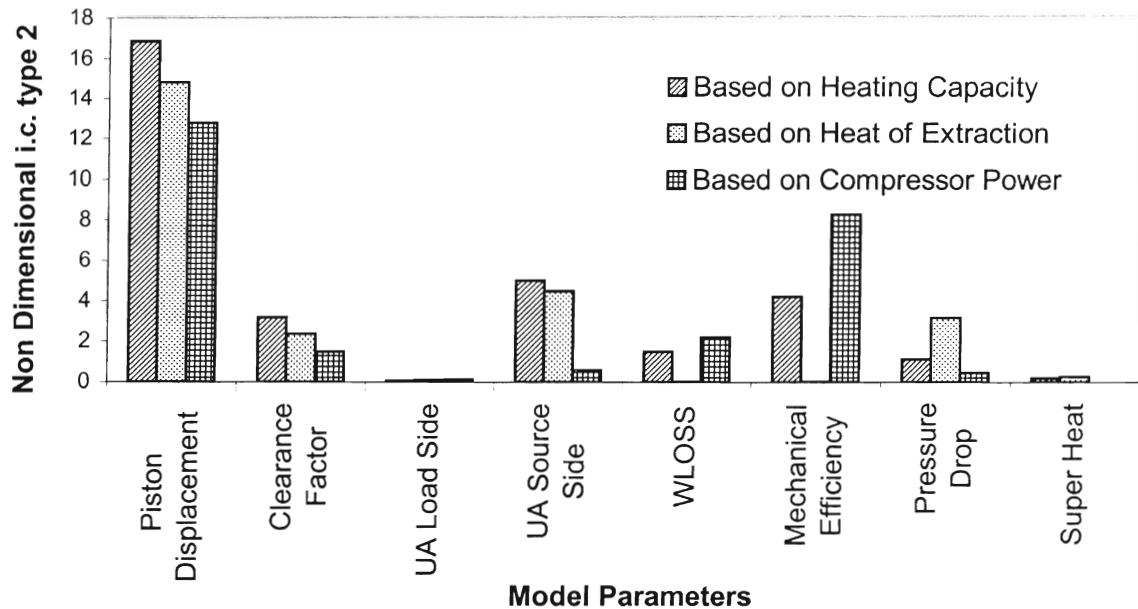
Figure 3.2 *Influence coefficients of model parameters based on heating capacity, heat extraction and compressor work.*

3.3.2. Sensitivity to changes in model inputs

A similar type of influence coefficient analysis was carried out on the model inputs. The same heat pump configuration used in the previous section was used for this analysis. The test was performed on all the inputs to the model namely, the load side inlet temperature and its mass flow rate and the source side inlet temperature and its mass flow rate. To compare the relative influence of the parameter among others, influence coefficients were calculated based on five different results: heating capacity for the heat pump, the rate of heat extraction of the source and the compressor power and the outlet temperature of the source and load sides. The base case values of the inputs were chosen as their nominal values as shown in Table 3.2 – Table 3.6. The base case results for all five were obtained at these nominal values. Then each input value was perturbed from the base case and results were obtained for the same five cases. Dimensional type-2 influence coefficients were calculated for each input, based on all five results and are listed in Table 3.2 – Table 3.6. But the influence coefficients shown in the tables have different dimensions, to compare them among each other they have to be non dimensionalized. This is done by estimating the error in each input. Then the error in result is obtained by using the equation 3.10

$$\left| \textit{Error in Result} \right| = \frac{\varDelta R^{*}}{\varDelta P} \times \left| \textit{Est. parameter error} \right| \tag{3.10}$$

Table 3-2 *Influence coefficients and error analysis based on load side outlet temperature of the water-to-water heat pump model.*

Input Parameter	Base-case value	Est. Error in Input	Dimensional type 2 i.c.	Est. Error in Result [%]
Load side inlet temperature	26.6 [°C]	1 [°C]	0.03414 [°C^{-1}]	3.41
Load side mass flow rate	0.437 [Kg/s]	0.1 [Kg/s]	0.12298 [s/Kg]	1.229
Source side inlet temperature	-3.8 [°C]	1 [°C]	0.00309 [°C^{-1}]	0.31
Source side mass flow rate	0.437 [Kg/s]	0.1 [Kg/s]	0.00050 [s/Kg]	0.005

Table 3-3 *Influence coefficients and error analysis based on source side outlet temperature of the water-to-water heat pump model.*

Input Parameter	Base-case value	Est. Error in Input	Dimensional type 2 i.c	Est. Error in Result [%]
Load side inlet temperature	26.6 [°C]	1 [°C]	0.00315 [°C^{-1}]	0.314
Load side mass flow rate	0.437 [Kg/s]	0.1 [Kg/s]	0.00725 [s/Kg]	0.072
Source side inlet temperature	-3.8 [°C]	1 [°C]	0.17060 [°C^{-1}]	17.06
Source side mass flow rate	0.437 [Kg/s]	0.1 [Kg/s]	0.05121 [s/Kg]	0.51

Table 3-4 *Influence coefficients and error analysis based on heat capacity of the water-to-water heat pump model.*

Input Parameter	Base-case value	Est. Error in Input	Dimensional type 2 i.c.	Est. Error in Result [%]
Load side inlet temperature	26.6 [°C]	1 [°C]	0.00521 [°C^{-1}]	0.52
Load side mass flow rate	0.437 [Kg/s]	0.1 [Kg/s]	0.01150 [s/Kg]	0.115
Source side inlet temperature	-3.8 [°C]	1 [°C]	0.03921 [°C^{-1}]	3.92
Source side mass flow rate	0.437 [Kg/s]	0.1 [Kg/s]	0.00635 [s/Kg]	0.063

Table 3-5 *Influence coefficients and error analysis based on the rate of heat extraction of the water-to-water heat pump model.*

Input Parameter	Base-case value	Est. Error in Input	Dimensional type 2 i.c.	Est. Error in Result [%]
Load side inlet temperature	26.6 [°C]	1 [°C]	0.01126 [°C^{-1}]	1.12
Load side mass flow rate	0.437 [Kg/s]	0.1 [Kg/s]	0.02593 [s/Kg]	0.25
Source side inlet temperature	-3.8 [°C]	1 [°C]	0.05255 [°C^{-1}]	5.25
Source side mass flow rate	0.437 [Kg/s]	0.1 [Kg/s]	0.00837 [s/Kg]	0.0837

Table 3-6 *Influence coefficients and error analysis based on compressor power of the water-to-water heat pump model.*

Input Parameter	Base-case value	Est. Error in Input	Dimensional type 2 i.c.	Est. Error in Result [%]
Load side inlet temperature	26.6 [°C]	1 [°C]	0.00662 [°C^{-1}]	0.662
Load side mass flow rate	0.437 [Kg/s]	0.1 [Kg/s]	0.01670 [s/Kg]	0.167
Source side inlet temperature	-3.8 [°C]	1 [°C]	0.01312 [°C^{-1}]	1.31
Source side mass flow rate	0.437 [Kg/s]	0.1 [Kg/s]	0.00239 [s/Kg]	0.024

Figure 3.3 compares the influence of different input parameters based on the five different results. It is seen from the figure that the load side mass flow rate and the load side temperature each have a significant influence on the load side outlet temperature calculated by the model. Similarly, the source side inlet temperature and its mass flow rate have a significant influence on the source side outlet temperature. The results based on the compressor power shows that the source inlet temperature has significant influence followed by load side inlet temperature, and mass flow rates. Source side inlet

temperature has a significant influence on the result based on heating capacity and rate of heat extraction, followed by the load side inlet temperature.
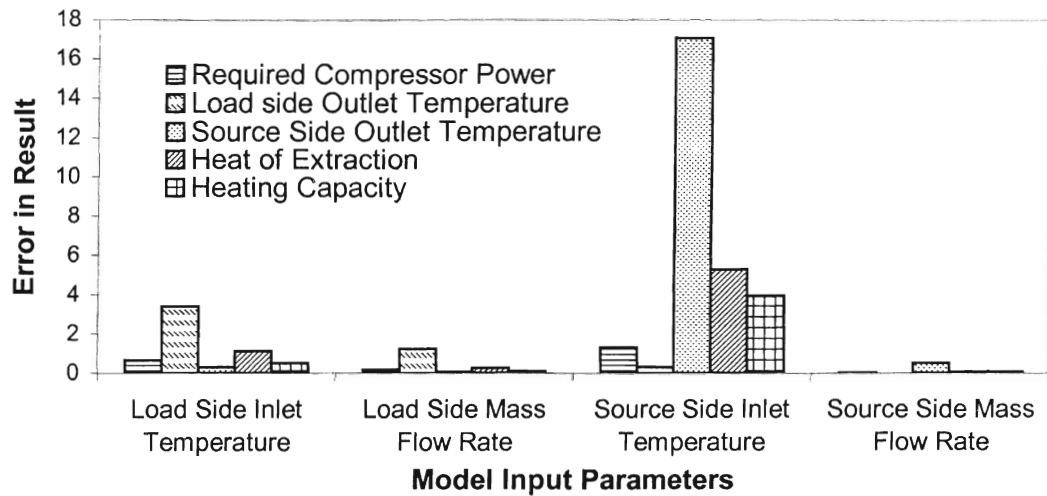
Figure 3.3 *Comparison of influence of model inputs on different model outputs.*

These results could be very helpful in model implementation. Where an insight about the influence of the model due to change in the input could be useful in predicting the stability of the model in the simulation environment. This also provides the model implementer with information on the convergence of the model in the simulation.

3.4. Model implementation

The model explained in Section 3.1 was implemented in EnergyPlus. Guidelines to implement a new model/component in the EnergyPlus simulation environment as specified in EnergyPlus Guide for Module Developers, EnergyPlus (2002), were followed in implementing the water-to-water heat pump model.

Figure 3.4 shows a typical EnergyPlus network of HVAC system and plant equipment. The components are connected together by air duct and fluid pipes called 'loops'. The structure of the network is defined with branch and connector objects. These are specified in the EnergyPlus input (IDF) file, discussed in Section 3.4.1.

The water-to-water heat pump (WWHP) model is connected in the plant loop as shown in Figure 3.4. As shown in the figure, EnergyPlus has two plant demand side loops, one each for cooling and heating. Since heat pump can both serve cooling and heating, which requires that the heat pump model to be connected to both the hot water loop and the chilled water loop. This is accomplished by defining two different virtual systems for the heat pump (one for cooling and another for heating) each of which is connected to its respective loop. As a result, the heat pump was implemented as two component models.
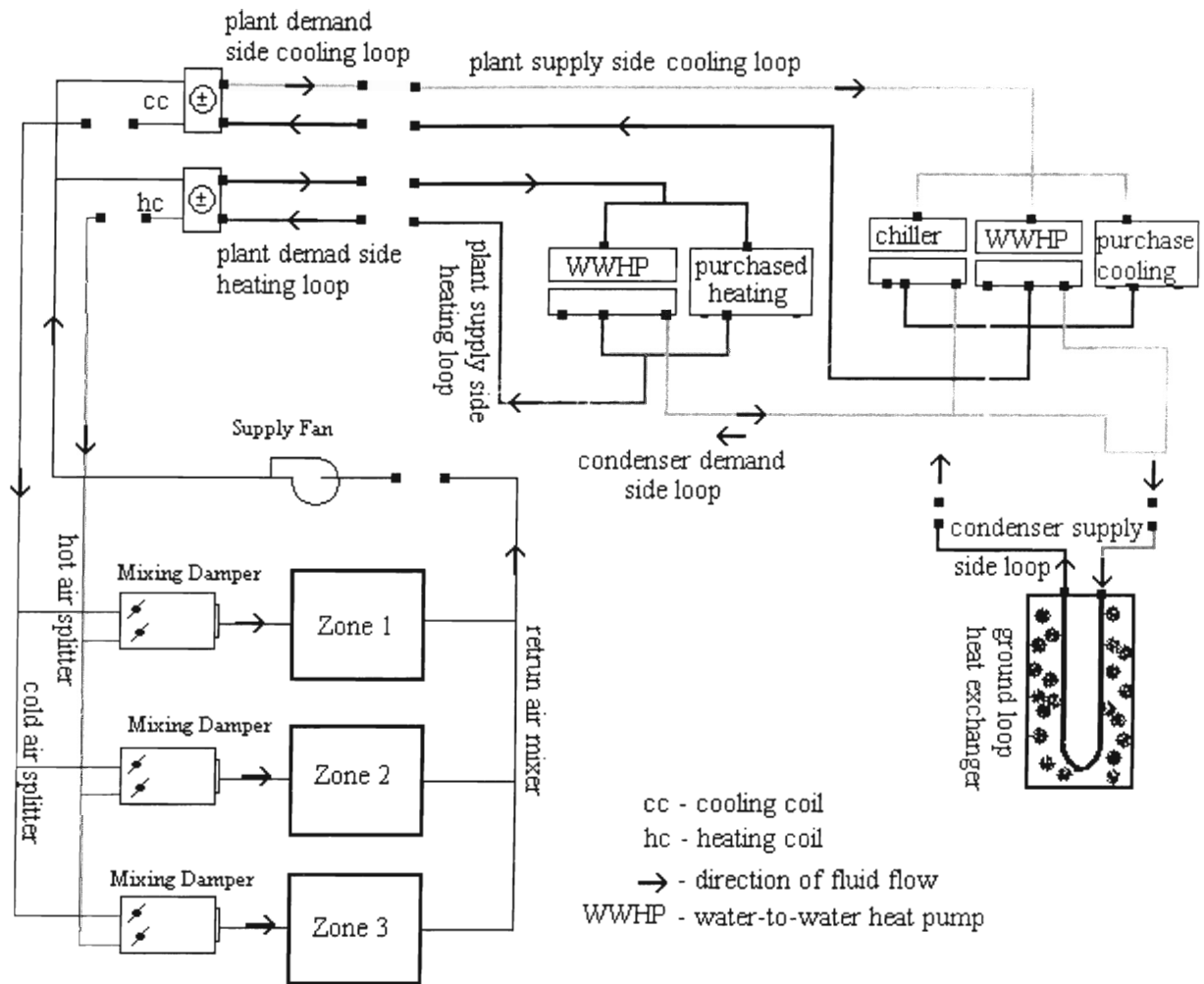
Figure 3.4 *The zone dual duct system connections.*

Initially the water-to-water heat pump component was written by Jin and Spitler (2002) in Fortran 77. The original model needed the following modification to comply with the EnergyPlus Standards:

1. Two input objects, one each for cooling and heating mode, were defined.

2. Two separate EnergyPlus component modules, one for cooling and one for heating, with their accompanying data structures were written.

3. EnergyPlus calling conventions and subroutine definitions were adapted. Input, initialization and output routines were written.

4. EnergyPlus data structure and variable definitions styles were adapted.

5. The code was upgraded to Fortran 90 "strict" conventions.

6. EnergyPlus fluid property routines were implemented in place of the equation based fluid property routines used in the original model.

7. A cyclic operation control algorithm was developed for the heat pump.

3.4.1. Input Specification

EnergyPlus Input requires that a unique class or keyword be specified in the IDD (input data dictionary) file for each component model. The IDD organizes information about each keyword specification and servers to interpret the input from the IDF (input data definition) file. This type of input specification is illustrated in Figure 3.5. The data is organized into blocks identified with a unique keyword, with one to one correspondence between each definition and data value. All the inputs are handled by a separate module in EnergyPlus called "InputProcessor". Each computational module uses the InputProcessor module to read its input from the definition file. InputProcessor provides the module developer with a number of service routines including: "GetNumObjectsFound" and "GetObjectItem". GetNumObjectsFound returns the number of objects found of a specific keyword. GetObjectItem gets the string (alpha) and numeric values of the specified object through two arrays a numeric and a character. Detailed information about the services and their usage can be found in the EnergyPlus Module Developers Guide EnergyPlus (2002).

```
Keyword 1                                    Keyword 1
  Data value 1          1 to 1                 Definition 1
  Data value 2      correspondence            Definition 2
      :            <------------->                :
Keyword 2                                    Keyword 2
      :                                          :
      :                                          :

   in.idf                                  EnergyPlus.idd
```
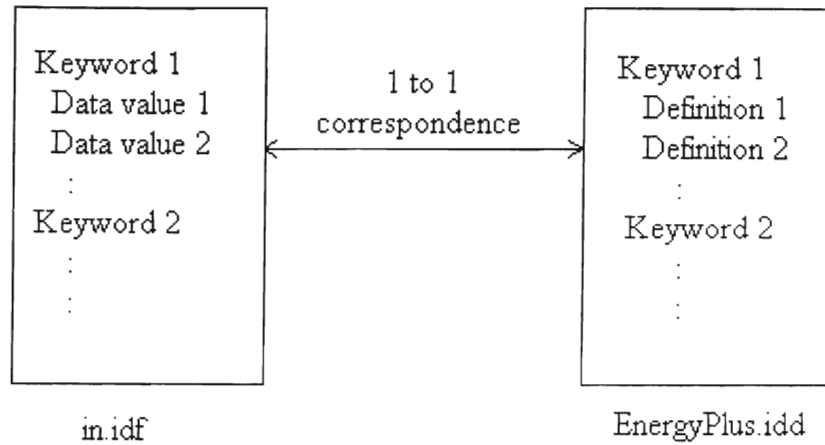
Figure 3.5 *EnergyPlus input scheme.*

Figure 3.6 shows the input definition for the water-to-water heat pump cooling object. An analogous object is created for heating mode. "HEATPUMP:WATERTOWATER COOLING" is the keyword or class name assigned to the heat pump model input definition. The keyword is followed by character field A1, which identifies a particular heat pump in the plant loop. The four text fields (A2, A3, A4, A5) are used to define the inlet and outlet connections of the heat pump to the plant loop. The source side is connected to the condenser loop and the load side to the chilled or hot water loop depending on the mode. The rest of the numeric fields are used to specify the model parameters, which are obtained from the manufacturer's catalog data.

```
HEATPUMP:WATERTOWATER COOLING,
  A1,\Field Water to Water Heat Pump Name
        \required-field
  A2,\Field Source Side Inlet Node
  A3,\Field Source Side Outlet Node
  A4,\Field Load Side Inlet Node
  A5,\Field Load Side Outlet Node
  N1,\Field COP
  N2,\Field Nominal Capacity
        \units W
  N3,\Field Min PLR
        \minimum 0.0
  N4,\Field Max PLR
        \minimum 0.0
  N5,\Field optimum PLR
        \minimum 0.0
  N6,\Field Load side Volumetric Flow Rate
        \units m3/s
        \minimum 0.0
  N7,\Field Source Side Volumetric Flow Rate
        \units m3/s
        \minimum 0.0
  N8,\Field Load side Heat Transfer Coefficient
     \units W/K
  N9,\Field Source Side Heat Transfer Coefficient
     \units W/K
  N10,\Field Piston Displacement
     \units m$^3$/s
  N11,\Field Compressor Clearance Factor
  N12,\Field Compressor Suction And Discharge Pressure Drop
  N13,\Field Superheating
     \units C
  N14,\Field Constant Part Of Electro Mechanical Power Losses
     \units W
  N15,\Field Loss Factor or mechanical efficiency
  N16,\Field High Pressure Cut off
  N17,\Field Low Pressure Cut off
  N18;\ Cycle time in hour
```

Figure 3.6 *The input object for water-to-water heat pump as defined in the data dictionary file.*

3.4.2. Model Implementation

Figure 3.7 shows the algorithm and the calling structure for the heat pump heating and cooling modules. The discussion focuses on the implementation of the cooling mode

45

model but can also be applied to the heating mode model. The driver routine "SimHPWatertoWaterCOOLING", which is the only public routine in the module "HeatPumpWaterToWaterCOOLING", acts as the interface between the model and the rest of the simulation. This subroutine is called by a high level HVAC manager routine in module "PlantSupplySideManager" which determines the cooling demand on the heat pump. A call to the heat pump driver routine is made in "SimPlantEquipment", a private routine in PlantSupplySideManager. This routine makes the call to all the plant components.

The heat pump's driver routine, "SimHPWatertoWaterCOOLING" calls the input routine "GetGshpInput" once at the beginning of the simulation. This input routine loads the heat pump local simulation variables with model parameter values and gets the node numbers for the heat pump connections on the load and source side inlets and outlets.
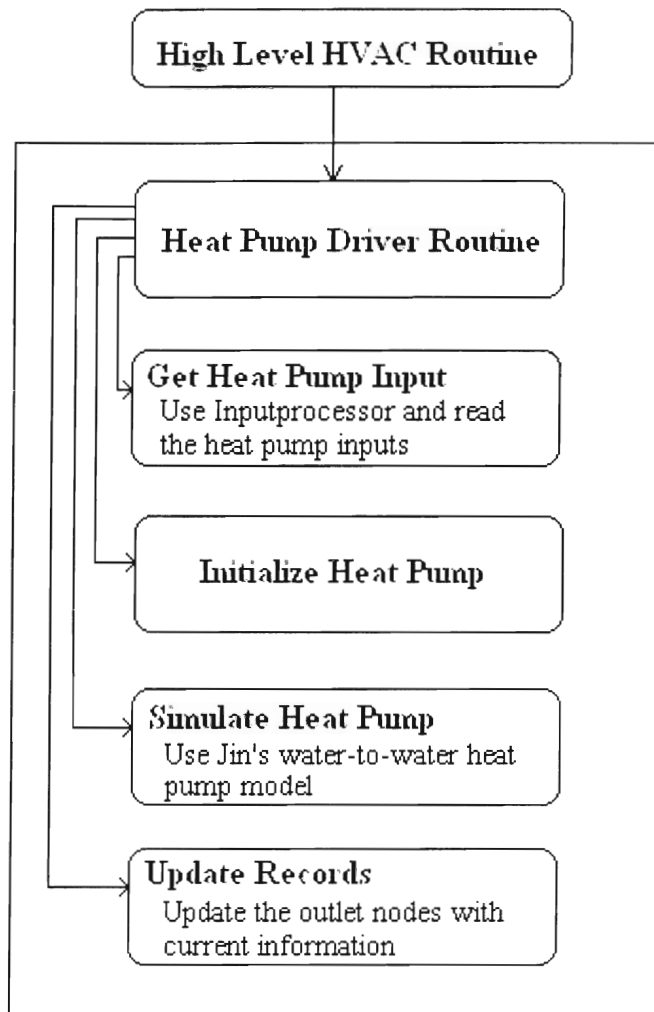
Figure 3.7 *Frame work of the water-to-water heat pump module.*

The initialization routine "InitSimVars" handles the initialization and re-initialization of the variables at the beginning of each environment, day, hour or time step as needed. It also updates node information from the heat pump inlet node data structure to local simulation variables for every iteration.

Once the initialization is done, the heat pump driver routine calls the model routine "CalcGshpModel", which simulates the water-to-water heat pump. It simulates the model for inlet conditions using the estimated parameter values and predicts the outlet conditions. Since the predicted outlet conditions are based on the catalog data used to

47

estimate the parameters there is no guarantee that the model would match the load

assigned by the simulation. That is, unless the operation of the heat pump is controlled by

a 'duty cycle' algorithm, it will run for the entire time step, regardless of demand on the

fluid loop.

To adjust the model's prediction to the demand requested by the high level

HVAC manager, the control strategy shown in Figure 3.8 was developed. When the

model's prediction of heating/cooling capacity (QLoad) for the given inlet condition is

more than the required demand, a duty factor is computed. The duty factor is calculated

as the ratio of the plant demand and the predicted heating/cooling capacity (QLoad).

Using this duty factor, the other outputs are scaled. Using the new-scaled values, the

outlet conditions are recalculated. Finally, the new outlet conditions are updated at the

respective outlet nodes.
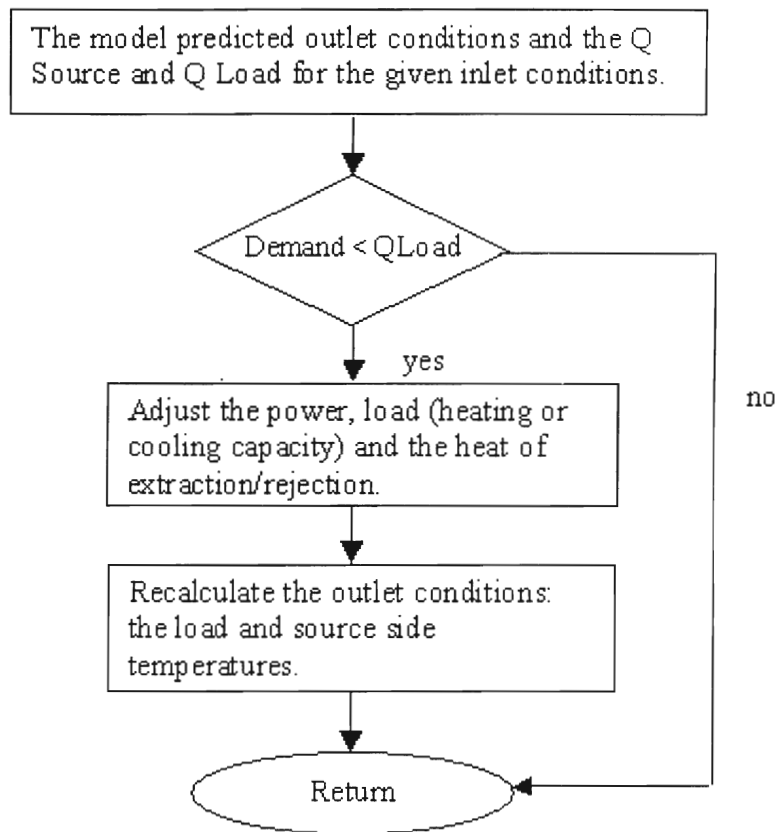
Figure 3.8 *Flow chart showing the load adjustment scheme- the duty cycle.*

Output variables like power, heat transfer rates and outlet temperatures are made available for reporting by calling the EnergyPlus output variable setup routine. These variables can be included in output reports by making a request in the IDF file at different frequencies (time-step, hourly, daily etc.) supported by EnergyPlus reporting.

To prevent 'short-cycling' of the model, an additional control algorithm was developed to ensure that the simulated heat pump, like a physical heat pump, would stay on or off for a specified time period after switching. To implement this behavior in the EnergyPlus heat pump model the input specification were modified to include the cycle time. The Figure 3.8 shows the logic for the cycle time control.
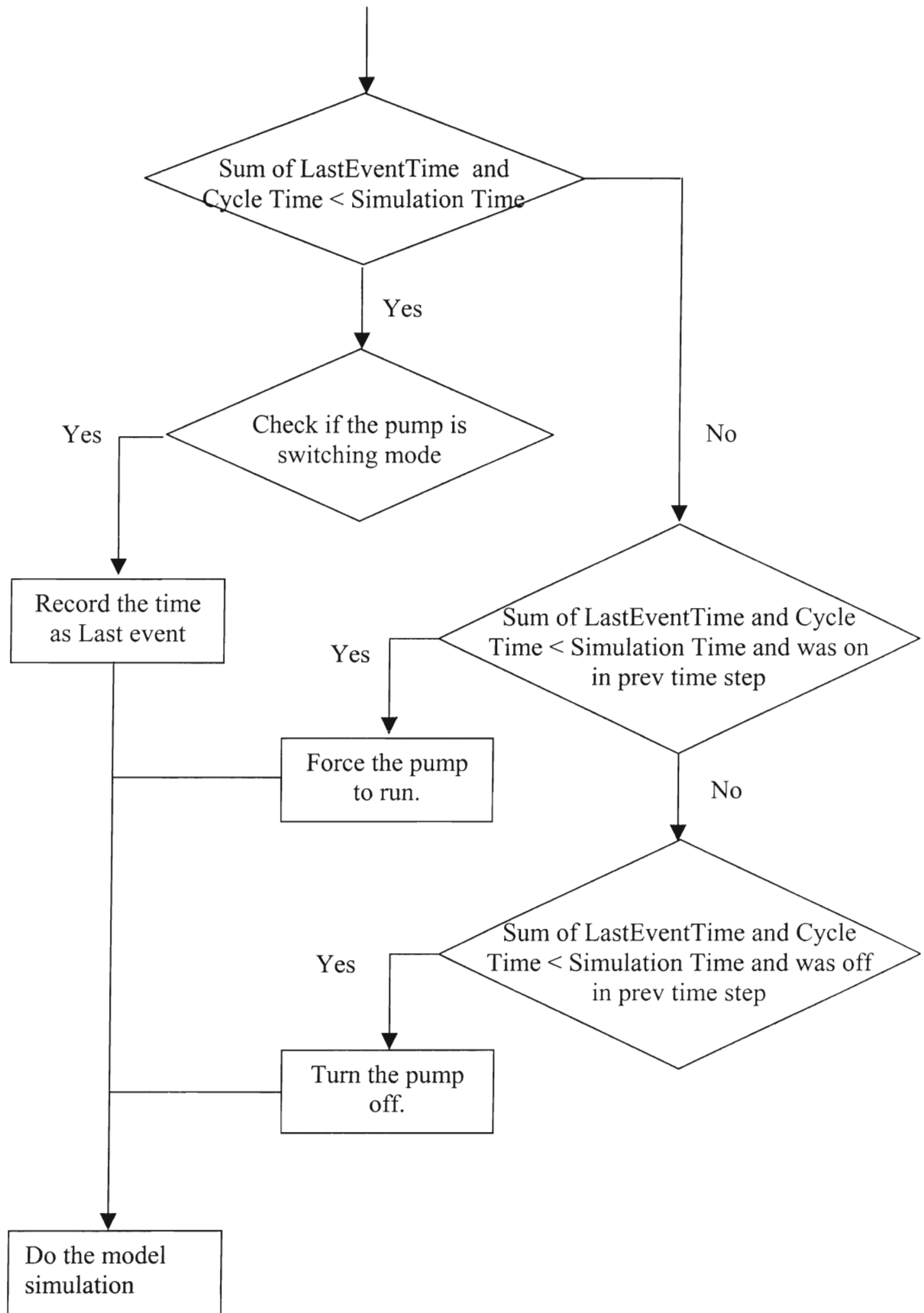
Figure 3-9 *Flow chart of the cycle time control logic implemented in the heat pump model.*

Cycle time logic is applied if the current system time-step is less than the cycle time. In this case it is possible that the heat pump has not stayed on or off for the required amount of time. From Figure 3.9 it can be seen that if the sum of LastEventTime (which stores the time when the heat pump last switched states) and CycleTime is not greater than CurrentSimulationTime, then, in that case the heat pump hasn't stayed on or off for the required time. Therefore, we check to see if it was on or off during the previous time step using the WasOn variable (which holds the heat pump on/off information from the previous time-step) and force it to continue to stay in that state in spite of the higher-level manager's decision to change its state. If the current simulation time is larger than the sum LastEventTime and CycleTime, which suggests that the heat pump has stayed on beyond the required cycle time, then, the decision of the higher-level manager is executed. When the heat pump switches states, then the simulation time at which that event occurred is recorded for future use.

3.5. Summary

A sensitivity analysis was performed on the parameter estimation based water-to-water heat pump model. An enhancement to the model to avoid "short-cycling" was developed. Finally, the model was implemented in the EnergyPlus environment according to the specifications of the EnergyPlus Module Developer's Guide.

Several case studies were performed to analyze the performance of the ground source heat pumps. These case studies investigated the combined performance of the heat pump model and the vertical ground loop heat exchanger model, which is explained in the next chapter.

Chapter 4. Variable Short Time Step Model of Vertical Ground Loop Heat Exchangers

Most ground loop heat exchanger models fail to account for short-term fluctuations in inlet water temperatures. Fluctuations of less than a day or hour, are typical in practice and can affect the sizing of both the ground loop heat exchanger and the ground source heat pump that is attached to the ground loop. Recent work reported by Yavuzturk and Spitler (1999) developed borehole temperature response factors for short time-steps and modeled the ground loop heat exchanger down to a one-hour time-step. Though Yavuzturk & Spitler successfully developed a true hourly model, sub-hourly models that work in energy simulation environments, with variable, sub-hourly time-steps are not reported in the literature.

Simulation environments, which operate with time-steps of less than an hour require models that can predict the system response to short time-step fluctuations of the model input parameters. Such an environment requires a ground loop heat exchanger model which can effectively and consistently predict short-term variations in the ground loop heat exchanger exiting fluid temperature. This enables the ground source heat pump installed in the system to be sized correctly.

4.1. Variable System Time Step in EnergyPlus

EnergyPlus uses a variable system time-step, which can go down to one minute, in order to calculate the system response to the zone load. The fixed length zone time-step is decoupled from the system time-step which changes continuously in order to

achieve convergence of the system simulation. Thus, an unspecified number of system time-steps occur during each zone time-step. The loads not met for a zone time-step are reflected as adjusted space temperatures in the next time-step. This ensures that an energy balance is achieved while maintaining a reasonably accurate prediction of space temperature. The latter is important for exact sizing of plant equipment and occupant comfort, but it does present some problems in implementing system models. In order to implement the vertical ground loop heat exchanger model in EnergyPlus, a method of accounting for the variable system time-step had to be developed first as discussed in Section 4.3

4.1.1. System Simulation in EnergyPlus

The EnergyPlus HVAC simulation environment is a cross between a component based and system based environment. EnergyPlus utilizes the system-based concept of a fluid loop, which represents the piping or ducts in a system. The modular components are defined and connected to the fluid loop in the input file. The combined environment uses a Manager-Interface simulation protocol Fisher et al. (1999).

The Manager-Interface protocol enables the simulation of subsystems independently of each other. A system is defined by first specifying hydronic and air loops. These model the ducts and pipes of the actual physical system. Once the loops are defined then components such as fans dampers, coils, boilers, chillers etc. are added to the loops to define the system. The type and order in which components are specified on each loop determines the system type. The loops are separated logically into different blocks corresponding to groups of functionally similar components. Each block is

controlled by a respective managing routine independently of the others. Six managers are defined in EnergyPlus for this purpose. They are the Plant Loop Supply Side Manager, the Plant Loop Demand Side Manager, the Condenser Loop Demand Side Manger, the Condenser Loop Supply Side Manager, the HVAC Manager and the HVAC Interface Manager.

The HVAC Interface Manger passes data between the other managers. The most recent values of all state variables are passed from the outlet of one loop to the inlet of its companion loop. The overall simulation is controlled by a higher-level manager, the HVAC Manager, which successively calls the loop managers until the system converges.

The variable short time-step vertical ground loop model was implemented in the condenser loop supply side manager as shown in Figure 3.4. This manager calls the source side components in the loop. The components can be as simple as a cooling tower or as complex as a hybrid system consisting of a ground loop heat exchanger with a supplemental heat rejecter like a shallow pond, pavement system or cooling tower.

4.2. Ground Temperature Response Factors

Eskilson (1987) and Yavuzturk and Spitler (1999) developed the long and short time-step borehole temperature response factors respectively. Response factors are an infinite series of numbers, which relate the current value of a variable to past values of other variables at discrete time intervals. In this literature, borehole temperature response factors are referred as *g*-functions. The variable time-step vertical ground loop heat exchanger model presented here uses both long time-step *g*-functions and short time-step

g-functions to predict the boreholes response to long and short term fluctuations in the load.

4.2.1. Long Time-Step Response Factors

Eskilson developed long time-step g-functions using a hybrid model, which is a combination of analytical and numerical solution techniques. He developed the g-functions for a basic step pulse using a forward explicit difference method on a two dimensional radial-axial mesh. Constant initial and boundary conditions were used. The variations in thermo-physical properties of the ground were ignored. The contributions of individual borehole elements such as pipe wall and grout were also neglected. The thermal resistance due to the individual borehole elements was calculated separately and added to the total resistance. The end effects were modeled using a finite borehole length.

The temperature response of a predefined configuration of the borehole field (characterized by the ratio of borehole spacing and borehole length) to a unit step function pulse is determined by spatial superposition of the response from a single borehole. When responses of the borehole outer wall temperature with respect to time is non-dimensionalized and plotted against non-dimensional time the resulting curve is called a g-function curve. The g-function gives the temperature response of the unit pulse at the borehole wall. Once we have the temperature response to a unit pulse, we can find the response to any heat extraction/injection rate by the superposition technique explained in Section 4.4.2.

Eskilson developed g-functions for various borehole configurations. He plotted the g-function curves against the non-dimensional time defined as $\ln(t/t_s)$ (where

$t_s = H^2 / 9\alpha$). Eskilson (1987) gave the g-function curves for 38 different configurations

for different sets of borehole spacing to borehole length ratio B/H typically for 0.05,

0.1, 0.15, 0.2, 0.3 and ∞ ($B/H = \infty$ represents the single borehole configuration). All the

plots were for the ratio of 0.0005 between the borehole radius and the borehole length

r_b / H . For any other radius a simple relation between the two radii as given by Eskilson

(1987) can be used.

Figure 4.1 shows the g-functions for various configurations of vertical boreholes

with B/H ratio of 0.1 along with a single borehole. It is seen from the Figure that the

thermal interaction between boreholes increases with time and with the number of

boreholes in field.
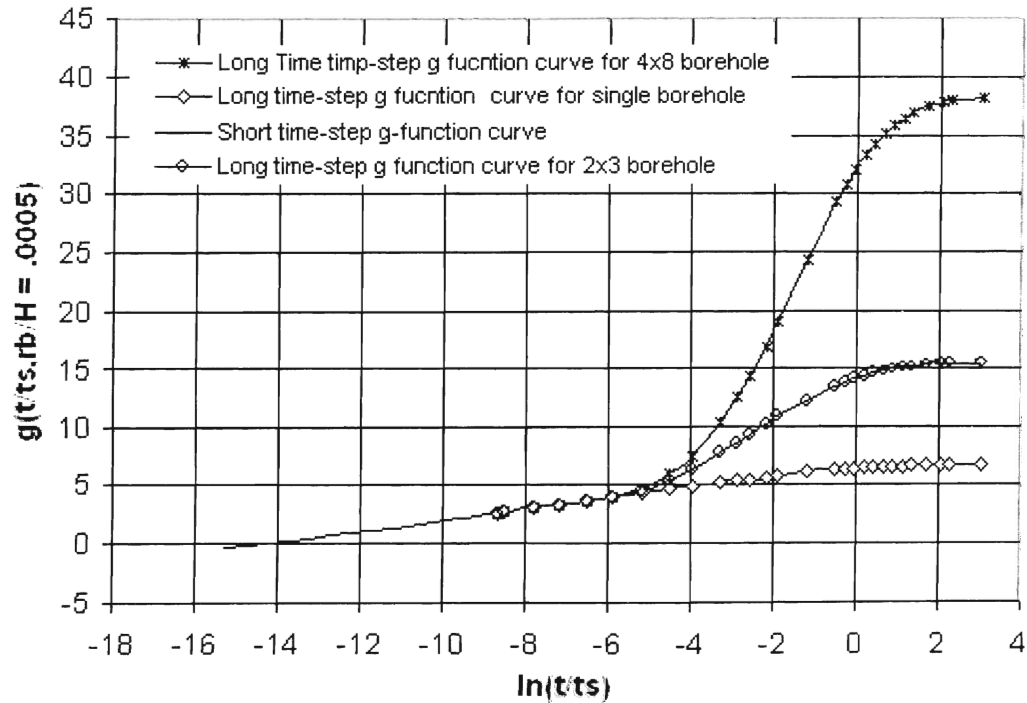
Figure 4.1 *Short time-step g-function curve as an extension of long time-step g-function curves for different configuration of boreholes (Eskilson 1987, Yavuzturk and Spitler 1999).*

56

The *g*-functions developed by Eskilson are valid only after a time estimated by Eskilson as $5r_b^2 / \alpha$. This time varies from 3-6 hours for a typical borehole field. This is because the analytical line source model, on which the Eskilson's model was based does not give a prompt increase in borehole wall temperature at $r = r_b$. It gives acceptable results only after the non-dimensional times of $\alpha t / r_b^2 > 5$. However, to model the short time responses of a borehole we need response factors, which can give accurate results down to minutes.

4.2.2. Short Time-Step Response Factors

Yavuzturk and Spitler (1999) developed short time-step response factors using a transient, two-dimensional, implicit finite volume model on a polar grid.

The circular u-tube pipe in the ground loop heat exchanger was approximated as a pie sector of equivalent perimeter. A constant heat flux for the heat transfer from/to the U-tube, a zero heat flux in the angular direction and a constant far field temperature in the radial axis make up the three boundary conditions. The undisturbed far field temperature is the initial condition. The numerical model accounts for the thermal resistance due to individual borehole elements; such as resistance of the pipe and grout material and the convection resistance due to the heat transfer fluid in the pipes. The long time-step *g*-functions discussed in the previous section do not account for these effects. Due to this discrepancy between the models, the short time-step *g*-functions need to be adjusted to match the long time-step *g*-functions developed by Eskilson (1987). The temperature rise due to borehole resistance for a specific time-step is subtracted from the short time-step model's temperature prediction for the corresponding time-step, which gives the actual

temperature rise for that time-step. These resulting temperature adjusted short time-step g-functions (the adjusted ones) when plotted with the long time-step g-functions line up very well with the long time-step g-functions. Figure 4.1 shows the short time-step g-functions as an extension of long time-step g-functions for a single, a 2x3 and a 4x8 borehole configuration.

The short time-step g-functions are the same for different borehole configurations. This is because there is no thermal interaction between the boreholes for times less than 200 hrs during which the short time-step g-functions apply. So it is appropriate to use the short time-step g-function for time-steps in the range of 2.5 min and 200 hours and the long time-step g-functions for time-steps longer than 200 hours. The g-function for any time can be found by linear interpolation between the bounding known values.

4.3. Development of the EnergyPlus Variable Short Time Step Model

The EnergyPlus variable time-step model was developed as an extension of the model presented by Yavuzturk and Spitler (1999). The variable, short time-step model uses a similar algorithm and extends it to accommodate sub-hourly responses and variable time-steps. The model includes an explicit calculation of the outlet fluid temperature of the ground loop heat exchanger.

The uniform time-step model developed by Yavuzturk and Spitler (1999) is able to pre-calculate all the g-functions at the beginning of the simulation. The variable time-step model on the other hand must calculate the g-functions when the borehole response calculation for each time-step is carried out. For every time-step a different set of g-

functions is needed in the variable time-step model as the time at which the g-function is to be applied for the past loads changes for each time-step. This is illustrated in Figure 4.2, which shows a simulation in progress. The boxes with numbers represent the sub-hourly loads. The time (in hrs) at which these loads occurred are shown by solid arrows above the respective load boxes. The right-most solid arrow gives the current simulation time, which is 3.31 hrs. The times given below the boxes, pointed by dashed arrows, are the time at which the g-functions are to be estimated and applied to the respective sub hourly loads (boxes) for the current time.

For example, let us take the sub hourly loads 1,2 & 3. These loads occurred at 0 hrs, 0.16 hrs & 0.28 hrs. The response of the borehole temperature for the current time-step is calculated by applying the g-functions at 3.15 hrs, 3.03 hrs & 2.5 hrs respectively. Thus to calculate the present borehole temperature, the sub hourly loads 1-12 are superposed using the corresponding g-functions at times given by the dashed lines. This gives the borehole temperature at hr 3.31. However, for the previous time-step, which occurred at 3.15 hrs, the g-functions for the loads 1, 2 & 3 are at 2.99 hrs 2.87 hrs and 2.42 hrs, and the over all response is obtained by superposing the loads 1-11.

Thus for each time-step, since the time-step increments are not uniform, we need to store the simulation times at which these time-steps occurred, and calculate corresponding g-functions at each time-step.
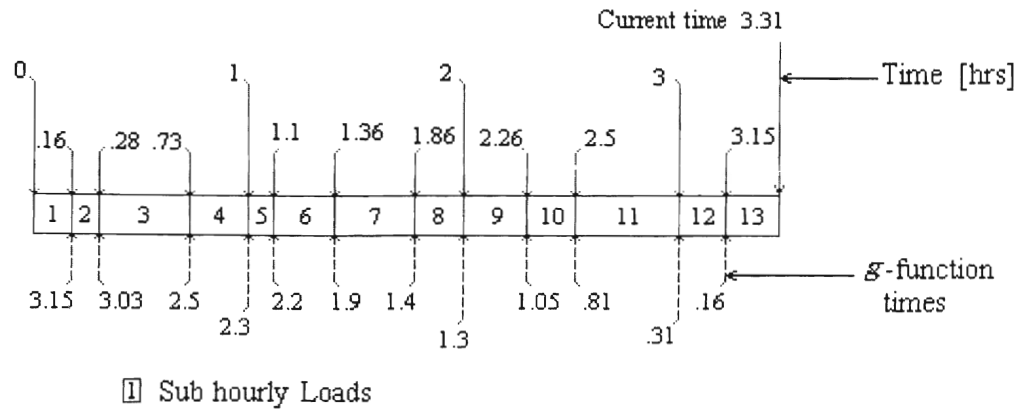
Figure 4.2 *Variable time-step ground loop heat exchanger model schematic explaining the g-fucntion estimation.*

The Yavuzturk and Spitler model calculates the outlet fluid temperature by iteration beginning with the undisturbed mean temperature of the surrounding ground as an initial guess. This increases the time taken by an already computationally intensive algorithm. To circumvent this a set of explicit equations were formulated to estimate the outlet fluid temperature.

The implementation of the variable short time-step vertical ground loop heat exchanger model in EnergyPlus is explained in Section 4.9.

4.4. Analytical Comparison

It order to validate the variable short time-step model, it was compared to an existing analytical line source approximation model. The results of the comparison of the simulation model with the line source approximation model are presented in this section. The line source theory was developed by Kelvin (1882) and was applied to vertical loop

60

heat exchanger analysis by Hellstrom (1991). This study follows the methodology

developed by Hellstrom to validate the EnergyPlus GLHE model.

4.4.1. The Line Source Model

Line source theory is based on simplification of the general 3-D heat conduction

equation with a cylindrical heat source as given by equation 4.1.

$$\frac{1}{\alpha}\frac{\partial T}{\partial t} = \frac{\partial^2 T}{\partial r^2} + \frac{1}{r}\frac{\partial T}{\partial r} + \frac{1}{r^2}\frac{\partial^2 T}{\partial \phi^2} + \frac{\partial^2 T}{\partial z^2} \tag{4.1}$$

Where

$$\alpha = \text{is thermal diffusivity} = k/\rho c \text{ in } m^2/s$$

This is the transient heat conduction equation in three dimensions for cylindrical

coordinates (r, z, ϕ). But in the analysis of ducts with circular cross-section, which is the

case of a ground loop heat exchanger, the heat equation is reduced to the radial

dimension, r, as the variation in axial direction is neglected. The equation for the thermal

process becomes:

$$\frac{1}{\alpha}\frac{\partial T}{\partial t} = \frac{\partial^2 T}{\partial r^2} + \frac{1}{r}\frac{\partial T}{\partial r} + \frac{\partial^2 T}{\partial z^2} \tag{4.2}$$

The boundary conditions to the ground loop heat exchanger are: prescribed

surface temperature, prescribed flux and heat flow proportional to the temperature

difference over a surface thermal resistance. Though the temperature of the borehole and

the ground varies in the vertical direction, an average value is taken for the entire length

of the borehole, neglecting the vertical effects.

Initial condition:

$$T(r,z,0) = T_{om}$$

1. Condition at pipe radius $r = r_b$

$$-2\pi r_b k \frac{\partial T}{\partial r}\bigg|_{r=r_b} = q_1 \qquad (t > 0)$$

2. Temperature at ground surface

$$T(r,0,t) = T_{om}$$

3. Temperature at borehole wall

$$T(r_b,z,t) = T_b(t)$$

The solution to the above problem can be obtained by a Laplace transform

approach Carslaw and Jaeger (1947). The Bessel function involved in the solution using

this method makes the integral difficult and time consuming to evaluate. Alternatively, a

line source approximation can be applied to obtain a simplified solution. The temperature

in the ground then becomes:

$$T^q(r,t) = \frac{q_1}{4\pi k} \int_0^t e^{-r^2/4\alpha(t-t')} \frac{dt'}{t-t'} = \frac{q_1}{4\pi k} \int_{r^2/4\alpha t}^{\infty} \frac{e^{-u}}{u} du = \frac{q_1}{4\pi k} E_1(r/4\alpha t) \qquad (4.3)$$

Here, E_1 is called the exponential integral. The tables and formula pertaining to

this function are given by Abramowitz and Stegun (1964). The temperature T_f is now a

function of just $r / \sqrt{\alpha t}$. The length $\sqrt{\alpha t}$ is a measure of the range of thermal influence around the pipe. Hellstrom demonstrated that the change in temperature is very small for values of $r / \sqrt{\alpha t} > 3$. For large values of the non-dimensional time $\alpha t / r^2$ the exponential integral E_1 can be approximated by the following relation Hellstrom (1991)

$$E_1(r^2 / 4\alpha t) = \ln\left(\frac{4\alpha t}{r^2}\right) - \gamma - \frac{1}{4}\left[r^2 / \alpha t - (r^2 / 4\alpha t)^2\right] \qquad \frac{\alpha t}{r^2} \geq 0.5 \qquad (4.4)$$

This can be further approximated by this simple and useful correlation

$$E_1(r^2 / 4at) = \ln\left(\frac{4\alpha t}{r^2}\right) - \gamma \qquad \alpha t / r^2 \geq 5 \qquad (4.5)$$

Where $\gamma = 0.577722\ldots$ is Euler's constant

This is valid when the thermal process in the region within the radius r reaches steady state, when the maximum error is 2% for $\alpha t / r^2 \geq 5$. The temperature at the pipe wall, which has more meaning and usefulness, is obtained by setting $r = r_b$ in the above formula.

$$T_b^q = \frac{q_1}{4\pi\lambda}\left[\ln\left(\frac{4\alpha t}{r^2}\right) - \gamma\right] \qquad (4.6)$$

Hellstrom (1991) compares the temperature at borehole wall for different solutions: Laplace solution, line source solution and the approximation used in the line source (equation 4.4). When he plotted the dimensionless temperature and dimensionless time it was found the Laplace solution gave a prompt increase of the pipe temperature

while the line source is delayed and the simple approximation were delayed. The non-dimensional time is defined as $\alpha t / r_b^2$. Hellstrom estimated the relative error between the exact solution and the line source solution for different non-dimensional times. He found that after non-dimensional times of $\alpha t / r_b^2 = 5$ the error drops to below 10%. He denoted this time as $t_b = \dfrac{5r_b^2}{\alpha}$ after which the error of the line source approximation is with in 10%. Swedish data given by Eskilson (1987) shows that the typical value of t_b is around a few hours. Once this time is reached the approximation $E_1(r^2/4at) = \ln\left(\dfrac{4\alpha t}{r^2}\right) - \gamma$ can be used to calculate the temperature at $r = r_b$.

The thermal resistance between the fluid and the ground (i.e. the resistance offered by the borehole against the heat transfer, R_b) determines the temperature difference between the fluid and the ground at $r = r_b$. The change in fluid temperature $T_f^q(t)$ due to a step change in the heat injection rate is given by Hellstrom (1991)

$$T_f^q(t) = \frac{q_1}{4\pi k}\left[\ln\left(\frac{4at}{r_b^2}\right) - \gamma\right] + q_1 R_b = q_1 R_q'(t) \qquad\qquad t \geq t_b \qquad\qquad (4.7)$$

Where R_b is the fluid to ground thermal resistance. This resistance is a measure of all the borehole elements including grout resistance and resistance due to convection and conduction in the pipe.

$R_q'(t)$ is the time-dependent thermal resistance for a heat injection step

64

$$R'_q(t) = \frac{1}{4\pi k}\left[\ln\left(\frac{4at}{r_b^2}\right) - \gamma\right] + R_b \qquad t \geq t_b \qquad\qquad (4.8)$$

$R'_q(t)$ is the thermal resistance between the fluid and the initial undisturbed

ground temperature level. This gives the temperature for a heat injection step with the

constant value q_1 *(W/m)* starting at time t=0. The following section discusses the more

general case of the heat injection steps, which include constant load, periodic load, and

pulse load.

4.4.2. Superposition of Pulses

The heat transfer rate to the fluid $q(t)$ can be represented as series of step-wise

constant values, where q_1, q_2, q_3, ...q_n, q_N, represent step changes in the heat transfer rate.

$$q(t)\begin{cases} q_1 & t_1 < t < t_2 \ (t=0) \\ q_2 & t_2 < t < t_3 \\ \vdots \\ \vdots \\ q_n & t_n < t < t_{n+1} \\ q_N & t > t_N \end{cases} \qquad\qquad (4.9)$$

Then the heat transfer rate $q(t)$ as a function of time at any time t can be

expressed as the sum of the step changes in heat transfer rate:

$$q(t) = \sum_{n=1}^{N}(q_n - q_{n-1})He(t - t_n) \ \textit{Where, } (q_0 = 0), \ He\begin{cases} 1t > 0 \\ 0t \leq 0 \end{cases} \qquad (4.10)$$

Where *He* is heavy side step function and N is the number of heat transfer pulses. Then the fluid temperature can be obtained by superposition of the contribution from each step as:

$$T_f(t) = T_{om} + \sum_{n=1}^{N}(q_n - q_{n-1})R(t - t_n)He(t - t_n) \qquad (4.11)$$

Any heat injection function $q(t)$ can be defined by superposition of single pulses. Figure 4.3 shows a single heat injection pulse of length t_1.
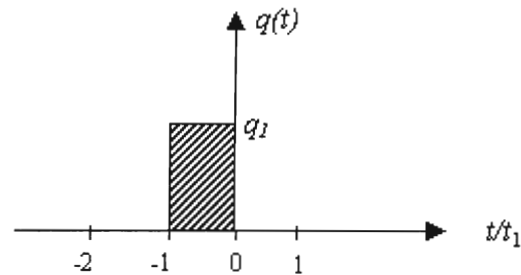
Figure 4.3 *Single heat extraction pulse.*

The increase in fluid temperature due to the injection pulse at the end of time $t = 0$ is given by equation 4.7

Another simple case, a balanced pair of heat extraction and heat injection pulses is shown in Figure 4.4. Both the extraction and injection pulse have same amount of energy. The length of the extraction pulse of strength q_1 is $\dfrac{\beta}{1-\beta}t_1$. The strength of the injection

pulse is $\dfrac{-\beta q_1}{1-\beta}$ and its length is βt_1. The change in fluid temperature at the end of the

pulses, $t = 0$, is given by superposition of the line source solution as,

$$T_f^q(0) = \frac{q_1}{4\pi k}\left[\ln\left(\frac{4\alpha t_1}{r_b^2}\right) - \gamma\right] + q_1 R_b - \frac{q_1}{4\pi \lambda}\left[\frac{1}{1-\beta}\ln\left(\frac{1}{\beta}\right)\right] \qquad (4.12)$$
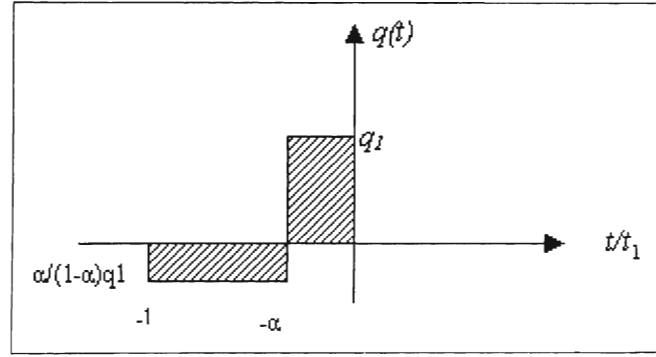
Figure 4.4 *Balanced pair of heat injection pulses.*

In general when heat transfer is expressed as a series of stepwise constant values

as described at the beginning of the section, the average fluid temperature relative to the

undisturbed ground temperature is given by the sum of all the contributions from each

step n:

$$T_f(t) - T_{om} = \sum_{n=1}^{N}\left(\frac{q_n - q_{n-1}}{4\pi k}\ln(t - t_n)\right) + q_N\left[R_b + \frac{1}{4\pi k}\left(\ln\left(\frac{4\alpha}{r_b^2}\right) - \gamma\right)\right] \qquad (4.13)$$

The first term gives the contribution of *1* to *n* pulses and the second term gives the temperature difference due to resistance offered by the individual borehole elements R_b as previously discussed.

4.4.3. Results of Stand-Alone Model Tests with no Load Aggregation

The variable short time-step model was compared with the analytical model discussed in the previous section. Four different Load profiles were considered.

1. Constant Heat Extraction: Heat is extracted constantly at the same rate q_0 throughout the simulation.

2. Pulsated Extraction: Heat is alternately extracted and injected every day of the year.

3. Periodic Extraction: Heat extraction is based on a sinusoidal function with amplitude, q_p and a period, t_p. The extraction rate at any time t is given by the expression, $q_p Sin(2\pi t / t_p)$.

4. Composite Extraction: The total heat extraction rate is obtained by superposition of the following three extraction rates.

   - Constant rate, q_0

   - Periodic rate, $q_p Sin(2\pi t / t_p)$

   - Pulsated load q_l for duration t_a-t_b, when the periodic component is maximum

The total heat extraction rate is given by

$$q(t) = q_0 + q_p Sin(2\pi t / t_p) + q_1[He(t - t_a) - He(t - t_b)] \qquad (4.14)$$

For each case, the simulation was run for one year at three-minute time-steps. The borehole parameters used in the test are given in the Table 4-1.

1. The constant heat extraction rate was $q_0 = 60.8W / m$ of borehole length

2. The pulsated $q_0 = \pm 43.4w / m$ of borehole length.

3. The periodic heat extraction had amplitude $q_p = 60.8W / m$ and a period $t_p = 720hrs$. The composite extraction is a combination of all the three different loads.

Table 4-1 *The Borehole and Ground Properties*

Parameters	Values
Number of Boreholes	1
Length of Bore holes	76.2 m
Radius of Borehole	0.0635 m
Thermal Conductivity Ground	0.692 W/m-K
Heat Storage Capacity Ground	2347 KJ/m^3-K
Specific Heat Fluid	4182 J/Kg-K
Far Field Temperature	19.3 °C
Grout Conductivity	0.6926 W/m-K
Pipe Conductivity	0.3913 W/m-K
Fluid Conductivity	0.6026 W/m-K
Fluid Density	998.2 Kg/m^3
Dynamic Viscosity Fluid	0.000987 m^2/s
Pipe Outer Dia	0.0266 m
U tube shank distance	0.0253 m
Pipe Wall thickness	0.00241 m

4.4.3.1. Constant Load

Figure 4.5 compares the analytical model and the simulation model for a single

borehole configuration. The test was run for one year at a 3-minute time-step. It is noted

from Figure 4.5 that the model behaves well and matches the analytical solution closely.

Figure 4.6 shows the difference between the analytical and the simulation temperature

predictions. The difference drops to less than 1°C within a few minutes of the simulation start. After a few hours it diminishes to less than 0.1°C. The larger differences between the analytical and simulation temperature prediction in the first few time-steps are due to the value of the initial guess, which is the undisturbed mean temperature of the ground.

Figure 4.7 shows the results of a 32-borehole configuration. The boreholes were arranged in a rectangular 4x8 configuration. The multi-borehole configuration also seems to behave well. The model prediction closely matches the analytical prediction of the borehole temperature.

Figure 4.5 *Comparison of borehole temperature predicted by analytical and simulation models for a single borehole configuration.*

71

Figure 4.6 *Difference between of borehole temperature predicted by the analytical and simulation models for a single borehole & 32-borehole.*

Figure 4.7 *Comparison of borehole temperature prediction between analytical and simulation models of a 4x8 rectangular borehole configuration.*

4.4.3.2. Pulsated Extraction/Injection

For this test, heat is injected and extracted alternately every day throughout the year. The amplitude of the heat transfer rate is ± 1500 KW. Figure 4.8 shows the predicted temperature for the analytical and simulation models for the first month of the simulation. The model prediction closely matches the analytical prediction. The temperature difference between the analytical and the simulation model for the pulsated heat extraction/injection is shown in Figure 4.9. The difference drops from $1.8°C$ to less than $0.05°C$ within a few hours of the simulation start. Larger differences in the early hours are expected as discussed in the previous section. The fluctuations in the temperature difference (delta temperature) as shown in Figure 4.9 may be attributed to the sudden change in the load profile and do not indicate model instability. After the initial few hours, the difference is much less than $\pm 0.05°C$. The difference is larger ($\pm 0.5°C$) at the end of every day when the load suddenly changes from extraction to injection or vice versa. The difference rapidly diminishes to less than $\pm 0.04°C$. This behavior closely resembles the constant load results discussed in the previous section, where the difference quickly drops from $4.5°C$ to $0.15°C$.

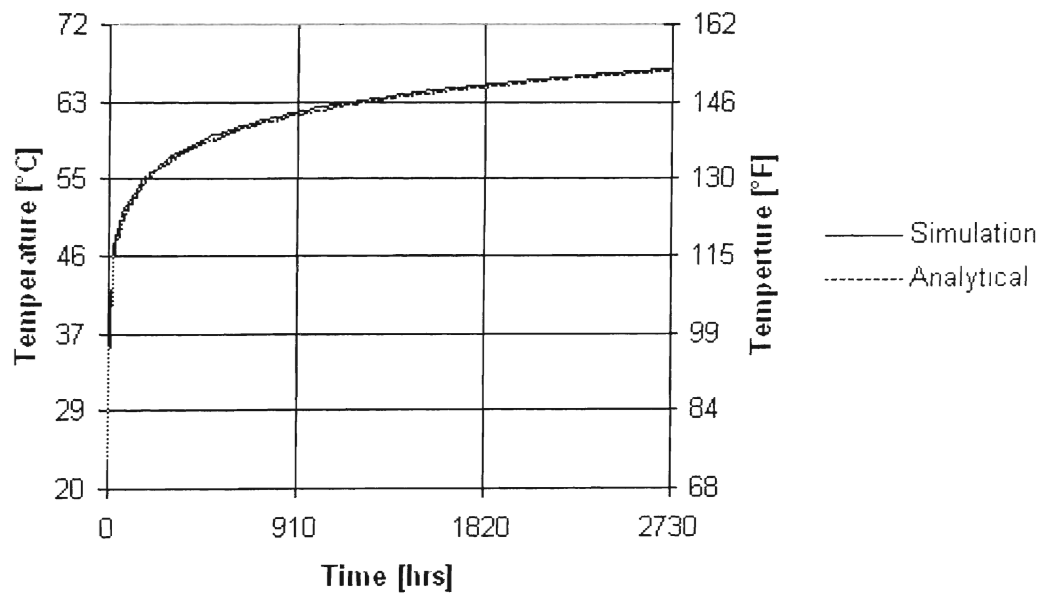**Figure 4.8** *Comparison of borehole temperature predicted by the analytical and simulation model for a single borehole configuration with pulsated a heat extraction of* ± *1500KW.*

Figure 4.9 *Difference between borehole temperature the predicted by the analytical and simulation models for a single borehole configuration with pulsated a heat extraction of* ± *1500KW.*

4.4.3.3. Composite Heat Extraction

This heat extraction pulse consists of a periodic component, a constant load and a pulse at the peak of the periodic loads, as explained in the previous section. Figure 4.10 shows the results obtained for the composite load profile for a single borehole configuration. Again this load profile behaves well with the model generated borehole temperatures closely matching analytical predictions. The difference between the analytical and the simulation temperature prediction is high, (around 2°C) in the beginning and drops to 0.5°C within a few hours of the start of the simulation as expected. The maximum differences occur when the pulse load is applied at hours 287, 1727, 3167 and so on. At these points the difference is 1.7°C. A spike in the error also occurs when these loads are removed at hours 432, 1872, 3312 and so on. This behavior closely resembles the pulsated characteristic as explained in the previous section. The rest of the time the error is within ±0.75°C.
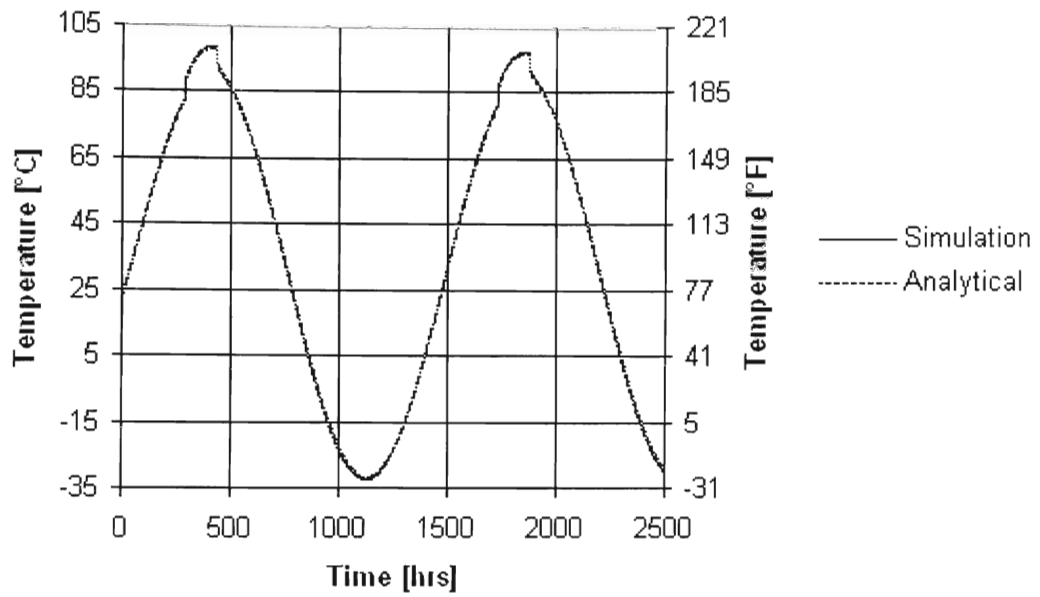
Figure 4.10 *Comparison of borehole temperature predicted by analytical and simulation model for a single borehole configuration with composite load.*
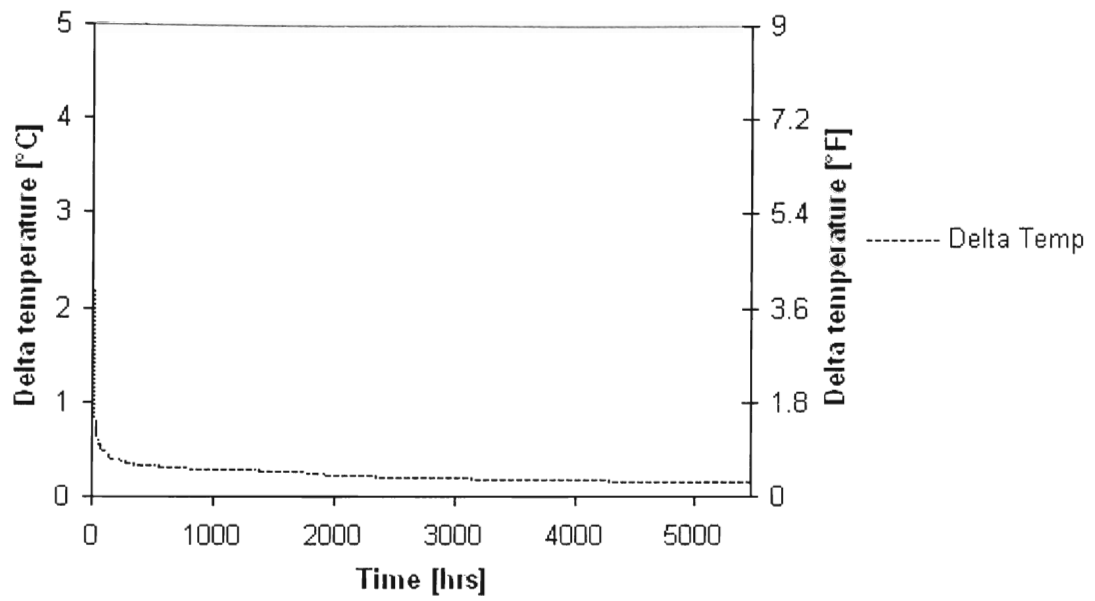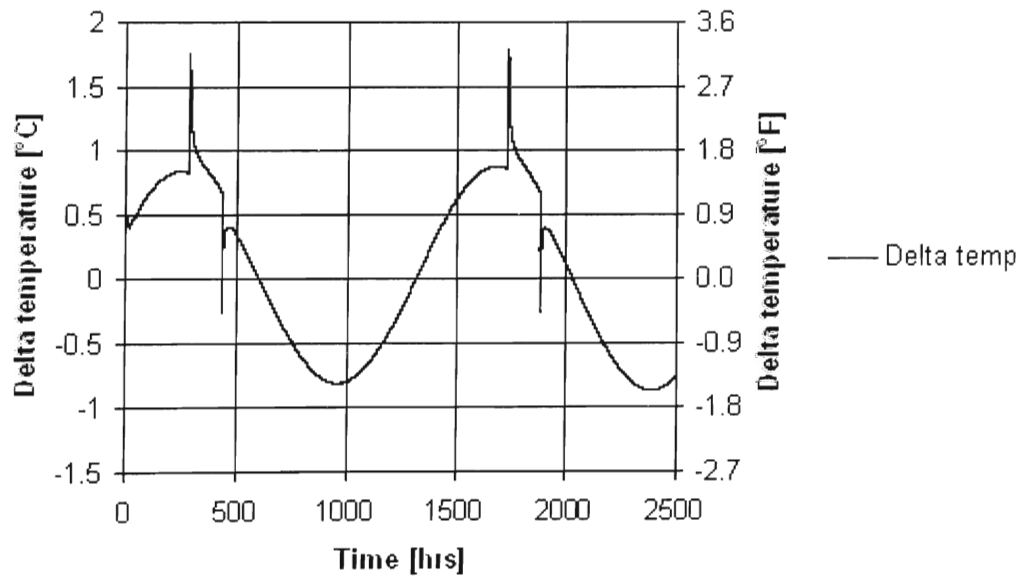

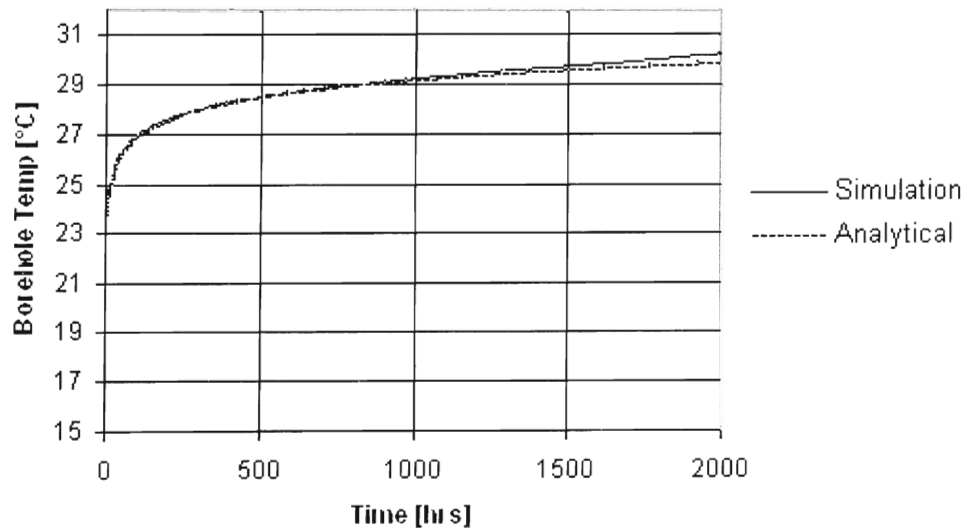**Figure 4.11** *Difference between borehole temperature predicted by the analytical and simulation models for a single borehole configuration with composite heat extraction.*

4.4.3.4. Random Heat Extraction

For this test, the load was applied as a series of random heat extraction pulses. The model's response and the analytical prediction are shown in Figure 4.12. Though the simulation prediction overshoots the analytical prediction at each time-step, the simulation curve follows the same trend as the analytical curve. Overshoot is again due to sudden changes in load. This test was performed to check the model's behavior under extreme conditions. The difference between the analytical and simulation prediction of borehole temperature is given in Figure 4.13. A statistical analysis showed that the standard deviation of the error was 1.67 and the range is 5.4 and -3.2. The median of distribution was 0.0605.
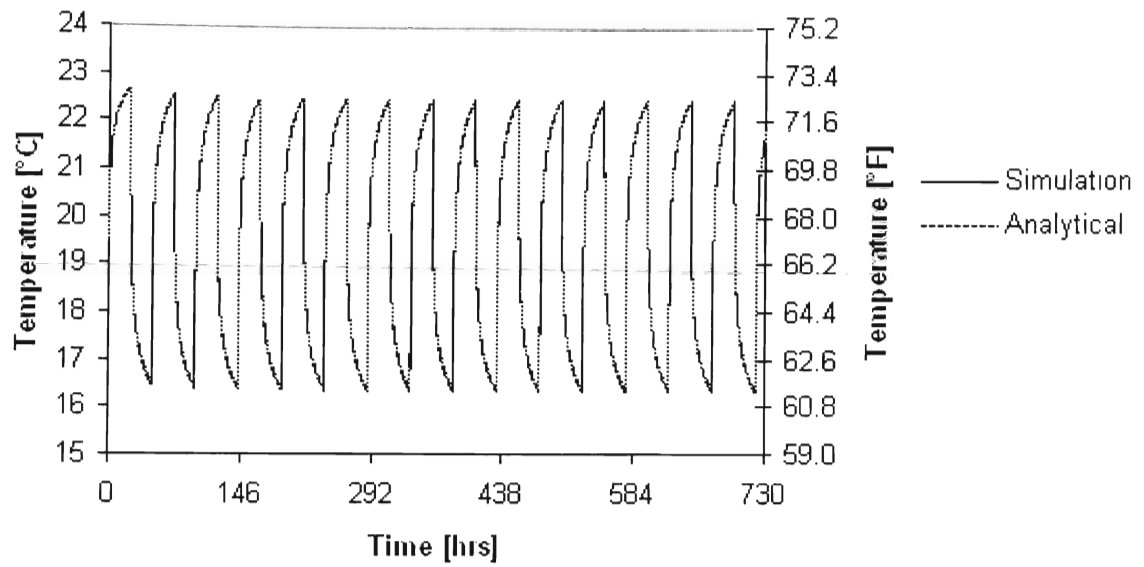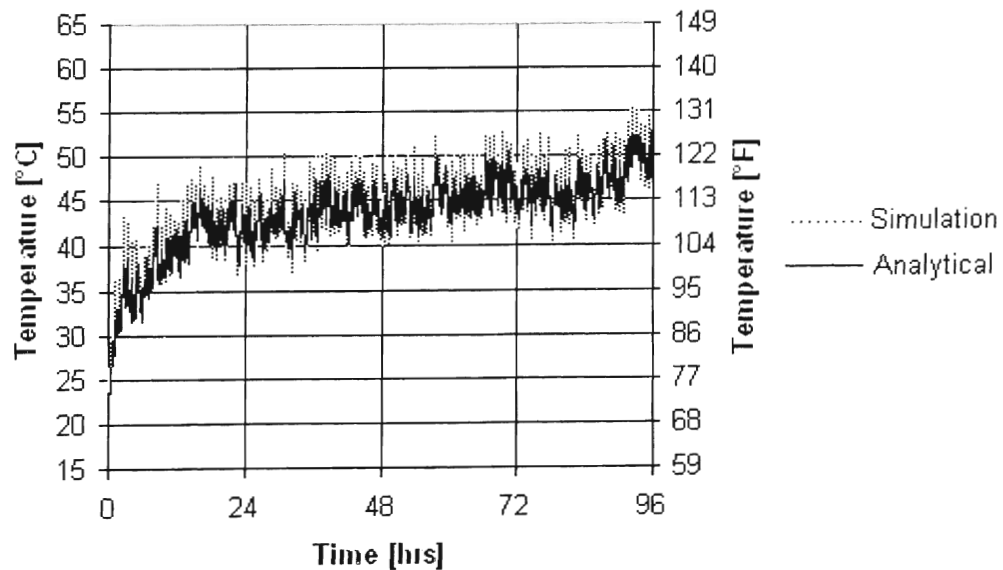

Figure 4.12 *Comparison of borehole temperature predicted between the analytical and simulation model for a single borehole configuration with random extraction pulses.*
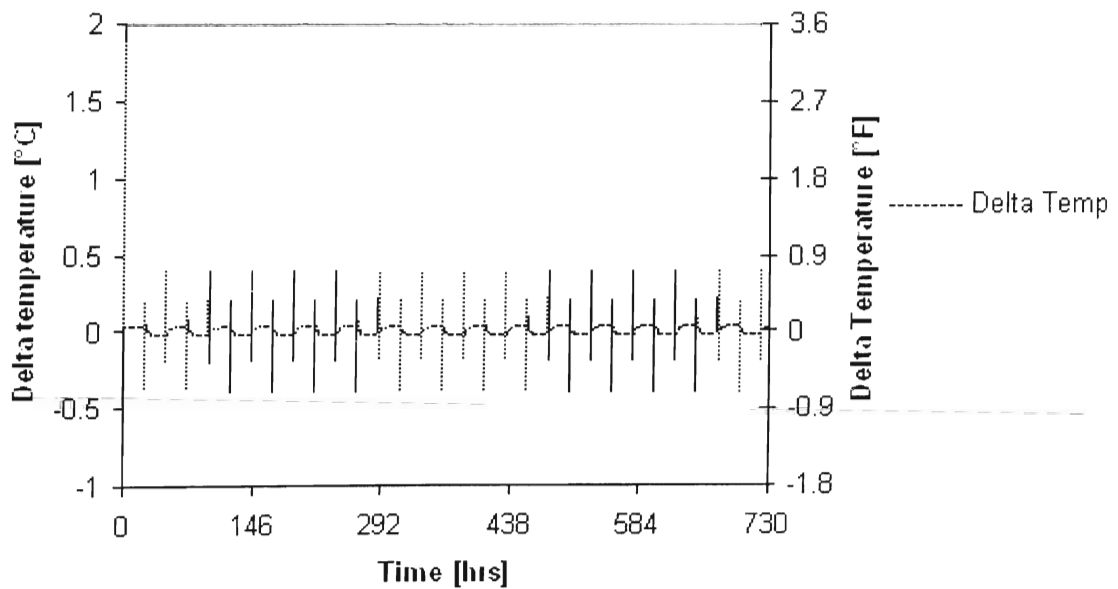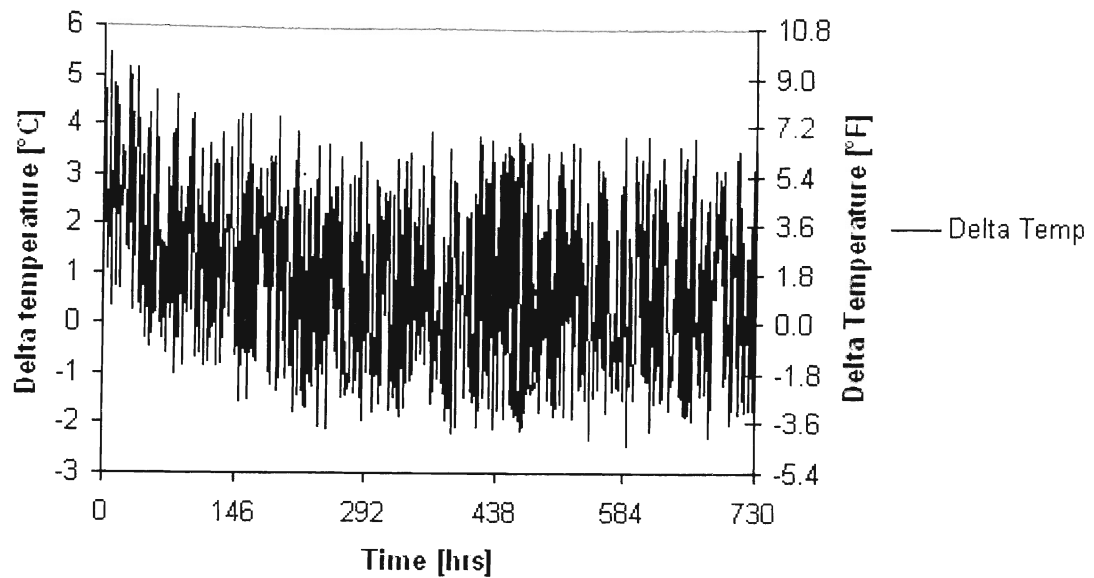
Figure 4.13 *Difference between borehole temperature predicted by the analytical and simulation models for a single borehole configuration with composite heat extraction.*

4.5. Load Aggregation

The short time-step model described above runs in "quadratic time." This means that the time to run an annual simulation of a system with a time-step of one minute would be proportional to 2.76e11 units of time ((8760 hours * 60 minutes/hour)^2). The number of superposition calculations is proportional to the square of the number of time-steps in the simulation. This is because in short time-step models the ground loads are devolved into individual step pulses and are superimposed in time for each time-step using short time-step g-functions. This model though theoretically good, cannot be used in a simulation program/environment without improving the computation time. The g-function model developed for analytical studies uses an accurate but inefficient algorithm to determine the short time temperature variations of the ground loop heat exchanger. To overcome this inefficiency a load aggregation algorithm, similar to the algorithm

78

developed by Yavuzturk and Spitler (1999), was implemented in the model. The results obtained using the aggregation algorithm were compared with the baseline model results and with the analytical results shown the in previous sections.

4.6. Description of the Load Aggregation Scheme

The load aggregation scheme implemented in the EnergyPlus vertical ground loop heat exchanger model utilizes the fact that the contribution of previous time-steps' loads to the calculation of the current effective borehole/fluid temperature diminishes progressively as one moves back in time. Since the importance of the contribution of a load at a given time-step diminishes in subsequent time-steps, these past loads can be lumped together into a sequence of larger blocks without introducing significant error in the calculation. Each block represents an average load for a specific past time period. The borehole temperature variations for each time-step can be found by superposing the past history of load blocks onto more recent ones.

The load aggregation algorithm developed in this section extends the algorithm developed by Yavuzturk and Spitler (1999) to account for sub hourly, variable time-steps. Since this model was extended to account for sub hourly variations, there is an additional burden of sub-hourly ground loop loads. In addition to the user definable "blocks" (usually 730 hours equivalent to a month as suggested by Yavuzturk and Spitler) the aggregation algorithm must also keep track of a sub-hourly load history. Keeping all the sub hourly loads requires a large amount of memory, for example an annual simulation with a one minute time-step would require approximately 2 MB of memory, assuming a

Real (4)* data type which takes 4 bytes of memory. Generally, a few hours of sub hourly load history terms are enough to account for the sub hourly variation in the ground temperature. A block of 10 hrs or even 5hrs of sub hourly history terms would adequately reflect sub hourly variation for each time-step. This reduces the memory requirement by more than 99%.

A load aggregation scheme was developed for EnergyPlus with variable short time-steps down to one minute. A major issue in the development was the calculation of the *g*-functions. As discussed previously in the variable time-step environments, the time-step increments are not uniform. As a result, *g*-functions cannot be pre-calculated. Figure 4.14 shows a schematic of the variable time-step ground loop heat exchanger model. The figure shows the larger monthly block loads, hourly loads and sub hourly loads along with the time of occurrence of those loads. The figure also shows the time at which the *g*-functions are applied to different load blocks.

---

* Real(4) is a basic data type in FORTRAN for real numbers.
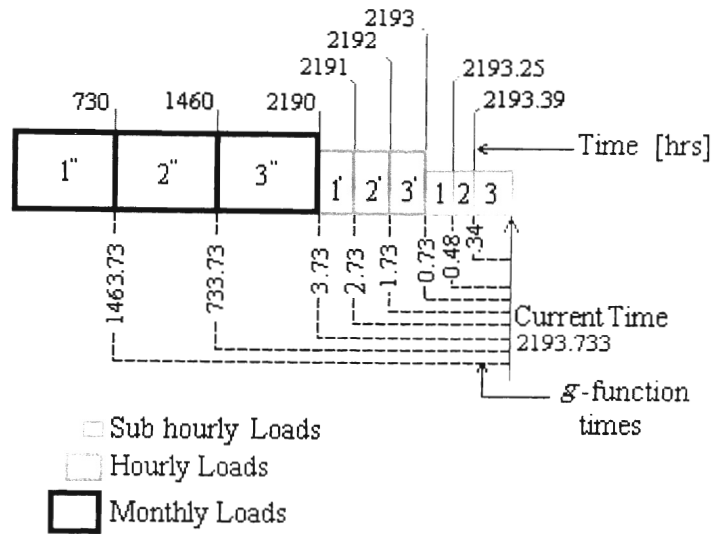
Figure 4.14 *Schematic of variable time-step model g-function calculation.*

To calculate the response of a past load on the borehole temperature we apply the
g-function corresponding to the time elapsed since the load was applied. This is easily
understood from the schematic. For example, to calculate the response of the aggregated
load 1" (at the end of 730 hrs.) for the current time-step (2193.73 hrs) we apply a *g*-
function at 1463.73hrs. The *g*-function for the same block 1" at the previous time-step,
which occurred at 2193.25 hrs, would be at 1463.25 hrs. From the schematic it is also
seen that for the other two aggregated monthly loads 2" and 3", the *g*-functions are
applied at 733.73 hrs and 3.73 hrs for the current time-step and at 733.25 hrs and 3.25 hrs
respectively for the previous time-step. The same scheme applies to hourly and sub-
hourly blocks. Thus to estimate the time at which the past monthly, hourly or sub-hourly
loads occur, we might be tempted to store the simulation times at each time-step for the
entire simulation. But storing load times for the whole length of the simulation for a
multi-year simulation with a variable short time-step would require a large amount of

memory. Since the monthly and hourly loads occur at equal intervals of time 730 hrs and 1hr respectively, the g-functions can be estimated with the current simulation time and the time at which the load block ends, which is a multiple of the monthly duration of the block size. Only the sub-hourly loads require storage of simulation times.

For example from the schematic (Figure 4.14), for the sub hourly load 1, which occurred at the end of 2193.25, a g-function at 0.48 hrs has to be applied; and for the next load 2, a g-function at 0.34 hrs has to be applied. Since the time intervals are not even for the sub hourly loads, we need to store the time-steps at which those loads occurred. These times are required to estimate the time elapsed between the current simulation time and the time at which the sub hourly loads occurred.

Thus, the algorithm keeps track of the sub hourly loads along with their time of occurrence for a user-defined length of time during which the sub hourly calculations are made. The algorithm also estimates the time weighted hourly load from their corresponding sub hourly loads as each hour passes. The sub-hourly loads are time weighted because of the irregular intervals at which the time-step occurs. This is also illustrated in Figure 4.14. The sub hourly loads 1, 2 & 3 occur for varying lengths of time. Load 3 occurs for a longer duration than 1 and 2 in that order. This implies that load 3 has to be given more weight than 1 and 2. So the sub hourly loads for a particular hour are multiplied by the length of their respective period of occurrence and averaged over the hour. This is further explained by Figure 4.15.
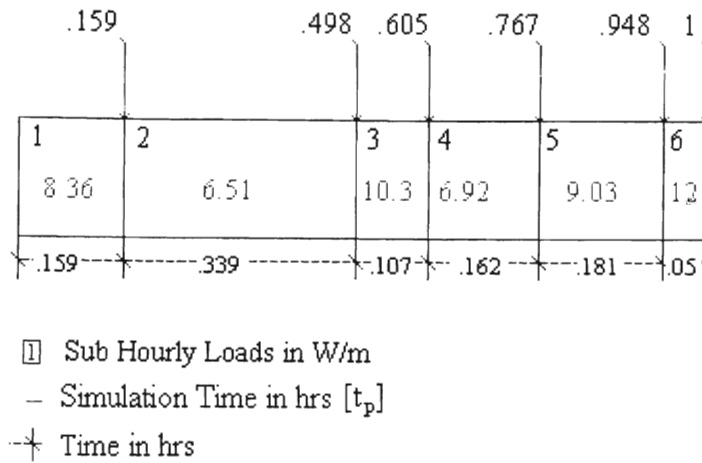
Figure 4.15 *Schematic showing the calculation of hourly load from the sub hourly loads.*

The bottom text in the boxes represents the magnitude of the sub hourly loads in W/m for each time-step. The duration of the occurrence of each time-step is shown below the respective block. The first hourly load is given by the equation 4.15

$$\bar{q}_1 = \begin{bmatrix} (8.36 \times .159) + (6.51 \times .339) + (10.3 \times .107) \\ + (6.92 \times .162) + (9.03 \times .181) + (12 \times .05) \end{bmatrix} = 7.993 W / m \qquad (4.15)$$

Where $\bar{q}_1$ = the first hourly load in W/m

The algorithm keeps track of enough of these past hourly loads to calculate the monthly load. As each month or user defined time passes, hourly loads over the entire month or user defined time "blocks" are averaged and stored in arrays for the respective monthly user defined block of time.

The borehole temperature for any time-step is computed by superposing the monthly (larger time block loads) hourly and sub-hourly loads for each time-step. To understand more clearly consider the schematic in Figure 4.14 where the borehole

temperature at 2193.733 hour is to be estimated. Here the monthly block time is 730 hrs.

We have three monthly aggregated load blocks for 730 hrs, 1460 hrs and 2190 hrs and

hourly loads from 2191st hr to 2193rd hour. For the remaining 0.733 hours a sub hourly

calculation is done. The three monthly aggregated load blocks when superposed using

long time g-functions, yield the borehole temperature at the end of 2190th hour. Then the

hourly loads from 2191st to 2193rd hrs are superposed using the corresponding short time-

step g-functions values yielding the borehole temperature at the end of 2193rd hour. The

sub-hourly variations for the current hour are obtained, by superposing the sub-hourly

loads. From the schematic, we see there are two sub-hourly loads, 1 and 2. Thus the

borehole temperature at the end of 2193.73 is expressed as:

$$T_{2193.73} = T_{ground} + \sum_{m=1}^{3} \left[\frac{\overline{\overline{q}}_m - \overline{\overline{q}}_{m-1}}{2\pi k_{ground}} g\left(\frac{t_{2193.73} - t_{730(m-1)}}{t_s}, \frac{r_b}{H} \right) \right]$$

$$+ \sum_{n=2190}^{2193} \left[\frac{\overline{q}_n - \overline{q}_{n-1}}{2\pi k_{ground}} g\left(\frac{t_{2193.73} - t_{n-1}}{t_s}, \frac{r_b}{H} \right) \right]$$

$$+ \sum_{p=2193}^{2193.73} \left[\frac{q_p - q_{p-1}}{2\pi k_{ground}} g\left(\frac{t_{2193.73} - t_p}{t_s}, \frac{r_b}{H} \right) \right] \quad (4.16)$$

Where

$\overline{\overline{q}}$ = the average monthly loads

$\overline{q}$ = the average hourly loads

q = the sub-hourly loads

m = index for monthly aggregated blocks

n = index for hourly loads

p = array index for sub hourly loads

t = time

t_p = the sub hourly time-steps over the history period. (here the time increment is not always unity)

Superposing the temperature responses of monthly (larger) blocks over the shorter, namely the hourly and sub hourly, introduces some error in the borehole temperature calculation at the beginning of every month. Yavuzturk and Spitler suggest a method to reduce the error in borehole temperature prediction by using a minimum hourly history period during which only the short time-step superposition is carried out. In the EnergyPlus model this idea is extended to sub hourly loads as well. Thus a user specified minimum sub-hourly history period is included along with the minimum hourly history period to model the sub-hourly variations. During this period only sub-hourly and hourly superposition are made. This guarantees that at any given time-step the superposition of temperature responses involves a minimum period of short time responses, which ensures a better estimation of borehole temperature. For example, a minimum hourly history period of 96 hrs and a minimum sub hourly history period of 5 hours would result in only 2 monthly aggregation blocks (1" and 2"). The last monthly aggregation does not occur because neither of the minimum hourly history period of 96 hours or sub-hourly history period of five hrs is met. So an hourly superposition of the

load is carried out for the third month until the minimum sub-hourly history period after which sub hourly superposition is carried out. The equation (4.17) becomes

$$T_{2193.73} = T_{ground} + \sum_{m=1}^{2} \left[\frac{\overline{\overline{q}}_m - \overline{\overline{q}}_{m-1}}{2\pi k_{ground}} g\left(\frac{t_{2193.73} - t_{730(m-1)}}{t_s}, \frac{r_b}{H} \right) \right]$$

$$+ \sum_{n=1460}^{2188} \left[\frac{\overline{q}_n - \overline{q}_{n-1}}{2\pi \kappa_{ground}} g\left(\frac{t_{2193.73} - t_{n-1}}{t_s}, \frac{r_b}{H} \right) \right]$$

$$+ \sum_{p=2188}^{2193.73} \left[\frac{q_p - q_{p-1}}{2\pi \kappa_{ground}} g\left(\frac{t_{2193.73} - t_p}{t_s}, \frac{r_b}{H} \right) \right] \tag{4.17}$$

Yavuzturk and Spitler have done a detailed analysis on the effect of minimum hourly history period. They found that a minimum hourly history period of 192 hrs for an annual simulation would reduce the running time by 90%. They also found that for a 20year simulation, the computation time of the aggregated load scheme is just 1% of the non-aggregated load scheme.

4.7. Summary of Variable Short Time Step Response Factor Model

The load aggregation scheme developed in line with the above example is summarized in eight steps as follows:

Step 1. Define monthly load blocks duration (mb) in hrs (generally 730 hrs) and the minimum hourly history period and minimum sub hourly history period.

Step 2. Read Borehole Geometry Parameters: number of boreholes, borehole length radius thickness of the pipe etc. Read Ground and Fluid thermal properties: Ground conductivity, volumetric specific heat capacity of the ground and heat carrier fluid. Read the short and long time-step g-functions into arrays with their respective non-dimensionalized times.

Step 3. Start Simulation from P=1 to nts. Here "nts" is the number of time-steps that have occurred since the start of simulation. (Note that P is not a count of number of hour elapsed in the simulation)

Step 4. Compute the hourly loads as each hour passes. This is done by averaging the sub hourly loads during the past hour. The monthly loads are calculated by averaging the hourly loads during that month. This is done by summing the hourly loads during that monthly period and dividing the sum by 730 hours NumMonths (the number of months used in aggregation calculations) is set to the number of months of simulation (current number of aggregated load blocks)

Step 5. If the simulation time is less than the minimum sub hourly history period the borehole temperature is estimated with no aggregation. Only sub hourly loads are superposed as given by equation 4.18.

$$T_{nts} = T_{ground} + \sum_{p=1}^{nts} \left[\frac{q_p - q_{p-1}}{2\pi \kappa_{ground}} g\left(\frac{t_{nts} - t_p}{t_s}, \frac{r_b}{H} \right) \right]$$ (4.18)

Step 6. If the simulation time is less than the sum of the minimum hourly and sub hourly history periods, then decomposed hourly aggregated loads are superposed using their corresponding g-function. Then the sub hourly temperature differences are

found by superposing the decomposed sub-hourly loads with their short time-step g-functions. The average borehole temperature is found by superposing the hourly and sub-hourly temperature differences with equation (4.19)

$$T_{nts} = \sum_{n=1}^{nh-sh} \left[\frac{\overline{q}_n - \overline{q}_{n-1}}{2\pi\kappa_{ground}} g\left(\frac{t_{nts} - t_{n-1}}{t_s}, \frac{r_b}{H} \right) \right] + \sum_{p=nts-sh}^{nts} \left[\frac{q_p - q_{p-1}}{2\pi\kappa_{ground}} g\left(\frac{t_{nts} - t_p}{t_s}, \frac{r_b}{H} \right) \right] \qquad (4.19)$$

Step 7. If the simulation time is greater then the sum of a monthly period, sub hourly history and the hourly history period, the monthly load aggregation is performed. If the difference between the simulation time and product of a monthly block period and the current number of monthly blocks is greater than the sum of the minimum hourly history and sub hourly history periods, the average borehole temperature is found by the equation (4.20).

$$T_{nts} = T_{ground} + \sum_{m=1}^{calb} \left[\frac{\overline{\overline{q}}_m - \overline{\overline{q}}_{m-1}}{2\pi\kappa_{ground}} g\left(\frac{t_{nts} - t_{mb[m-1]}}{t_s}, \frac{r_b}{H} \right) \right]$$

$$+ \sum_{n=nh-[calb(mb)+sh]}^{nh-sh} \left[\frac{\overline{q}_n - \overline{q}_{n-1}}{2\pi\kappa_{ground}} g\left(\frac{t_{nts} - t_{n-1}}{t_s}, \frac{r_b}{H} \right) \right]$$

$$+ \sum_{p=nts-sh}^{nts} \left[\frac{q_p - q_{p-1}}{2\pi\kappa_{ground}} g\left(\frac{t_{nts} - t_p}{t_s}, \frac{r_b}{H} \right) \right] \qquad (4.20)$$

Step 8. If the difference between the simulation time and the product of a monthly block period and the current number of monthly blocks is less than the sum of the minimum hourly history and sub hourly history periods, then NumMonths is set to one month less than the actual number of months of simulation completed. The average borehole temperature is calculated by superposing the long and time-step temperature differences using the equation 4.21.

$$T_{nts} = T_{ground} + \sum_{m=1}^{calb-1}\left[\frac{\overline{\overline{q}}_m - \overline{\overline{q}}_{m-1}}{2\pi\kappa_{ground}}g\left(\frac{t_{nts} - t_{mb[m-1]}}{t_s}, \frac{r_b}{H}\right)\right]$$

$$+ \sum_{n=nh-[(calb-1)(mb)+sh]}^{nh-sh}\left[\frac{\overline{q}_n - \overline{q}_{n-1}}{2\pi\kappa_{ground}}g\left(\frac{t_{nts} - t_{n-1}}{t_s}, \frac{r_b}{H}\right)\right]$$

$$+ \sum_{p=nts-sh}^{nts}\left[\frac{q_p - q_{p-1}}{2\pi\kappa_{ground}}g\left(\frac{t_{nts} - t_p}{t_s}, \frac{r_b}{H}\right)\right] \quad (4.21)$$

Figure 4.16 shows the EnergyPlus vertical ground loop heat exchanger computational algorithm. The previously discussed steps in the algorithm are referenced in the pseudo-code.

```
Define Monthly, hourly and sub hourly periods (step 1)
Read parameters, properties and g-functions. (step 2)

Do until p = 1 to number of time-steps (nts) (step 3)
     Compute current hourly and monthly loads. Calculate the number of
     monthly blocks (NumMonths)(step 4)

     If (Current time less than minimum sub hourly history)

          use Equation 4.19 (step 5)

     Else If (Current Time less than sum of minimum hourly and sub
          hourly histories)

          use Equation 4.20 (step 6)

     Else
          If (Difference between current time and duration of the
               total number months is Greater than sum of minimum
               hourly and sub hourly history periods)

               use Equation 4.21 (step 7)

          Else

               use Equation 4.22 (step 8)

          End if
     End if
End do
```

Figure 4.16 *Pseudo code showing the load aggregation algorithm.*

89

4.8. Effect of Load Aggregation

The base model described in Section 4.3 was developed mainly for analytical comparison purpose, and could not be used effectively in the simulation environment because of the amount of time required to predict the borehole temperature. In order to reduce the computation time, a Load aggregation scheme was implemented as described in the previous Section 4.7. The time required to run the base model for an annual simulation with a time-step of 3 minutes was on average 5 hrs and 30 minutes on a Pentium III 500 MHz, running on Win NT4.0 SP6.0 with 128 MB of RAM. A multi-year simulation with the same parameters would take a time quadratically proportional to the time required for an annual simulation, which would be undesirably large. So, the base model cannot be considered for any serious applications. Alternatively, the load aggregation scheme model, which could reduce the computation time by a factor of 90% - 95%, would introduce error in the simulation, depending on the level of aggregation. A study on predicted borehole temperatures for different aggregation schemes was performed, and recommendations are made based on these results.

Tests were carried out on three different load profiles:

1. constant

2. composite load profile with a period of 730 hrs (Figure 4.18 (A))

3. composite load profile with a period of 1095 hrs (Figure 4.18 (B))

The test measured the effect of various sub hourly and hourly history periods on the final borehole temperature. The input parameters used were the same, as given in Table 4-1 with different combinations of sub-hourly and hourly history periods used.

90

Table 4-2 lists the root mean square of the difference between the predicted borehole temperature of the analytical and aggregation model for different combination of hourly and sub-hourly aggregations. Table 4-3 shows the computation time required for an annual simulation for those combinations of hourly and sub hourly history periods shown in Table 4-2. Table 4-2 shows that as the number of history periods increases, the root mean square of the temperature difference between the analytical and the aggregation model decreases. For combinations of hourly and a sub-hourly aggregation of 200 hrs and 240 hrs respectively, the RMS is 0.46 °C, which is comparable to the RMS value of the base model around 0.43°C. However, the base model takes around 5 hrs to run while the model incorporated with the aggregation scheme for a minimum history periods of 200 hrs as sub-hourly and 240 hrs as hourly takes only 12.19 minutes, which is a 96% reduction in run time.

Table 4-2 *Root mean square of the temperature difference between the analytical and simulation models for various hourly and sub-hourly history periods for load profile (A).*

Sub Hourly History Periods	0	25	50	100	200
Hourly history Periods					
0	0.94	0.86	0.80	0.70	0.55
24	0.86	0.80	0.75	0.66	0.52
96	0.71	0.70	0.63	0.56	0.47
192	0.56	0.53	0.50	0.47	0.46
240	0.51	0.49	0.47	0.46	0.45

Table 4-3 *Computation time in minutes for different combination of hourly history periods and sub-hourly history periods for load profile (A).*

Sub Hourly History Periods	0	25	50	100	200
Hourly history Periods					
0	1.265	2.590	3.841	6.405	11.509
24	1.321	2.611	3.905	6.469	11.562
96	1.522	2.812	4.107	6.674	11.774
192	1.792	3.082	4.375	6.943	12.038
240	2.006	3.217	4.510	7.077	12.192

Figure 4.18 shows Table 4-2 as a chart. The first series is curve of minimum sub-hourly period of zero hours for different hourly history periods (for Zero sub-hourly: superposition is done only for the current hour's fraction). As the hourly history period increases from 0 to 240 hrs, the error falls to around 0.51°C (RMS) from 0.97 with a small increment in time from 1.2 minutes to 2 minutes. It is also seen from the chart that for different sub-hourly history periods, the time increases from 2 minutes to around 12 minutes as the sub-hourly history period increases from 0 to 200 hrs. For example, if one goes along the curve for the sub-hourly history of 0 hours the hourly history increases from 0 to 240 hrs with a reduction in RMS from 0.94°C to 0.51°C with time increasing from 1.2 minutes to a mere 2 minutes. On the other hand if we go along the sub-hourly period from 0 hours to 200 hours of hourly history, the error goes down from 0.94°C to 0.55°C with time increasing from 1.2 minutes to 11.5 minutes. This shows that using a large value of sub-hourly history takes longer when compared to using a similar value of hourly history with no noticeable change in error. However, to adequately represent the

sub-hourly variations it is advised to include some sub-hourly calculations say for a period of 25 hrs to 50 hrs.

The RMS error with an hourly history of 192 hrs is less than 0.6°C for all sub-hourly history periods. So in conclusion it is suggested to use an hourly history period of 192 hrs and sub-hourly history period of 25-50 hrs.

It is also interesting to note that the error changes as the load profile changes. A test with a different load profile as showed in Figure 4.18(b) gave better results than the one with the load profile in Figure 4.18(a). Figure 4.19 shows the computation time vs the RMS for the load profile (B). It is evident from that figure that as the number of pulse loads decreases the error decreases. But no change in computation time was seen as expected. This implies that if the load profile is erratic with a large number of pulse loads, it is advisable to use more hourly and sub-hourly history periods. The author also found that for constant load there was no noticeable difference in the root mean square value for different combinations of hourly and sub-hourly history periods.

Figure 4.17 shows load profiles (A) and (B) respectively. Comparing Figures 4.18 and 4.19 which shows the running time vs RMS for the two profiles A and B respectively we can see that RMS is higher for profile A than B, which is because profile A has more step loads per load block on the average. The running time for different sub-hourly and hourly combination is mostly the same as the running time doesn't depend on the profiles of the load. It solely depends on the history periods requested. Figures 4.20 and 4.21 show the error in predicted temperature between the no aggregation and different sub-hourly and hourly configuration for the two load profiles A and B respectively.
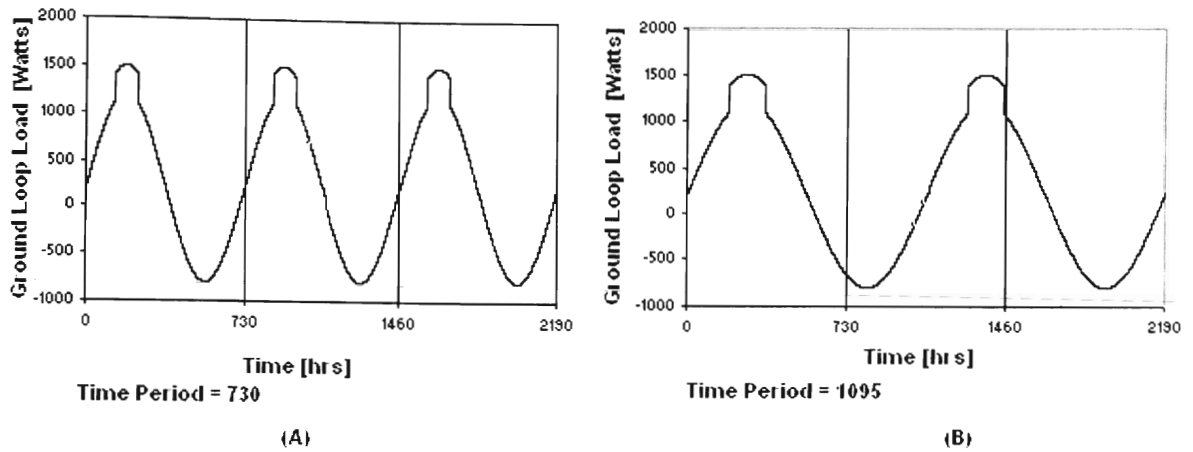
Figure 4.17 *Sinusoidal load with different time periods.*

Figure 4.18 *Comparison of running time vs sum of the square of the errors between the analytical model and different combination of hourly and sub-hourly history periods for load profile (A).*
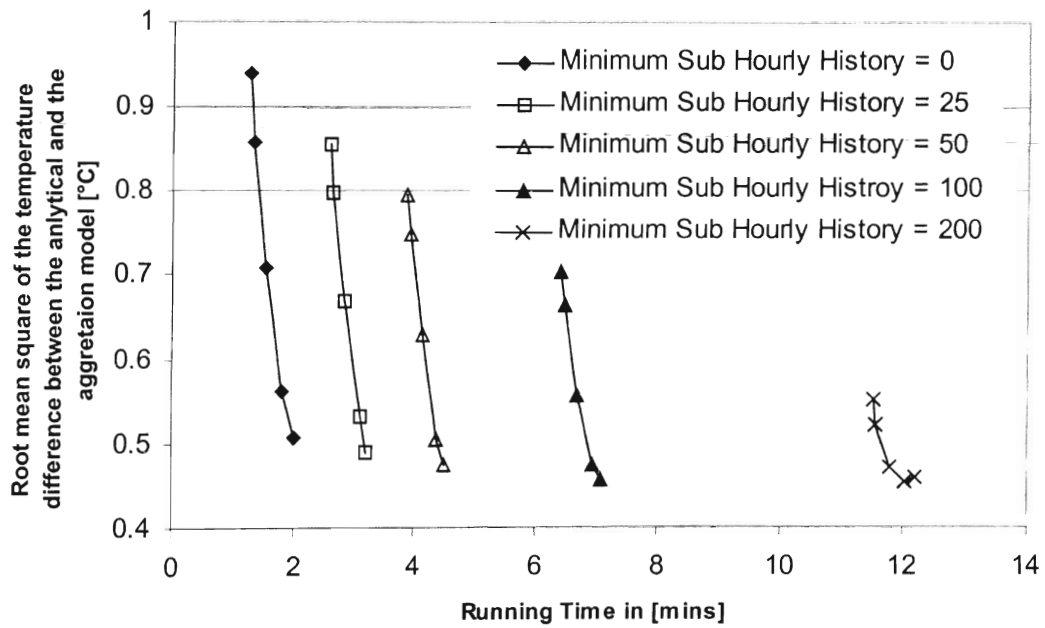
94
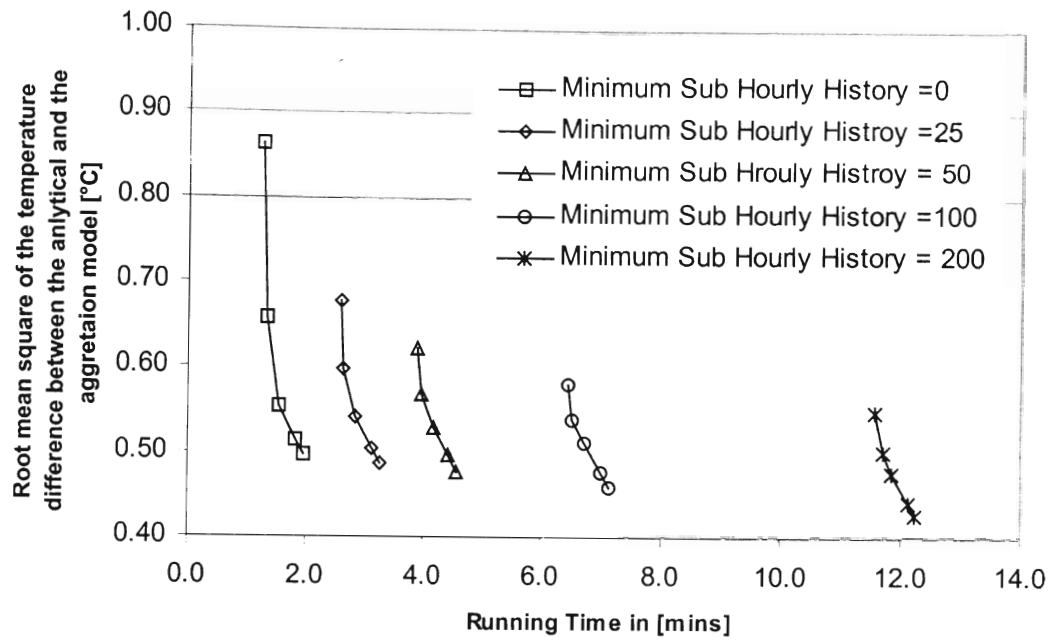
Figure 4.19 *Comparison of running time vs sum of the square of the errors between the analytical model and different combination of hourly and sub-hourly history periods for load profile (B).*
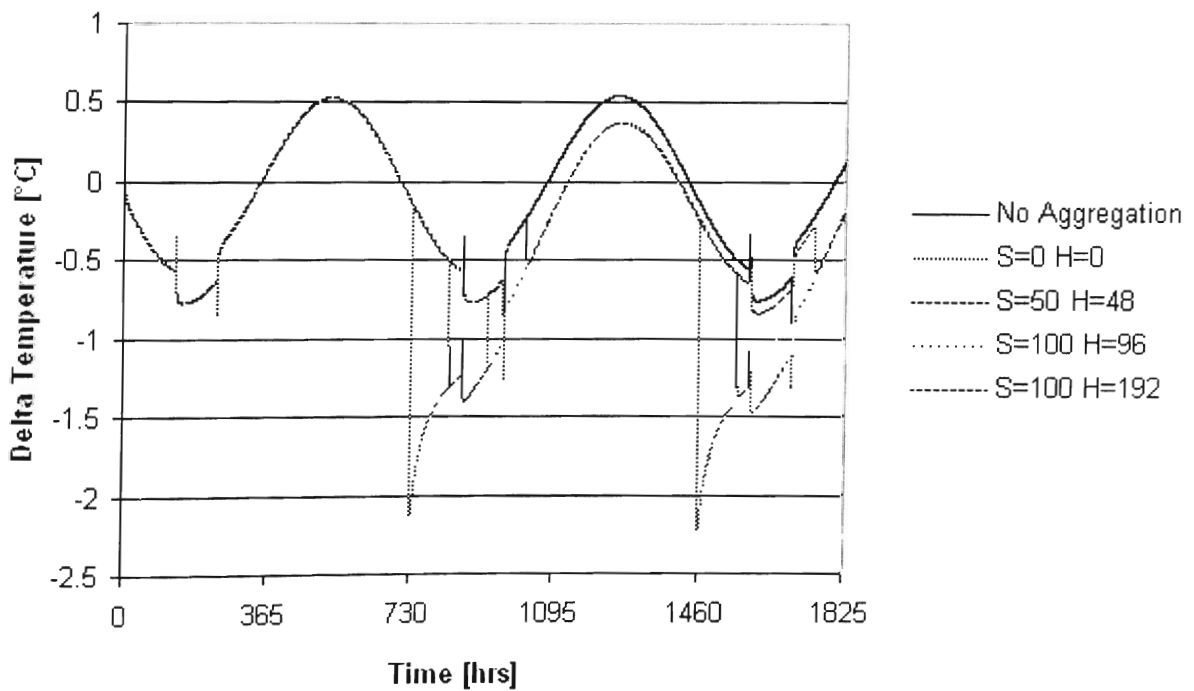
Figure 4.20 *Comparison of borehole temperature prediction for different histories periods for load profile (A).*
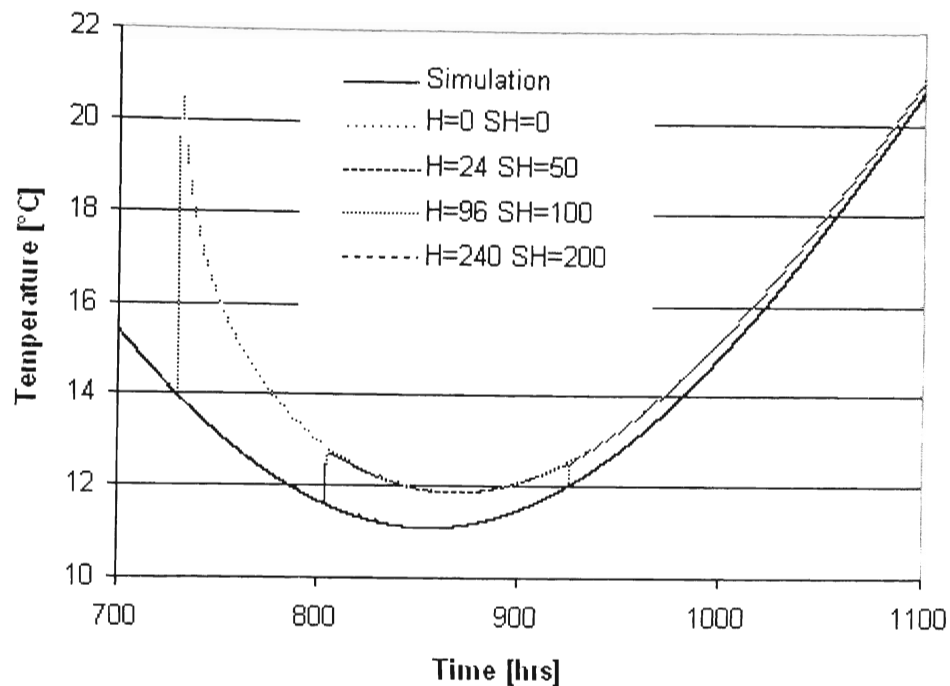
Figure 4.21 *Comparison of borehole temperature prediction for different histories periods for load profile (B).*

4.9. Implementing Vertical Ground Loop Heat Exchanger Model in EnergyPlus

The EnergyPlus implementation of the variable short time-step vertical ground loop heat exchanger model is similar to the Heat Pump Implementation explained in the previous chapter. The guidelines to implement a component in the EnergyPlus environment were strictly followed. The input object specification for the vertical ground loop heat exchanger is defined as shown in Figure 4.22. The keyword "GROUND HEAT EXCHANGER:VERTICAL", identifies the input object for ground loop heat exchangers. The accompanying comment for each field explains the purpose of the field and gives its units.

```
GROUND HEAT EXCHANGER:VERTICAL
  A1,    \field Ground Loop Heat Exchanger Name
  A2,    \field GLHE Inlet Node
  A3,    \field GLHE Outlet Node
  N1,    \field GLHE Max Volumetric Flow Rate [m3/s]
  N2,    \field Number of Boreholes
  N3,    \field Bore Hole Length [m]
  N4,    \field Bore Hole Radius [m]
  N5,    \field K of Ground [W/m-C]
  N6,    \field rhoCp of Ground [J/m3-C]
  N7,    \field rhoCp of Fluid [J/m3-C]
  N8,    \field Temp. of Ground [C]
  N9,    \field GLHE Design volumetric Flow rate [m3/s]
  N10,   \field K of Grout[W/m-C]
  N11,   \field K of Pipe [W/m-C]
  N12,   \field K of Fluid [W/m-C]
  N13,   \field Rho of Fluid [Kg/m3]
  N14,   \field Nu of Fluid [m2/s]
  N15,   \field Pipe Out Diameter [m]
  N16,   \field U-Tube Distance [m]
  N17,   \field Pipe Thickness [m]
  N18,   \field Maximum length of simulation [years]
  N19,   \field Number of data pairs of the G function
  N20,   \field LNTTS1
  N21,   \field GFNC1
  N22, N23,
  N24, N25,
  N26, N27,
  N28, N29,
  N30, N31,
  N32, N33,
  N34, N35,
  N36, N37;
```

Figure 4.22 *The input data definition for the EnergyPlus vertical ground loop heat exchanger model.*

A number of challenges were encountered when implementing the variable short time-step ground loop heat exchanger model in EnergyPlus.

1. Getting current simulation time; there is no variable provided in the EnergyPlus simulation environment, which gives the current simulation time.

2. Storing the sub-hourly, hourly loads and the times at which each time-step occurred.

3. EOSHIFT intrinsic function crashes when the array size exceeds 32000, to circumvent this problem custom shifting routines were written.

4. Multi-year Simulation; EnergyPlus can only run annual simulations. It was extended to run multi-year simulations.

Current simulation time is required by the model to estimate the g-functions for every time-step. It is computed using equation 4.22, which uses EnergyPlus time keeping variables.

$$CurrentSim\ Time = (DayOfSim-1)*24 + HourOfDay-1 +$$
$$(TimeStep-1)*TimeStepZone + SysTimeElapsed \qquad (4.22)$$

Where,

CurrentSimTime = Local variable which holds the current simulation time (Module: "GroundHeatExchangers")

DayOfSim = Counter for number of days in simulation (Module: "DataGlobals")

HourOfDay = Counter for hours in a simulation day (Module: "DataGlobals")

TimeStep = Counter for time-steps (Module: "DataGlobals")

TimeStepZone = Zone time-step in fractional hours (Module: "DataGlobals")

SysTimeElapsed = elapsed system time in zone time-step (Module: DataHVACGlobals")

Storing different past loads for superposition and past times for g-function required a large amount of memory, which was minimized as explained in Section 4.6. The other problem with storing these values was with the intrinsic function "EOSHIFT"

98

which performs an end-off shift on a rank-one array, Compaq Visual Fortran, Language reference, caused a stack overflow for large arrays on a Pentium III, with 128MB RAM running on Windows NT 4.0. To avoid this problem custom shifting routines were written.

The present version of EnergyPlus could only run annual simulations. The vertical ground loop heat exchanger's behavior and its power savings, cost benefits etc. could be studied for only one year of operation. To facilitate geothermal studies the simulation was extended to run multi-year simulations.

In the usual way, an object was created for the multiyear simulation. This over rides the "RunPeriods" input, which is used to define annual simulation or semi annual simulation time periods.

The following block shows the multi-year object definition. It is simple and straightforward. The object's keyword is "MULTIYEAR" and has a single numeric field, which holds the number of years of simulation.

Specifying a "MULTIYEAR" object overrides any RunPeriod definitions. However, users can run design days along with multiyear simulations. The weather data for a multiyear simulation is read from the same annual weather file repeatedly for every year of the simulation.

The framework of the ground loop heat exchanger module, "GROUNDHEATEXCHANGERS", is shown in Figure 4.23. The only public routine "SimGroundHeatExchangers", acts as the interface between the higher-level HVAC manager and the condenser loop manager, "CondLoopSupplySideManager". This
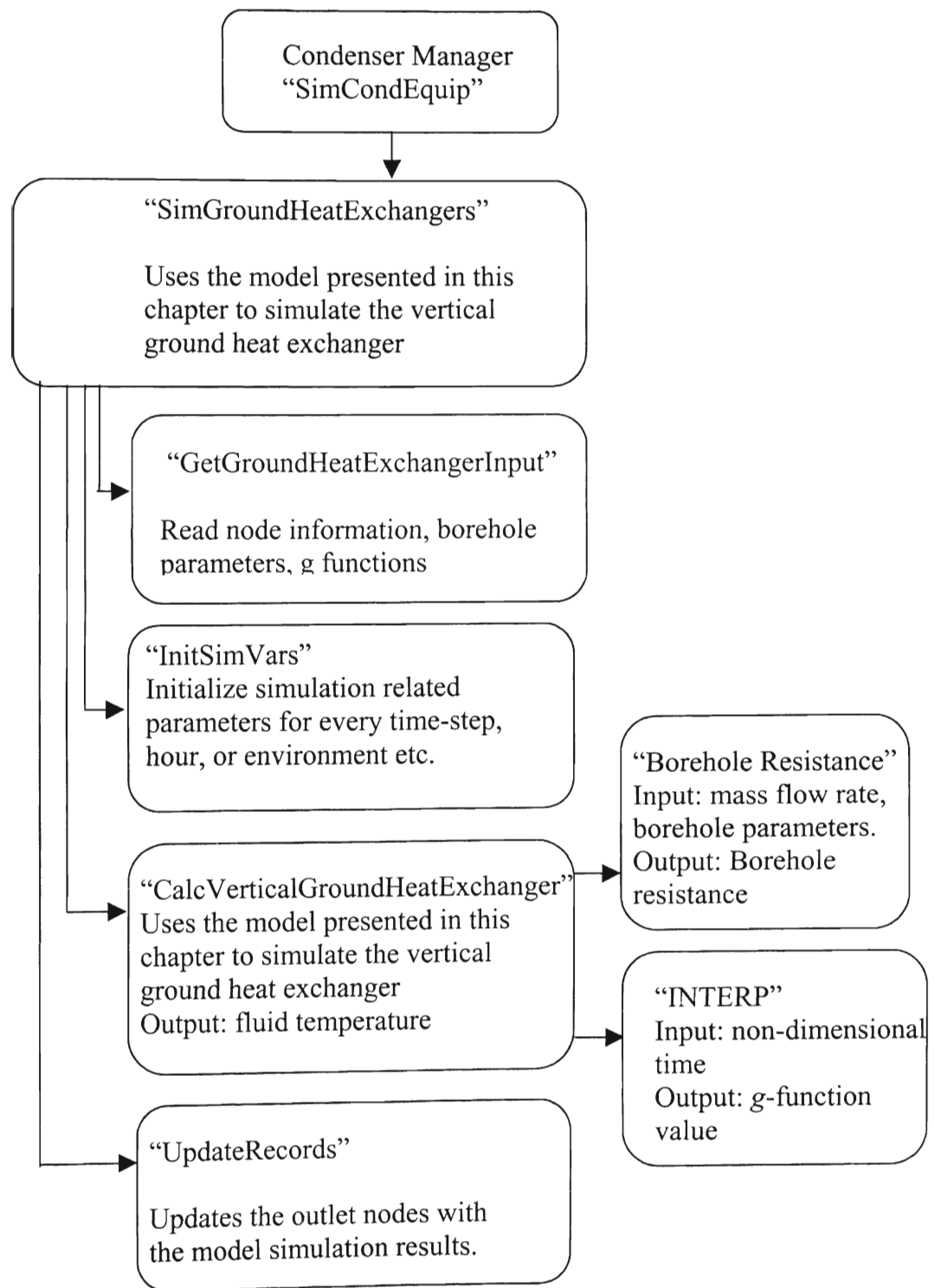
Figure 4.23 *The framework of the EnergyPlus model*

module manages the condenser side equipment simulation, by making systematic calls to the equipment modules based on availability and demands.

The public routine "SimGroundHeatExchangers", calls the private routine which simulates the vertical ground loop heat exchanger, as shown in Figure 4.22. It makes a one time call to the input routine "GetGroundHeatExchangerInput", which uses the input processor as explained in Section 3.4 in Chapter 3, to read the input, allocates space for the module arrays based input sizes and loads the local simulation variables with borehole properties, g-functions with their non-dimensional times and the inlet and outlet nodes of the ground loop heat exchanger.

"InitSimVars", an initialization routine is called for every time-step. "CurrentSimTime" is also updated every time-step. At the beginning of each environment, the various history arrays (like past monthly loads, hourly loads, sub-hourly loads etc.) are reset. The initialization routine also reads the inlet condition and updates the local simulation variable for every time-step.

Once the initialization is done, the model is simulated based on the current input information by calling the "CalcVerticalGroundHeatExchanger". This routine uses the model developed in Section 4.3 with the load aggregation scheme explained in Section 4.5. The simulation results are updated in a separate routine "UpdateRecords" which loads the outlets node with the current state of the node variables, obtained from the model simulation.

Several case studies were performed to demonstrate the performance of the EnergyPlus ground loop heat exchanger. These case studies are presented in Chapter 5.

Chapter 5. Case Studies

5.1. Introduction

The ground source heat pump and the ground loop heat exchanger models that were implemented in EnergyPlus as described in previous chapters were verified by analyzing their performance in the simulation environment. The ground loop exchanger analysis focused on the borehole field temperature over a long period of time. The heat pump performance was also analyzed over a long period, in order to see the effect of long-term changes in ground temperature on heat pump performance. The case studies were carried on an office building. Some architectural data from a real office building was used to model the zones. The plant was modeled using one of the air handling systems available in EnergyPlus, a single zone draw thru system. Simulations were run for three different ground loop heat exchanger configurations and two different climates: Anchorage, Alaska, and Tulsa, Oklahoma. The locations represent a heating dominated climate and a cooling dominated climate respectively. In each case the load profiles were unbalanced resulting in long term ground temperature changes.

5.2. Example Building and Plant Description

The example building shown in Figure 5.1 is similar to the office building used in a previous study by Yavuzturk and Spitler (2000). The building has a total area of 1,320m² (approx) and was modeled as eight thermal zones. The zones were served by a single zone draw through system. This building model with this air handling system was the basis for all the case studies. The building model , as shown in Figure 5.1, was useful

for the purpose of obtaining realistic load profiles. The plant supply side was served by a chilled water loop and a hot water loop. Single condenser loop served both the chilled water and hot water loops. A summary of the modeling assumptions are given in the following list.

1. The building is modeled as eight thermal zones.

2. The air handling system is modeled as a single zone draw through system.

3. The office occupancy is assumed to be one person per 9.3 m^2 with a total heat gain of 132 Watts/Person of which 70% is radiant heat gain.

4. The lighting loads are assumed as 10.8 W/m^2. The equipment plug load is 11.8 W/m^2 used as suggested in Yavuzturk and Spitler (2000)

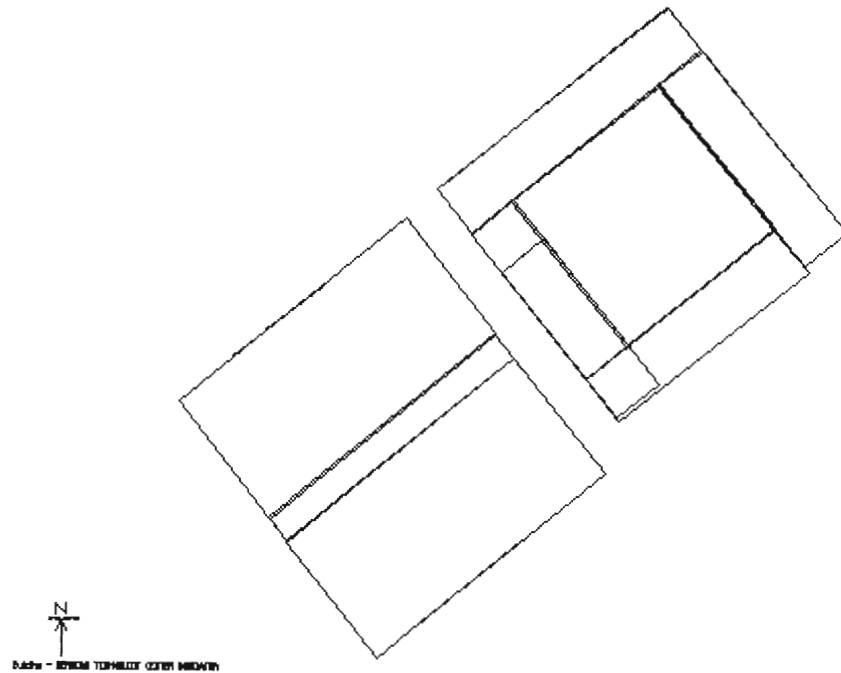5. The zone set points are specified at a constant 24°C.

Figure 5.1 *Plan view of the example building used for case study.*

The plant is modeled in EnergyPlus as follows.

1. The cooling coil is served by a chilled water loop that has a ground source heat pump in cooling mode and outside cooling sources. The loop has a constant speed pump that operates continuously. The loop set point temperature is set at 6.68°C. The Ground source heat pump in cooling mode is scheduled to work only during summer months.

2. The Heating coil and the reheat coils are served by hot water loop, which has a ground source heat pump in heating mode and an outside heating source. The ground source heat pump in heating mode is available for operation in winter. The hot water loop set point is set at 55°C. The loop is operated by a constant flow pump with continuous pump operation.
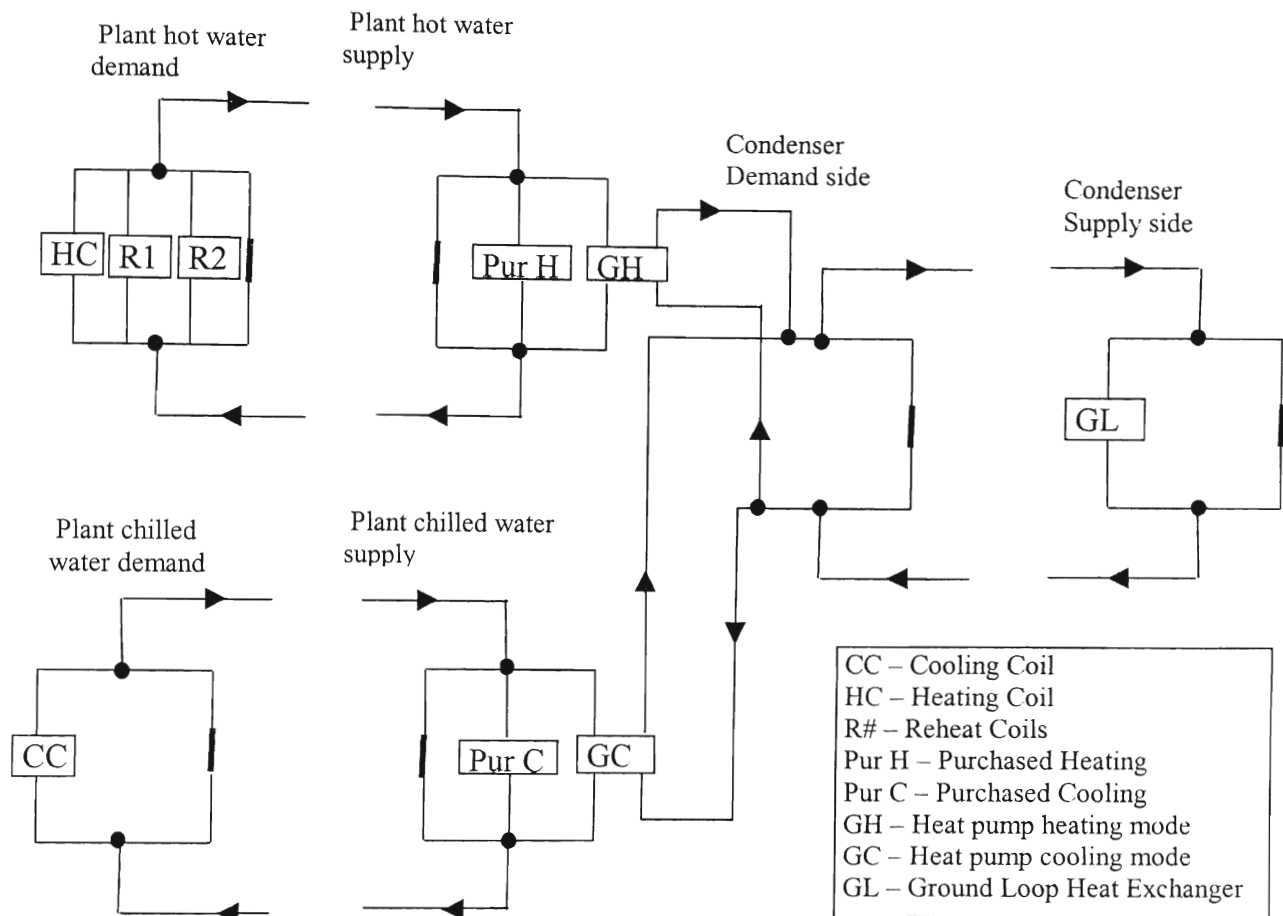
Figure 5.2 *Plant loop showing ground source heat pump and ground loop heat exchanger.*

3. Both chilled and hot water loops are served by a single condenser loop as shown in Figure 5.2. Refer to Chapter 2.1 for details on plant loop simulations. This has either one or two ground loop heat exchangers.

4. The constant speed circulation pumps in all the different loops are operated continuously. The nominal flow rate of each pump is set at 2.76 Kg/s, which is the nominal flow rate of the heat pumps used in simulation. Heat pumps run with design flow rates on both the load and source sides.

5. The heat pump was set to run on a cycle time of 10 minutes.

5.3. Building load Profiles

In order to see the effect of long-term changes in the borehole field temperature, two different climates were used in the simulations. One was a severely cold region, which resulted in a heating load dominated simulation. The other was a warmer climate that required more cooling than heating. The weather information was obtained from Typical Meteorological Year data files in Energy Plus weather format. Figure 5.3 shows the hourly zone cooling and heating loads for the example building, when simulated with Anchorage, Alaska, weather data. Heating loads are shown as positive loads and cooling as negative loads. It can be seen from Figure 5.3 that the building is heating dominated with a peak-heating load of around 80 KW and a peak- cooling load of around 25 KW.
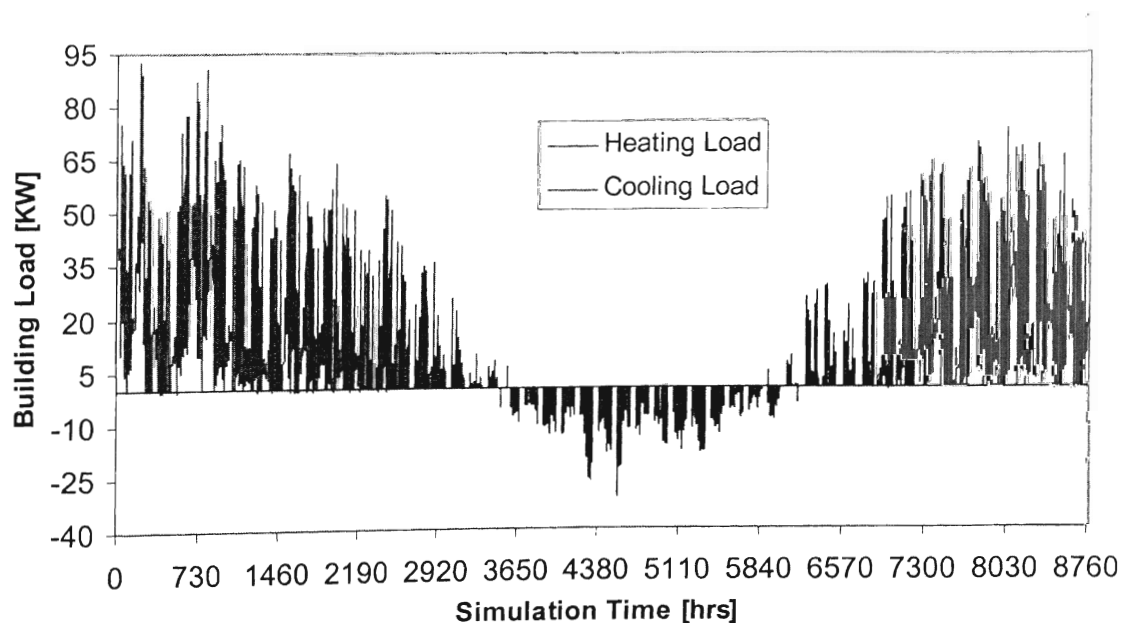

Figure 5.3 *Annual hourly building loads for the example building in Anchorage, Alaska.*

106

Figure 5.4 shows the annual hourly heating and cooling loads for the same building, when simulated in Tulsa, Oklahoma. The building now becomes cooling dominated, with a peak-cooling load of 75 KW and peak-heating load of 65 KW.
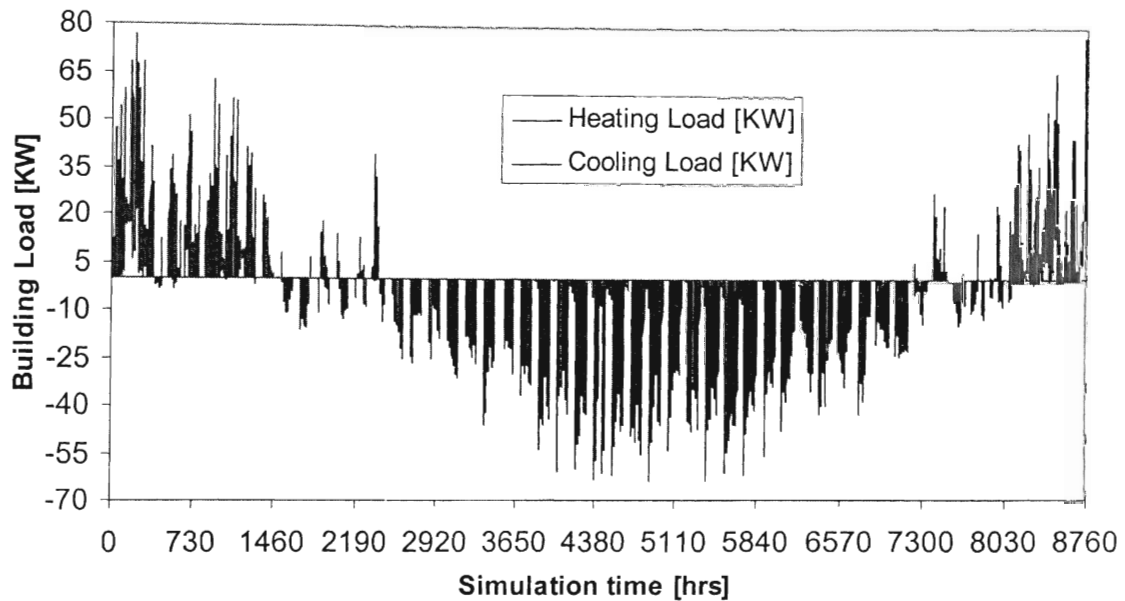
Figure 5.4 *Annual hourly building loads for the example building in Tulsa, Oklahoma.*

5.4. The Heat pump Selection

Model parameters were obtained for a commercially available heat pump (Florida Heat Pumps WP Series) with a nominal capacity of 45 KW. The heat pump is modeled as two heat pumps, one for cooling and another for heating which serves the chilled and hot water loops respectively. The nominal flow rate of the heat pump were 2.76 Kg/s on both load and source sides. The heat pumps are available throughout the year. However, to avoid operating the heat pump simultaneously in heating and cooling mode, a schedule was implemented. This schedule makes sure that only one of the modes is available at any given time. The cooling mode is made available only in summer and the heating

mode available only in winter. The heating requirements in summer and vice versa are handled by the outside energy sources. The heat pump parameters are calculated using the parameter estimation model of the heat pump by Jin and Spitler (2002). The heat pump parameters differ for cooling and heating because the two models (heating and cooling) use different sets of catalog data. The parameters values for the heat pump used in the case study is given in Table 5-1.

Table 5-1 *Heat pump parameters.*

Simulation Parameter	Cooling parameters	Heating parameters
Piston Displacement [m^3/s]	.012544	.01229
Clearance Factor	.05469	.05347
UA Load Side [W/K]	7760	8290
UA Source Side [W/K]	4000	4200
WLOSS [Watts]	2800	1460
ETA	.69	0.55
Pressure Drop [Pascal]	92200	93660
Super Heat [°C]	4.89	4.80

5.5. Ground Loop Configuration

Using the *g*-functions as input requires that the ground loop heat exchanger be sized prior to the simulation. Since this study doesn't concentrate on the economic analysis of the system no attempt was made to select an optimal borehole configuration. However, under sizing or over sizing the boreholes may have a detrimental effect on the performance on the heat pump and thereby defeat the economic feasibility of the ground source heat pumps as a practical alternative to conventional systems. This study focuses on the thermal aspects of the model: the borehole field temperature behavior and its impact on heat pump performance.

The parameter values used for the ground loop heat exchanger model are given in Table 5-2. These parameters were obtained from a previous study by Yavuzturk and Spitler (2000). A constant $T_{farfield}$ temperature (undisturbed mean ground temperature) of 2.6°C was chosen for Anchorage. For Tulsa, which is at a much lower latitude (35°N), a temperature of 17.2°C was selected.

A simulation period of 20 years was used in order to study the long-term thermal effect of the borehole field. Generally, temperatures in a well-sized borehole field will not change much during this period. In a cooling dominated region, a high temperature at the end of the first-year of simulation reflects an undersized borehole configuration. A large drop in temperature at the borehole field reflects the same for heating configuration. This large temperature change would have a detrimental effect on heat pump performance in succeeding years due high source side temperatures. The study was carried out by varying the size of the borehole field. In addition, a two-borehole field configuration was studied to check the model's capability to handle multiple borehole fields in a single simulation.

Table 5-2 *Borehole and ground parameters.*

Parameter	Value
Cp working fluid [J/Kg/k]	4182
K fluid [W/m-K]	0.6026
Rho Fluid Kg/m3	998.2
K ground [W/m-K]	2.08
K Grout [W/m-K]	1.47
K Pipe [W/m-K]	0.3913
Radius of bore holes [m]	0.0889
Pipe OD [m]	0.0267
U tube dist [m]	0.0254
Pipe Wall thickness [m]	0.0024

Case 1: 16 boreholes in 4x4 square configuration - This is the base case. The 16 boreholes are arranged in a square fashion. The length (H) of the boreholes is 73.2 m, which was adapted from a previous study by Yavuzturk and Spitler (2000). The spacing (B) between the boreholes is 3.66m for a B/H ratio of 0.05. The flow rate was set at 2.76 Kg/s, which is the nominal source side flow rate of the heat pumps. All other parameters remain the same.

Case 2: 32 boreholes in 8x4 rectangular configuration - Here the number of borehole is doubled keeping the other parameters the same. A new set of *g*-functions is required for this new configuration.

110

Case 3: 120 boreholes in 12x10 rectangular configuration - This case tests a large borehole field, which has the same parameter values of the base case for individual boreholes. However, a new set of g-functions is obtained for this configuration.

Case 4: Two borehole fields in parallel - This configuration has two isolated boreholes in parallel with the same configuration as in the base case. However, no thermal interaction between the two fields is accounted for (They are assumed to be thermally insulated fields.). The mass flow rate is split between the two borehole fields, with 1.38 Kg/s flowing to each borefield. Figure 5.5 shows how the parallel borehole fields are connected to the supply side of the condenser loop. The objective of this case was to check the model's ability to handle multiple borehole fields in the simulation.
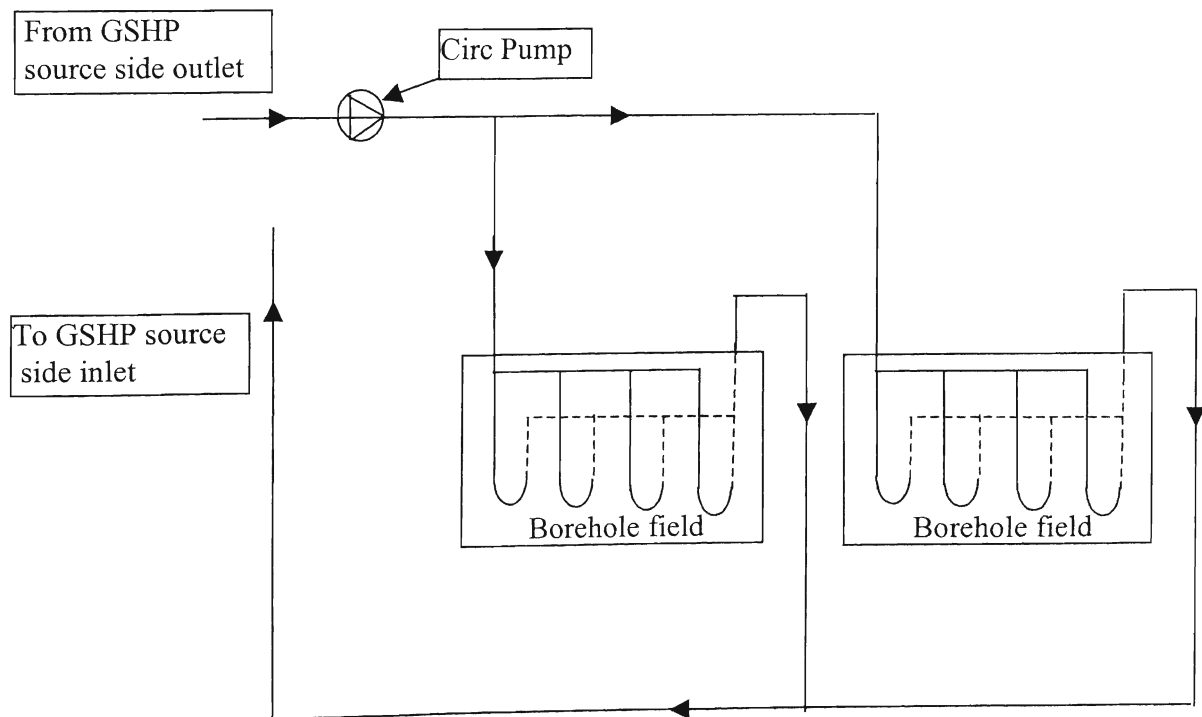

Figure 5.5 *Condenser Loop diagram showing two borehole fields in parallel.*

5.6. Results

5.6.1. Tulsa, Oklahoma

Case 1: 16 borehole in 4x4 square configuration

Figure 5.6 shows the daily average borehole wall temperature over the twenty-year duration of the simulation with the example building in Tulsa. It can be seen from the graph that the average borehole all temperature increases. This is due to the energy storage in the later years caused by unbalanced heat injection into ground. The rise in the borehole temperature for the second, tenth and the twentieth year of simulation is given in Table 5-3. It can be seen from Table 5-3 that the temperature of the borehole wall at the end of first year increases by 3.1°C and reaches a final temperature of 25.9°C at the end of 20 years. This is an increase of 8.7°C from the start of the simulation when the temperature was at the undisturbed mean ground temperature. The sharp increase in the average borehole wall temperature at the end of first year suggests that the ground loop is under sized. Higher borehole temperatures result in higher entering water temperatures on the source side of the Heat pump, which affects the cooling performance of the heat pump. This effect can be seen in Table 5-4 where the annual cooling energy consumption increases 10% from 34.3 MWh for the first year to 37.5 MWh for the 20th year. This shows that the cooling performance degrades over time. The rise in the borehole temperature has a small positive effect on the heating performance. This is seen from Figure 5.7, where the annual cooling energy consumption increases over the years and the annual cooling energy consumption slightly decreases. Though the cooling power increases over the 20 year period, there are some years that show a slight decrease in

112

power from the previous year. This result is not expected for a twenty year simulation where inputs for every year (including the weather data) are the same. The possible cause of this problem is presented in Section 5.7, and a stand alone simulation was performed to demonstrate that the ground source heat pump and ground loop heat exchanger models were performing correctly.

Figure 5.8 shows that the zone daily average temperature is maintained at the required set point for most of the year, though it rises above the set point for roughly seventeen days of the year, when the zone load is very small or none. Moreover, the daily average temperature of the zone drops below the set point for a couple of days in a year during high demand days. This shows that the heat pump is not able to meet the demand on those days.

Table 5-3 *Average borehole wall temperature with the building simulated at Tulsa, Oklahoma.*

Tulsa	Case 1: 16 boreholes			Case 2: 32 boreholes			Case 3: 120 boreholes			Case 4: 2-16 boreholes in parallel		
	2nd Year	10th Year	20th Year	2nd Year	10th Year	20th Year	2nd Year	10th Year	20th Year	2nd Year	10th Year	20th Year
Borehole temperature °C	20.31	24.25	25.9	19.8	23.1	24.7	18.3	20.2	21.3	19.3	24.3	25.4
ΔT from $T_{farfield}$	3.1	7.1	8.7	2.66	5.9	7.5	2.1	3.0	4.1	2.1	7.1	8.2

Table 5-4 *The energy consumption of the example building simulated at Tulsa, Oklahoma for different cases.*

| TULSA	Case 1: 16 boreholes			Case 2: 32 boreholes			Case 3: 120 boreholes			Case 4: 2-16 boreholes in parallel		
	1st Year	20th Year	20-Year Ave	1st Year	20th Year	20-Year Ave	1st Year	20th Year	20-Year Ave	1st Year	20th Year	20-Year Ave
Energy Consumption Cooling mode (MWh)	34.3	38.8	37.5	31.3	35.5	34.2	29.2	31.4	30.7	33.7	37.0	35.8
Energy Consumption Heating mode (MWh)	23.5	21.6	21.9	22.9	21.6	21.8	22.9	22.1	22.2	23.2	22.0	22.3
Circ Pump Energy Consumption (MWh)	.181	.181	.181	.181	.181	.181	.181	.181	.181	.181	.181	.181
Total Energy Consumption (MWh)	57.9	60.6	59.6	54.4	57.2	56.2	52.2	53.7	53.0	57.0	59.2	58.2
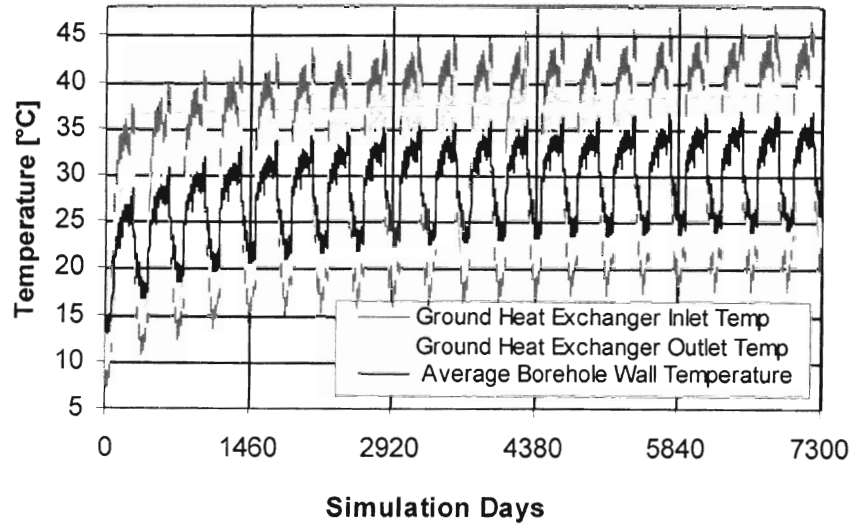
Figure 5.6 *Case1: Borehole temperatures for the example building at Tulsa, Oklahoma for the base case.*
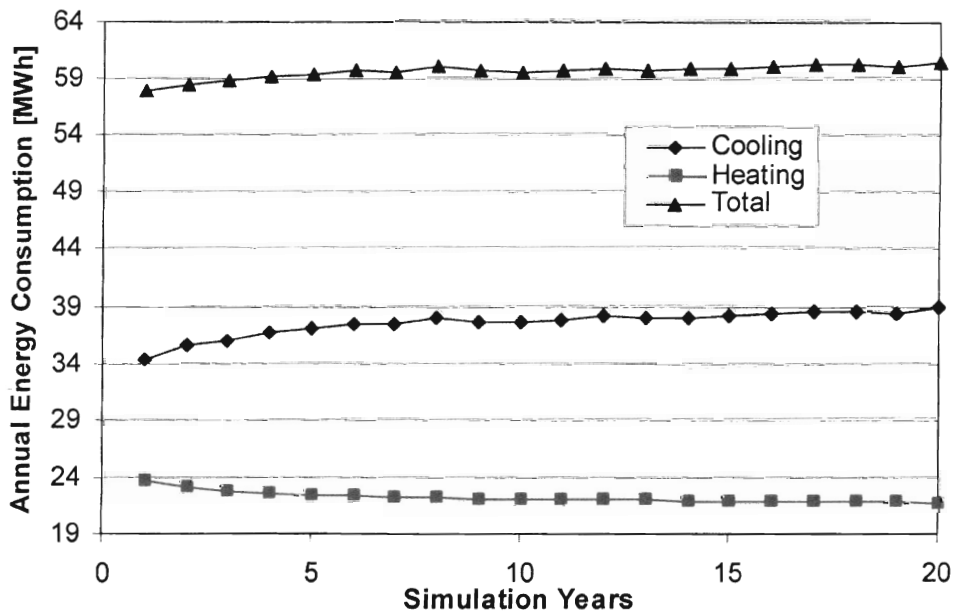

Figure 5.7 *Case1: Annual Energy consumption of the heat pump in cooling and heating mode for 20 years of simulation at Tulsa, Oklahoma.*

Figure 5.6 *Case1: Borehole temperatures for the example building at Tulsa, Oklahoma for the base case.*

Figure 5.7 *Case1: Annual Energy consumption of the heat pump in cooling and heating mode for 20 years of simulation at Tulsa, Oklahoma.*
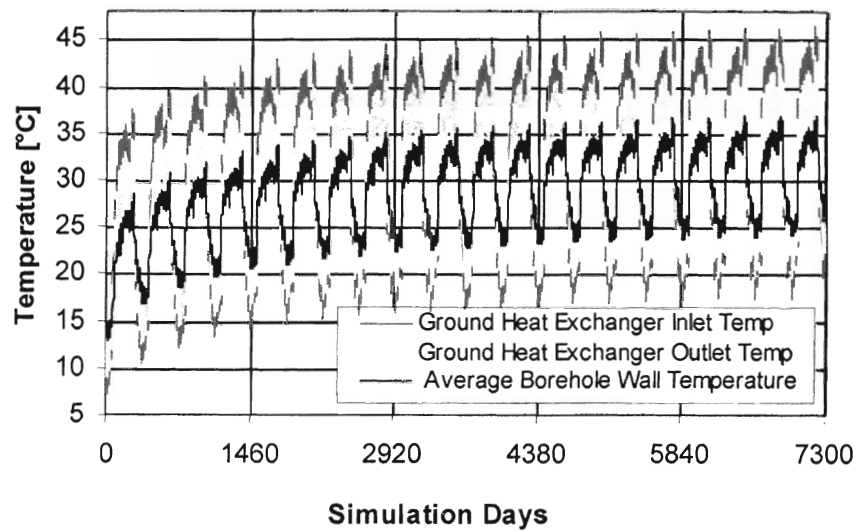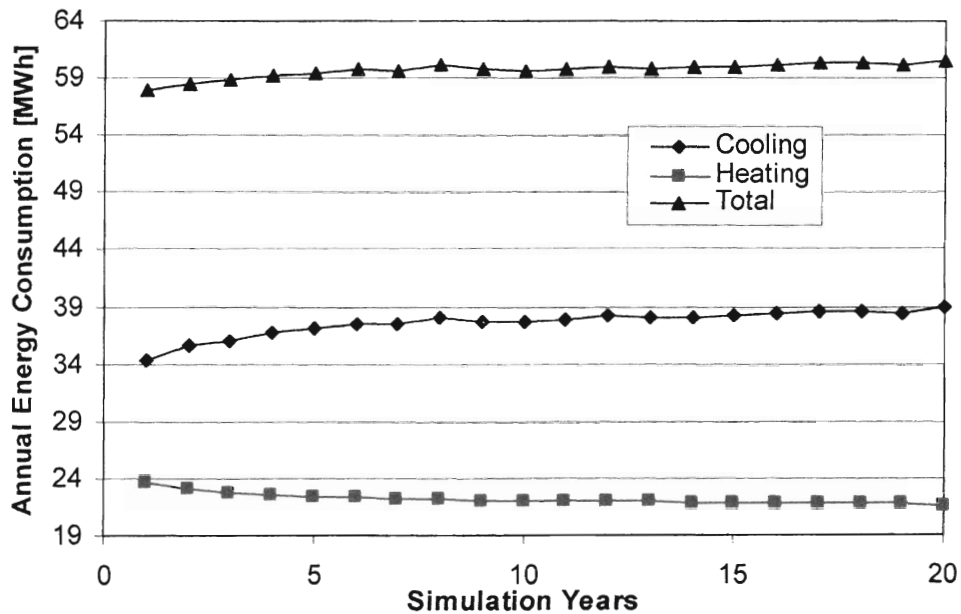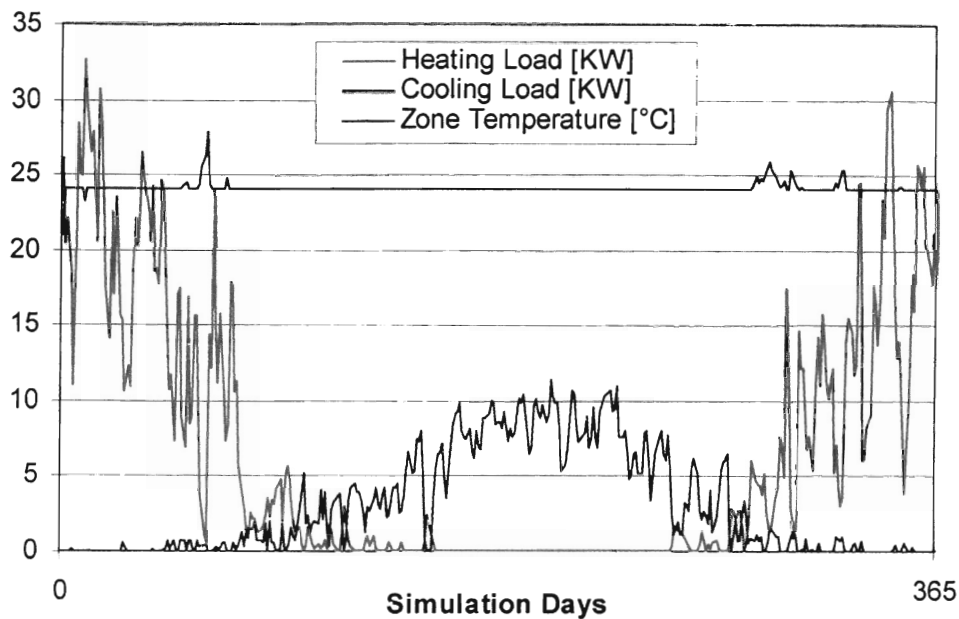
Figure 5.8 *Case1: The zone space temperature and the daily average building loads for a year when building simulated at Tulsa, Oklahoma.*

Case 2: 32 boreholes in 4x8 rectangular configuration

The Figures 5.9, 5.10 and 5.11 show the results from 32-borehole configuration. A significant improvement in the heat pump performance can be seen from Table 5-4, where the 20 year average annual energy consumption decreases by 5.7% from 59.6 MWh for case 1 to 56.2 MWh for case 2. From Table 5-3 it is seen that the borehole wall temperature increases at the end of the first year of the simulation and is reduced from 3.1 for case 1 to 2.6 for case 2. This shows that the borehole configuration is better than the previous case, however not necessarily the most economical one. It is also seen that the borehole wall temperature increases by 7.5°C at the end of the 20-year period, less than the increase of 8.7°C for case 1. All these improvements are due to the increased number of boreholes in the field.
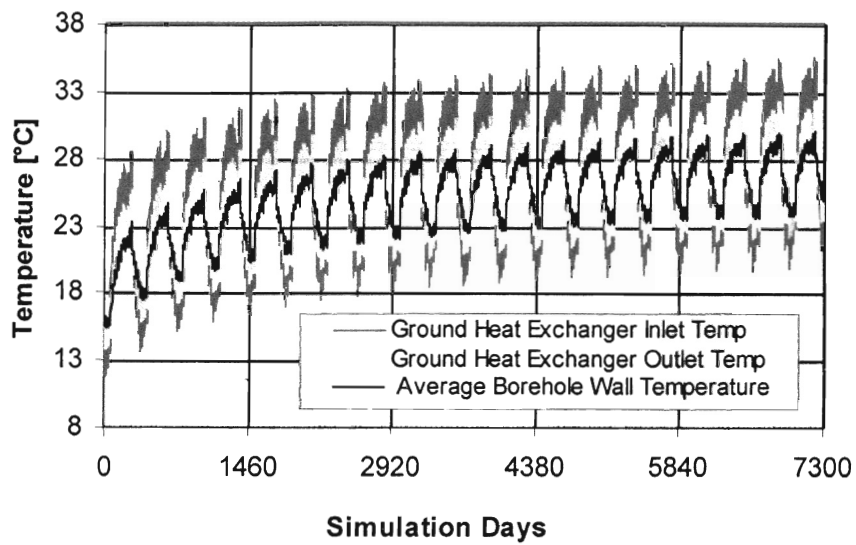
116

Figure 5.9 *Case2: Borehole temperatures for the example building at Tulsa, Oklahoma for a 32 borehole in 4x8 rectangular configuration.*
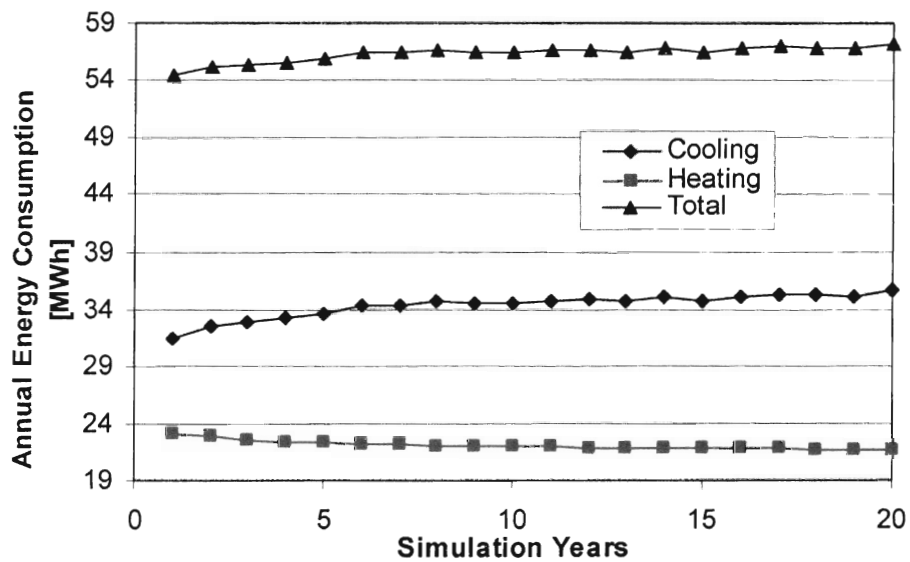

Figure 5.10 *Case2: Annual cooling power consumption for heating mode, cooling mode and the total, for 20 years of simulation at Tulsa, Oklahoma.*
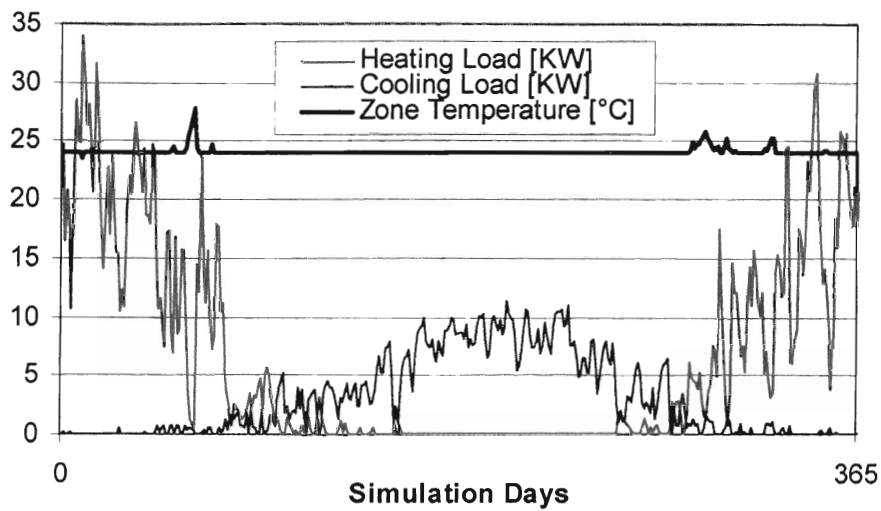
Figure 5.11 *The zone space temperature and the daily average building load for a year when the building simulated at Tulsa, Oklahoma with 32 boreholes.*

Case 3: 120 boreholes in 10x12 rectangular configuration

This configuration shows the same behavior as the previous cases for heating and cooling annual energy consumption. However, the 20-year average annual total energy consumption is the least for this case. From Table 5-3, we can see that the borehole temperature increases by 2.1°C, which is smaller than both of the previous two configurations. Figures 5.12, 5.13 and 5.14 show the trends for this configuration.
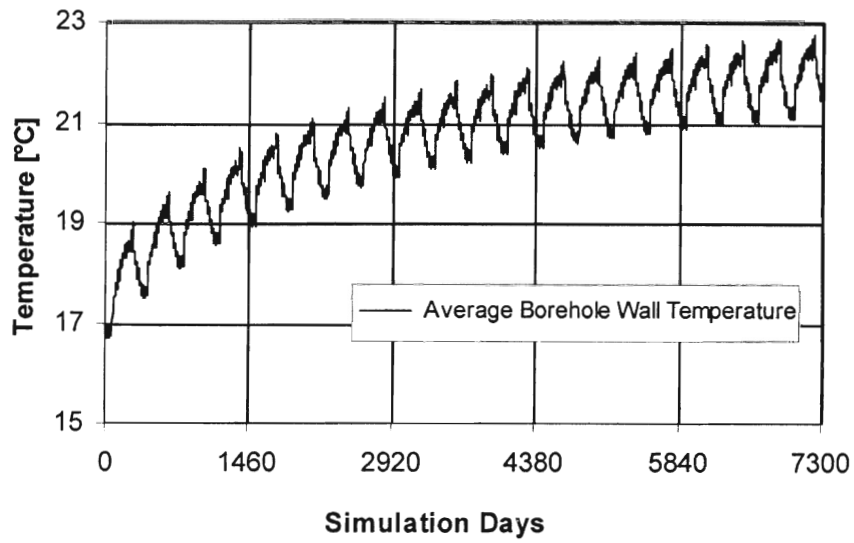
Figure 5.12 *Case3: Average borehole wall temperature for the example building at Tulsa, Oklahoma for a 120 boreholes in 12x10 rectangular configuration.*
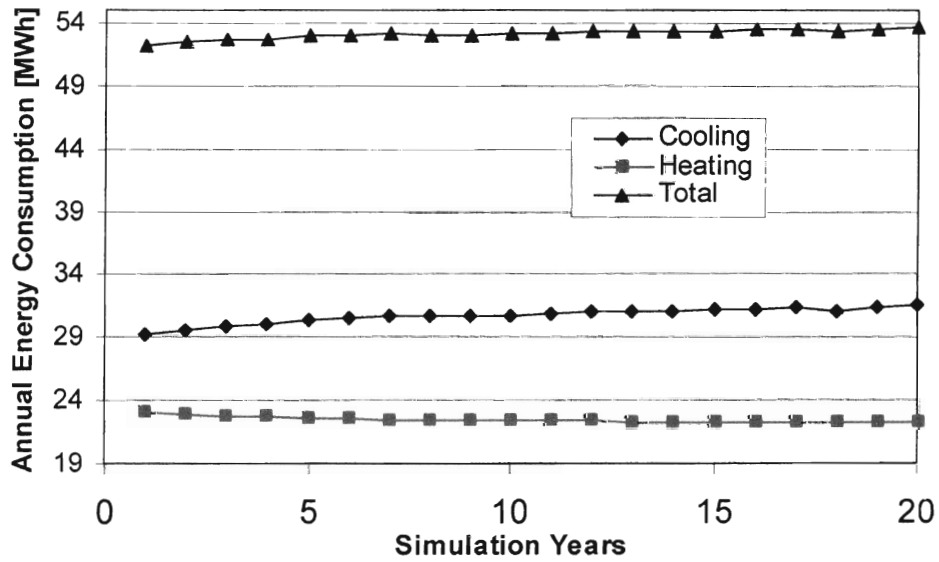
Figure 5.13 *Case3: Annual cooling power consumption for heating mode, cooling mode and the total, for Tulsa, Oklahoma, with 120 boreholes for 20 years of simulation.*
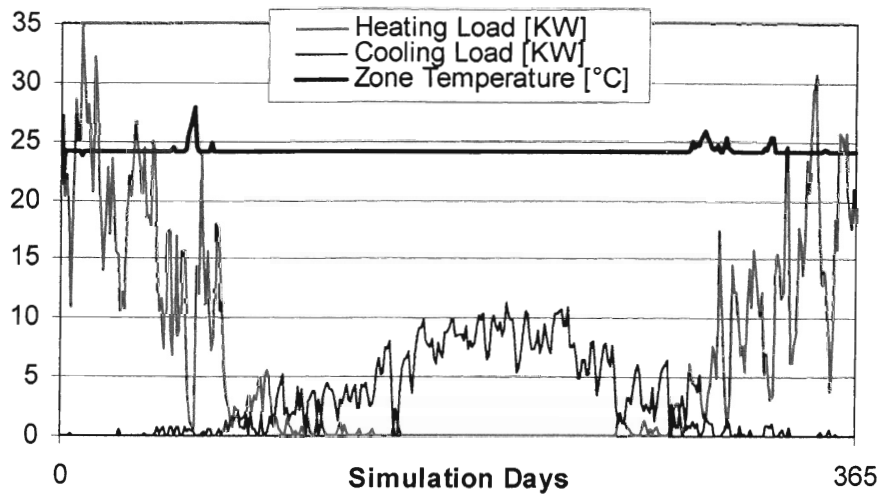
Figure 5.14 *The zone space temperature and the daily average building loads for a year when the building simulated at Tulsa, Oklahoma with 120 boreholes.*
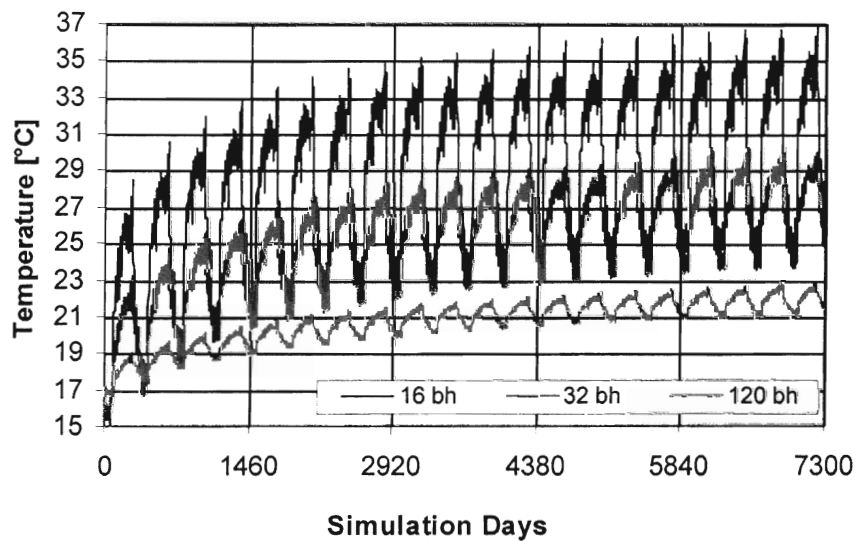
Figure 5.15 *Figure shows the comparison of the average borehole wall temperature for the three cases, in Tulsa, Oklahoma.*

Figure 5.15 shows the average borehole wall temperature over the period of the simulation. It can be seen that the annual borehole wall temperature fluctuation increases as the number of boreholes in the field decreases.

5.6.2. Anchorage, Alaska

Case 1: 16 boreholes in square configuration

From Figure5.16 it is seen that the average borehole temperature in Alaska drops over time as the heating dominated building (Figure 5.17) extracts energy from the ground. The actual temperature drops are given in Table 5-6 for all cases. The sixteen-borehole case has the highest drop in temperature, which is due to the smaller surface area of the ground coupled heat exchanger. Figure 5.18 shows the zone space temperature for a year for this case. Deviation from the 24°C set point occurs when the heating load on the building exceeds the capacity of the heat pump.

Figure 5.16 *Case1: Borehole wall temperature for the example building at Anchorage Alaska for a 16-borehole field in square configuration.*
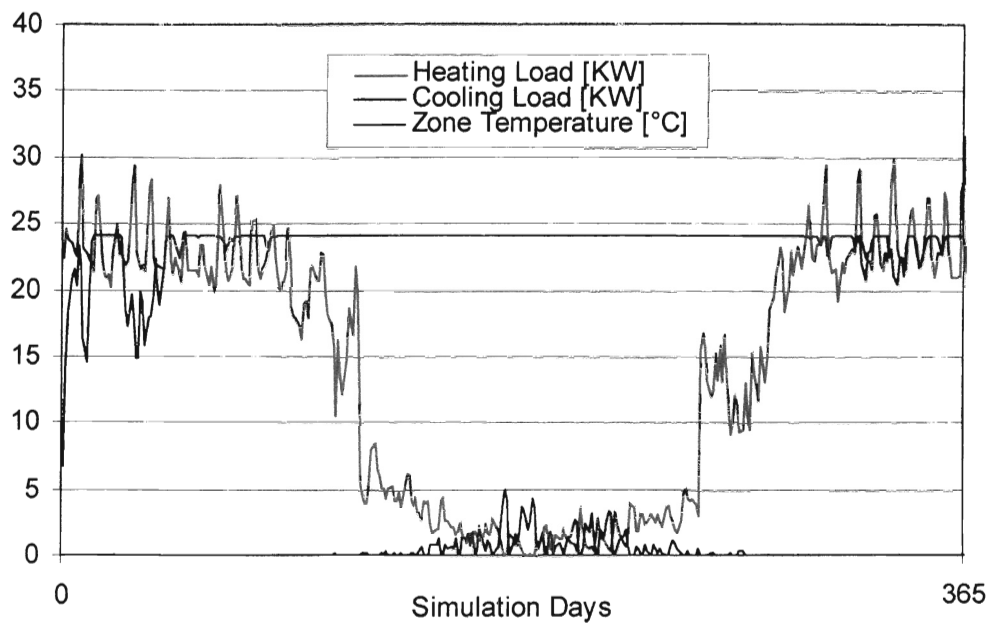
Figure 5.17 *The zone space temperature and the daily average building load for a year for the building simulated at Anchorage, Alaska, with 16- boreholes.*
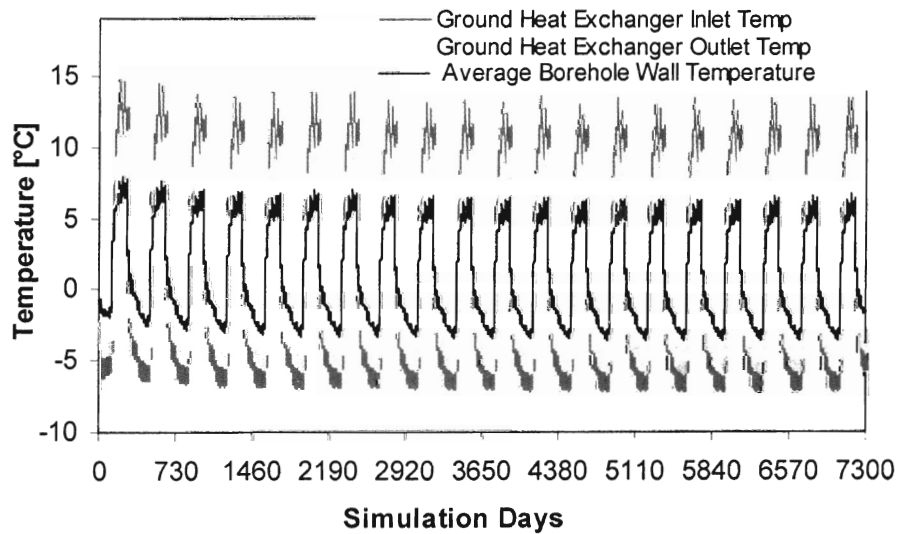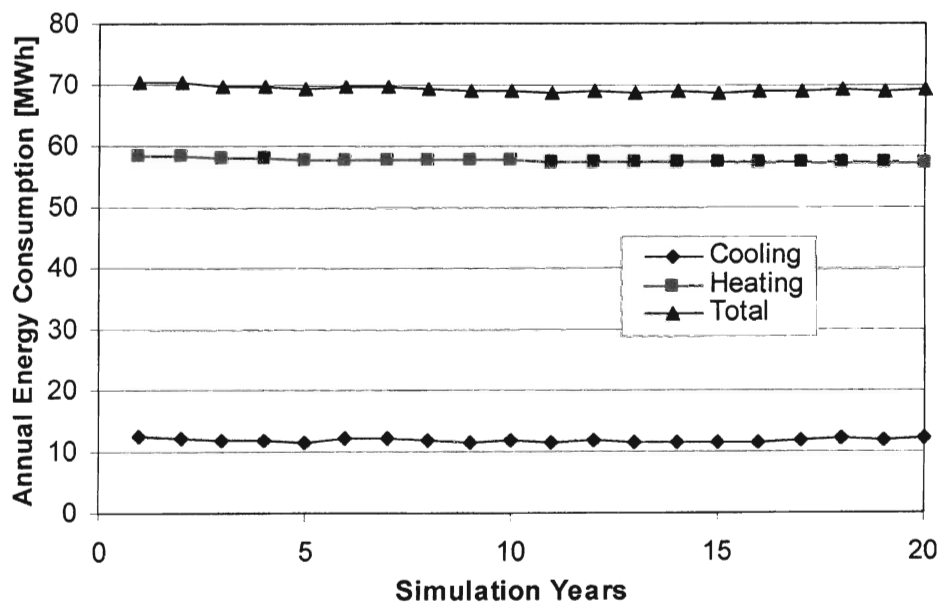

Figure 5.18 *Case1: Annual cooling power consumption for heating mode, cooling mode and the total.*

Case 2 & 3: 32&120 boreholes in rectangular configurations.

Figure 5-19 shows the borehole wall temperature for the three different cases in Alaska. From Table 5-5 it can be seen that 32 and 120 boreholes configurations have a smaller temperature drop than the 16 borehole field case, and 120 boreholes has the smallest drop which is around 0.8°C at the end of first year of simulation, compared to the 16 and 32 boreholes which are 4.5°C and 2.6°C respectively. Similar to the Tulsa results, the larger borehole configurations have lesser fluctuations in the borehole wall temperature.

Figure 5.19 *Figure shows the comparison of the borehole wall temperature in the cases for all the three cases.*

Table 5-5 *Borehole temperature with the building simulated at Anchorage, Alaska.*

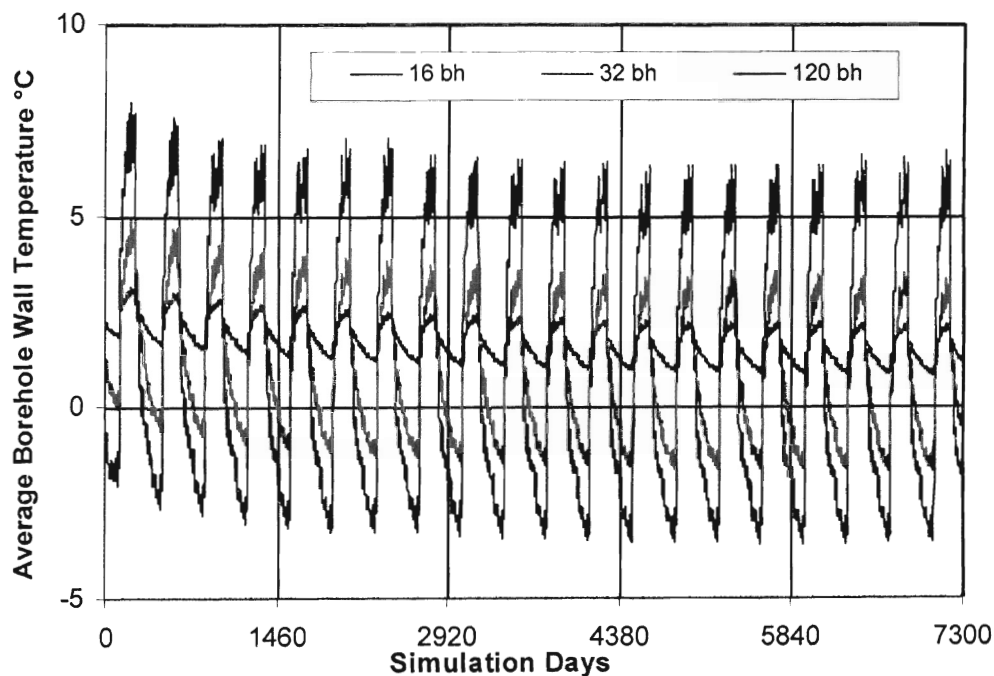| Anchorage	Case 1: Base case with 16 borehole			Case 2: 32 boreholes			Case 3: 120 boreholes		
	2nd Year	10th Year	20th Year	2nd Year	10th Year	20th Year	2nd Year	10th Year	20th Year
Borehole temperature °C	-.9	-1.5	-1.7	.4	-.2	-.5	1.8	1.4	1.1
ΔT from $T_{farfield}$	-3.5	-4.1	-4.3	-2.1	-2.8	-3.1	-.7	-1.1	-1.4

Table 5-6 *The Energy Consumption of the Example building at Anchorage, Alaska for different cases*

Anchorage	Case 1: Base case with 16 borehole			Case 2: 32 boreholes			Case 3: 120 boreholes		
	1st Year	20th Year	20-Year Ave	1st Year	20th Year	20-Year Ave	1st Year	20th Year	20-Year Ave
Energy Consumption Cooling mode (KWh)	12.3	12.0	11.7	10.6	10.2	10.4	10.1	10.2	9.9
Energy Consumption Heating mode (KWh)	58.2	57.3	57.3	61.0	60.4	60.3	62.4	62.4	62.2
Total Energy Consumption (KWh)	70.5	69.3	68.9	71.6	70.6	70.7	72.5	72.6	72.2

5.7. Discrepancy in the Cooling Power Consumption

Overall, the case studies performed on the geothermal heat pump models showed reasonable results. The ground loop heat exchanger performed in a physically reasonable way, and the heat pump model showed expected long term trends in efficiency due to

rising or falling condenser temperatures. There were, however, some unexplained results in the predicted annual energy consumption of the ground source heat pump. Annual energy consumption is expected to rise every year for a heat pump in a cooling dominated climate with an undersized ground loop heat exchanger coupled to the source side of the heat pump. Examination of Figures 5.7, 5.10, 5.13, 5.18 shows a few years when the energy consumption decreases when it is expected to increase or increases when it is expected to decrease. There are several possibilities for this inconsistency in the energy consumption results.

1. The annual weather file is not read in properly for every year. This possibility was eliminated by checking the output from energy plus for outside dry bulb and wet bulb temperatures for three years in a row.

2. The history term aggregation in the ground loop heat exchanger might be incorrect. This was checked by running the ground loop heat exchanger model in a stand alone simulation. The zone load from an annual energy plus simulation at the time-step level was used to run the ground loop heat exchanger over 20 years, with the loads repeated. The sign of the load was changed to reflect the phenomenon occurring at the ground loop heat exchanger for cooling and heating in the zone. The flow rates were held constant and the ground and bore hole parameters were the same as the case study (Table 5-2). Figure 5.20 shows the peak average borehole temperature for the 20 years of the ground loop heat exchanger. The

figure clearly shows that the ground loop heat exchanger model is working correctly.
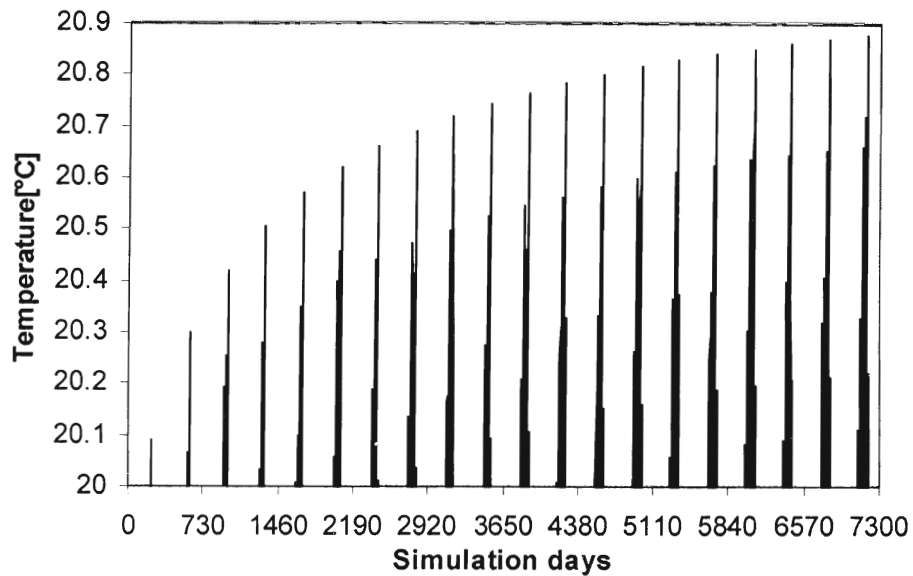
Figure 5.20 *Borehole wall temperature for 20 years of simulation with the variable short time-step ground loop heat exchanger model alone.*

3.   Instabilities or errors in the ground source heat pump model due to incorrectly bounded fluid property calls or incorrectly initialized variables could also cause the problem. To check this possibility, the heat pump was run as a stand alone simulation. An input file with the load side inlet temperature for both cooling and heating for one year was created from the EnergyPlus simulation results. The source side inlet temperature was increased logarithmically at the beginning of every year and was held constant for that year. The heat pump annual energy consumption for the cooling mode from this study is shown in Figure

126

5.21. As shown the energy consumption increases for each year of the
twenty year simulation as expected.
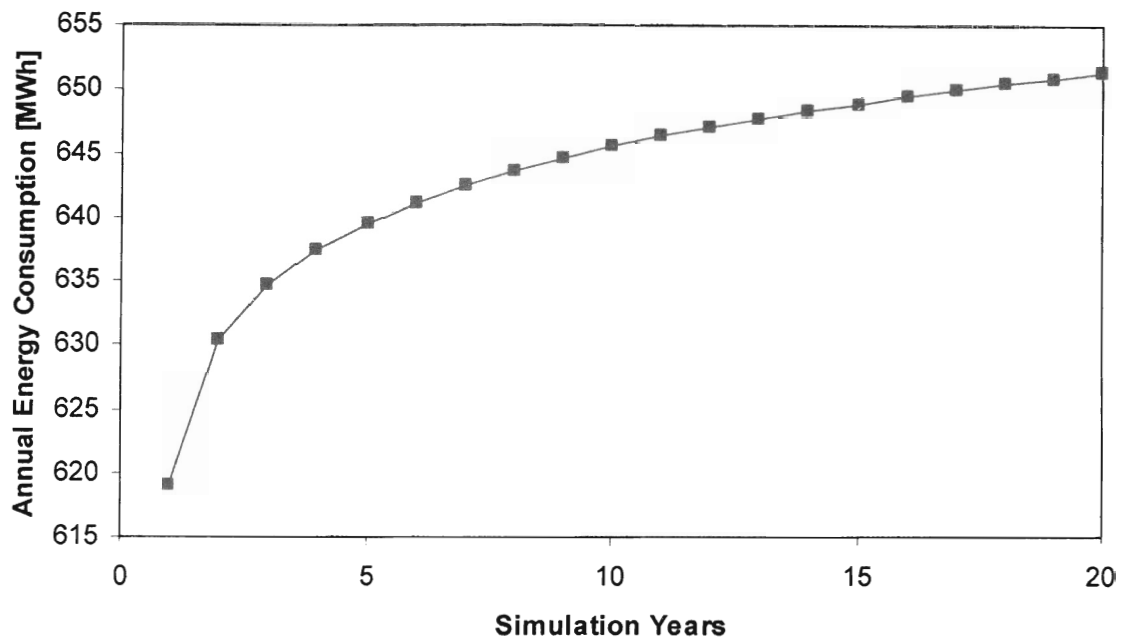
Figure 5.21 *Annual energy consumption of the heat pump in cooling mode when*
ran in stand-alone mode for 20 years.

4. Another possible cause of the "wiggle" in the power consumption curve
could be the system interaction between the heat pump and the ground
loop heat exchanger models. To investigate this possibility, the combined
ground loop heat exchanger and ground source heat pump simulation
were run as a stand alone simulation. Here again the load side inlet
temperatures to the heat pump were read from and a file with the hot and
cold water supply side inlet conditions obtained directly from EnergyPlus
simulation. Figure 5-22 demonstrates that incorrect interactions between

the ground source and heat pump models are not the cause of the problem.
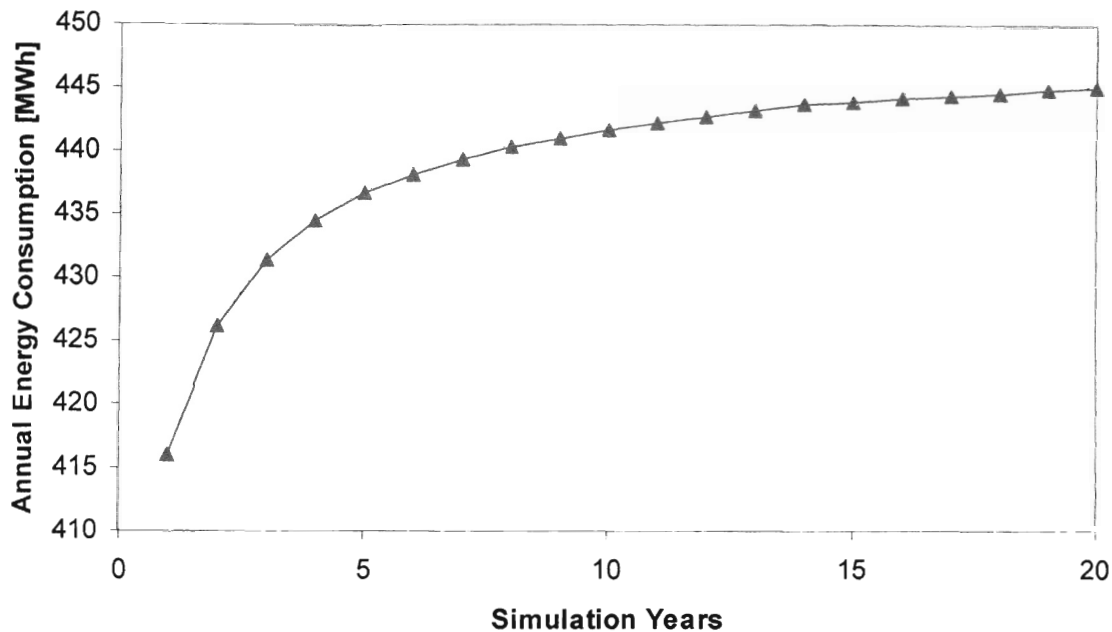
Figure 5.22 *Annual energy consumption of the heat pump in cooling mode when ran in stand-alone with ground loop heat exchanger for 20 years.*

5. This eliminates all possible problems with the model and suggests that the problem is caused by some other part of the EnergyPlus simulation. To demonstrate that the problem is unrelated to the ground source models, an electric chiller model from EnergyPlus was run with the ground loop heat exchanger for 20 years, in the EnergyPlus simulation environment. The result from the Energy Plus simulation is shown in figure 5.23. Figure 5-23 illustrates the same behavior as the heat pump model and demonstrates conclusively that the source of the problem is does not reside in the ground source models.
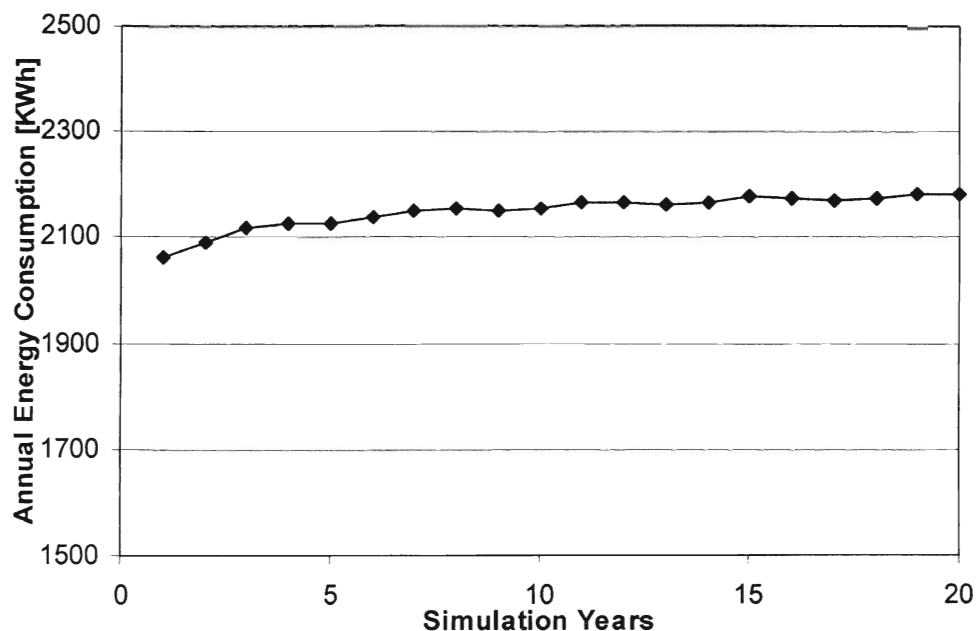
Figure 5.23 *Annual energy consumption of the EnergyPlus electric chiller model for 20 years, with ground source pump on the condenser side.*

Further investigation of the problem is beyond the scope of this work, however, it is recommended that the investigation be continued at the simulation manager level in the future.

5.8. Zone and Heat Pump System Interactions

Figure 5.24 shows various simulation metrics on the zone time-step scale, for case 1 in Tulsa, Oklahoma, for a day in the simulation where the building's heating demand peaks. When the heating demand peaks, the temperature drops in the hot water supply loop, demanding more heat from the loop. The heat pump is runs at full capacity to keep up with the demand, but the heat pump cannot meet the demand. Due to which the loop temperature drops, consequently the zone temperature also drops. This continues until the

zone demand is with in the capacity of the heat pump. Once the zone load is below the heat pump's capacity, the heat pump recovers and meets the demand, there by maintains the zone at the required set point temperature. Similarly, Figure 5.25 shows a day in the simulation where there was no load. Here the zone is over heated, in spite of the heat pump staying off, due to the continuous operation of the hot water loop circulation pump.

The days when the zone temperature fell below the set point temperature are eliminated if an additional heat pump is added to the plant loop. The additional pump takes care of the excessive load on the loop during high demand days. Figures 5.26 and 5.27 show the zone space temperature with two heat pumps for Tulsa and Anchorage respectively. It can be seen that there is a better control on the zone space temperature. However, the days where the zone temperature goes above the set point are not eliminated. This is because of the low demand days, which cannot be rectified with additional heat pump.

Legend shown in figure:
- ZONE 3 Air temp
- Zn Ht Load
- HW supply outlet temp
- HW supply inlet temp
- Loop Set Point
- Load Mdot

Loop temperature drops due to high demand

Heat pump turned on every time the loop inlet goes below set point

Zone temperature drops due to the high demand

Heat pump stays on to keep up to the demand

Zone time step
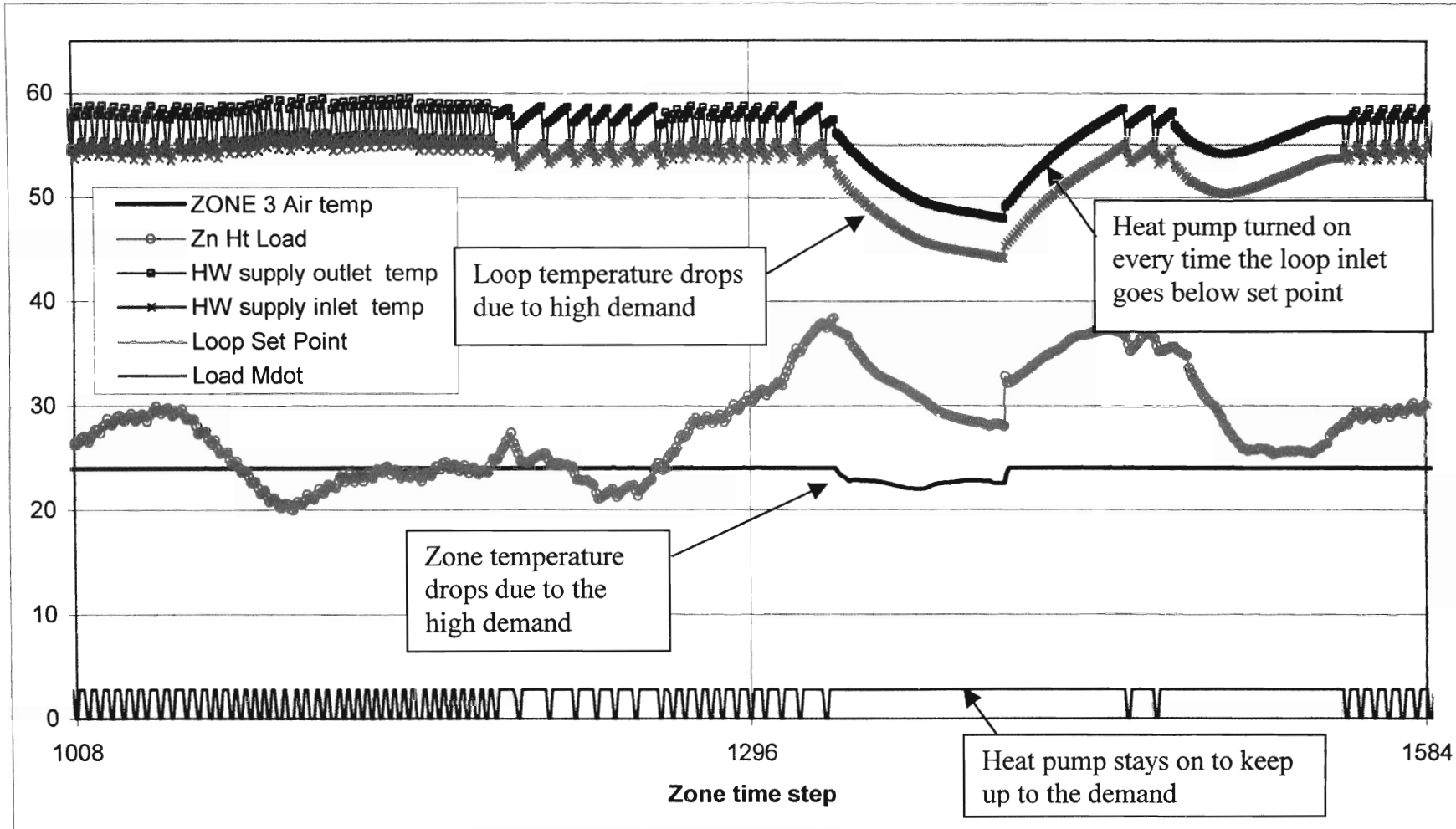
Figure 5.24 *Figure shows zone and heat pump system interactions on a day in simulation when the building's heating load peaks.*
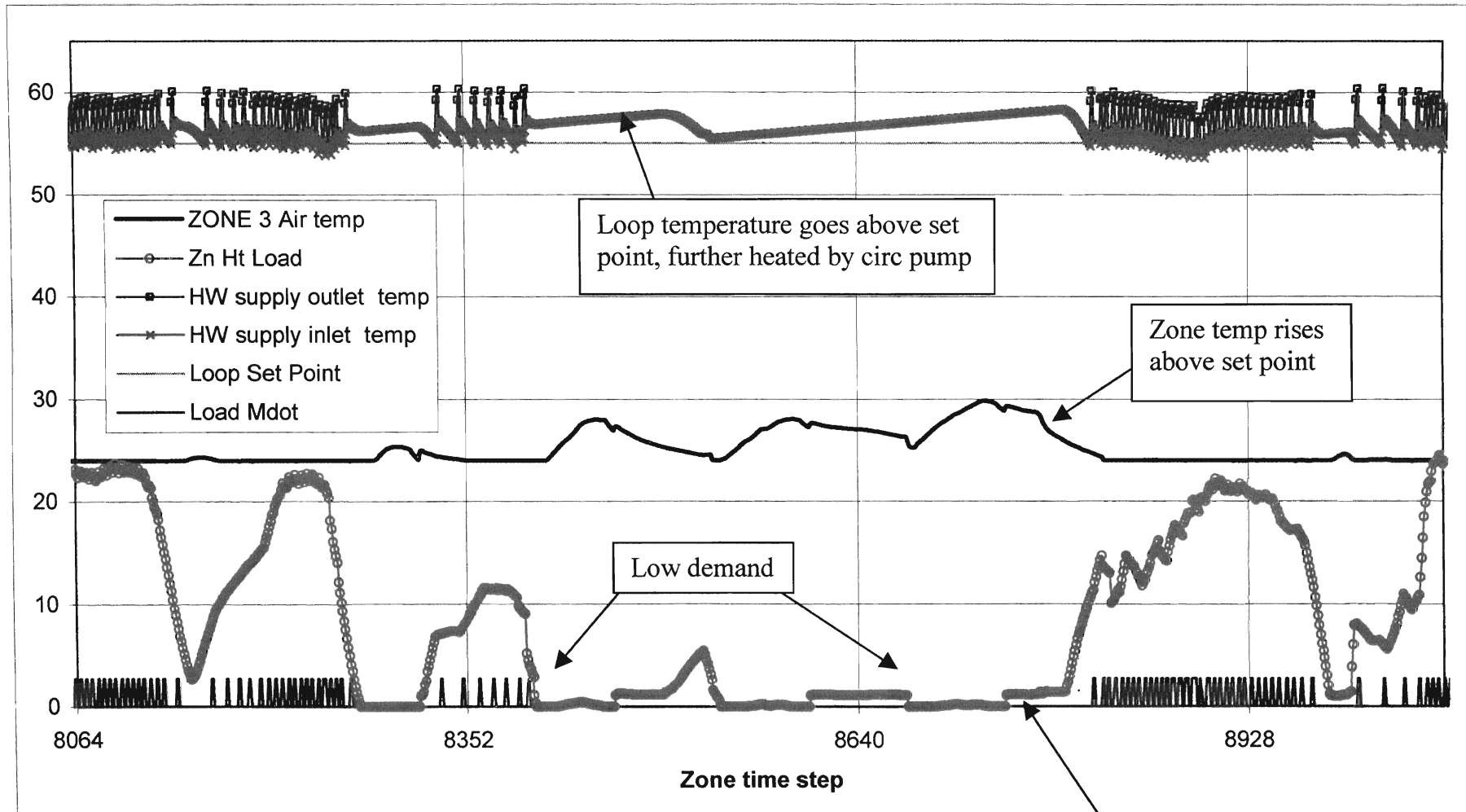
Figure 5.25 *Figure shows the zone and heat pump system interactions on a day in the simulation when there is no lo*
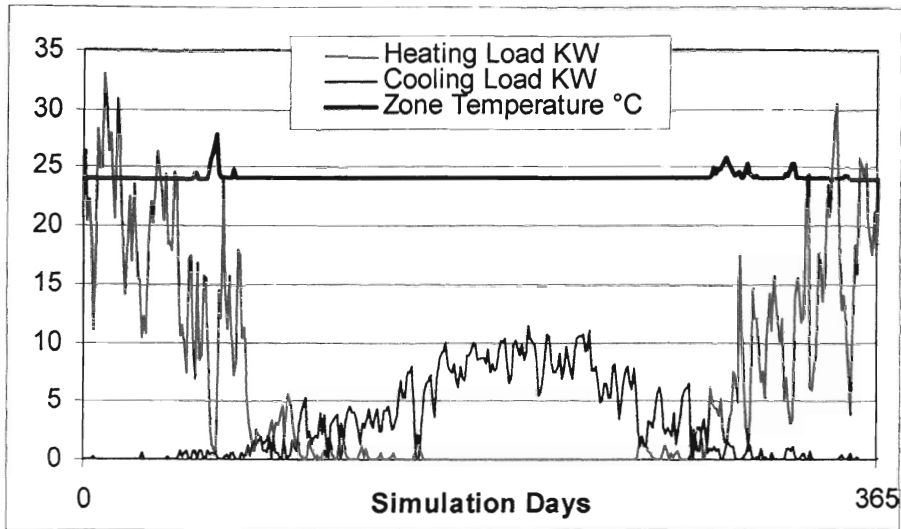
Figure 5.26 *The zone space temperature and the building loads with two heat pumps for 16 boreholes in square configuration case when the building simulated in Tulsa, Oklahoma.*

Figure 5.27 *The zone space temperature and the building loads with two heat pumps for 16 boreholes in square configuration case when the building simulated in Anchorage, Alaska.*

5.9. Conclusion

The ground loop heat exchanger and the ground source heat pump were found to show predictable behavior for a twenty-year simulation. In Tulsa, were the climate is cooling dominated the borehole field temperature increases due to unbalanced heat injection into the ground. Also as the number of year passes, the power required to provide cooling increases as the borehole field temperature increases, which is acting as a sink to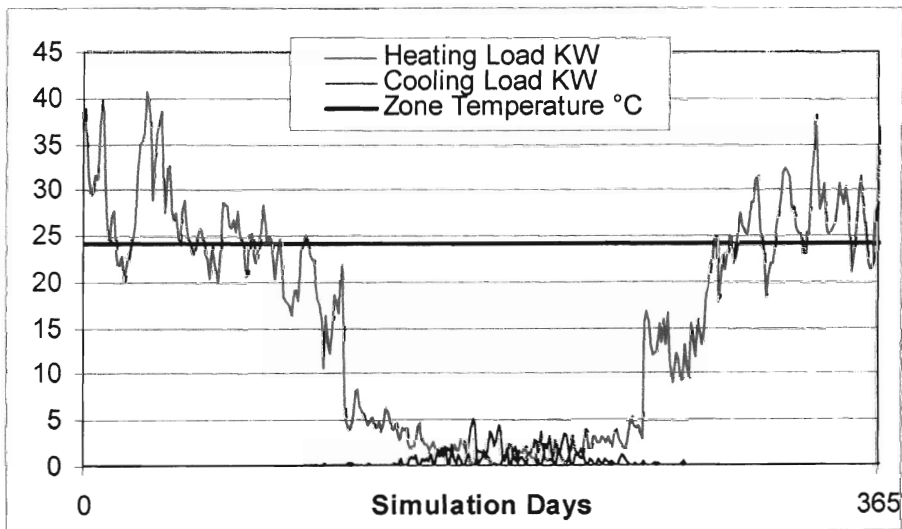 the heat pump. In Anchorage with a large annual net heat extraction rate, the borehole field temperature drops every year of the twenty-year simulation. Here the cooling performance improves as the sink is getting colder and colder, on the other hand the heating performance degrades, as the temperature drops. In addition, several other observations were made concerning model performance:

1. The testing showed the ground source heat pump models were stable in the simulation environment.

2. The models reflected the physics of the process correctly, which is evident from the higher power consumption in later years for cooling mode and lower consumption for heating mode in a cooling dominated region. (Tulsa)

3. The thermal history behavior of the ground loop heat exchanger correctly reflects the thermodynamics of the heat exchanging process. The temperature drops in a colder climate where the heat exchanger is the source and increases in a warmer climate where it acts as a heat sink.

4. The cyclic operation was reflected in the loop temperature. In the hot water loop when the temperature falls below the loop set point temperature, the heat

pump is turned on and remains on for the required cycle time or longer as needed. The heat pump switched off once the loop temperature reaches the loop set point temperature and stays off for the required cycle time or longer as needed.

Chapter 6. Conclusion and Recommendations

A geothermal system simulation, consisting of a ground source heat pump and ground loop heart exchanger, was implemented in the EnergyPlus simulation program. Choice of simulation environment was critical to the implementation the geothermal system. One of the key system design decisions is based on the long term change in ground temperature and its impact on heat pump performance. The simulation must support feedback from the ground loop heat exchanger to the plant equipment. Building energy analysis programs that use sequential simulation techniques cannot properly support the sort of feedback required to accurately model geothermal systems. EnergyPlus is built on an integrated simulation engine (simultaneous system and load simulation), which accounts for the interactions between the space, the air handling system, the plant equipment and the environmental heat exchangers. Also the feasibility of the geothermal system as a alternate to the conventional system depends on the economic benefits of the system. To make this option more attractive the ground loop has to be sized properly as the initial cost of installation of such a system is prohibitively high. Proper sizing of the system depends on the accurate prediction of the space temperatures. Though EnergyPlus provided the basic framework for implementing the geothermal systems, it lacked several features including suitable fluid property routines and multi-year simulation capabilities. Chapter 2 describes extensions and enhancements to EnergyPlus that were required for ground source heat pump system simulation. The

multi year simulation capability is particularly useful in the analysis of ground loop heat exchanger performance over an extended period of time, typically twenty years.

6.1. Conclusion:

The ground source heat pump model was based on a parameter estimation model of a water-to-water heat pump developed by Jin and Spitler (2002) . A sensitivity analysis was performed on this model before it was implemented. From the study it was concluded that the heat pump model was most sensitive to the parameters that govern the refrigerant flow rate, which were the piston displacement and the clearance factor.

The model was implemented in EnergyPlus as two component models one each for cooling and heating; schedule was used to select between the modes. This control scheme was imposed by limitations of EnergyPlus environment which doesn't support cooling and heating on a single loop.

The ground source heat pump model was enhanced to avoid short-cycling of the heat pump. Although the software model could be turned on and off in successive time steps without introducing instabilities into the simulation, a minimum cycle time was enforced during which period the heat pump model stays on or off. The control scheme more accurately reflects actual heat pump operation and gives a better prediction of power consumption and water temperatures.

The Ground loop heat exchanger model was based on the vertical borehole field model developed by Yavuzturk and Spitler (1999). Their model was based on

the Eskilson's model, which uses long time (more than a few hours) temperature response factor called *g*-functions. Yavuzturk and Spitler extended Eskilson's *g*-function model to include short time steps of less than an hour.

This work extended the Yavuzturk and Spitler model to handle variable time steps of less than one hour. The new model was designed to EnergyPlus specifications and implemented in Energy Plus. The model included a load aggregation scheme that was designed for variable time step simulation. Results from the model were compared to the response predicted by an analytical model of the borehole. Analytical study was based on the line source approximation solution by Kelvin (1882). Various load profiles were considered in this study like, constant, pulsated, periodic and composite (which includes all other loads profiles) were tested against the analytical solution. In conclusion, the constant load profile matched the analytical solution very well. This is because the *g*-functions are applied to the decomposed step pulses, which are zero for a constant load profile. The temperature prediction between the simulation model and analytical model was large when there was a sharp change in the load. Therefore, the other load profiles, which had varying loads, had a relatively higher error.

Finally, a case study was performed to check the performance of the new EnergyPlus models. The case study was based on an office building located south west of Stillwater Oklahoma. Two different climates were considered for the test: Anchorage, Alaska and Tulsa, Oklahoma. The case study analyzed different borehole and heat pump configurations. The following conclusions are based on the case study results.

i. The models reflect the expected trends of the thermal processes correctly. This is evident from the higher power consumption for cooling mode and lower consumption for heating mode after twenty years of operation in a cooling dominated region. (Tulsa)

ii. The thermal history of the ground loop heat exchanger also correctly reflects the expected trends of the ground heat transfer process. The temperature drops in a colder climate where the heat exchanger is the source and increases in a warmer climate where it acts as a heat sink.

iii. Cyclic operation was reflected in loop temperature. In the hot water loop when the temperature dropped below the loop set point, the heat pump was started and it stayed on for the cycle time. The heat pump was switched off once the loop temperature reached the set point and stayed off for the cycle time.

6.2. Recommendations:

1. It would be very useful to validate the model results against a working system. This study would include validation of the entire EnergyPlus simulation with all of the zone/system/plant interactions.

2. The parameter estimation models could be enhanced to reduce internal iteration and overall computation time.

3. A penalty function/factor for Heat pump startup performance could be implemented and the heat pump model could be refined further. This would give a better estimation of the model's energy consumption.

4. Other low energy systems like pond models, pavement heat rejection models etc could be implemented which would be very useful in the study of hybrid configurations.

5. A hybrid model of ground loop heat exchanger with cooling tower as supplementary heat rejecter can be analyzed.

6. EnergyPlus should be extended to provide a single loop for both cooling and heating. The models could then be modified to operate on the basis of a control algorithm instead of a schedule.

7. The possibility of using a single set of heat pump parameters for both heating and cooling should be investigated.

REFERENCES

Abramowitz, M. and I.A. Stegun, 1964. Handbook of Mathematical Functions. Dover Publications, NewYork.

Allen, J.J. and J.F. Hamilton. 1983. Steady-State Reciprocating Water Chiller Models. ASHRAE Transactions, Vol. 89(2A), pp. 398-407.

Bourdouxhe, J-P H., M. Grodent, J.J. Lebrun, C. Saavedra, K.L. Silva. 1994. A Toolkit for Primary HVAC System Energy Calculation—Part 2: Reciprocating Chiller Models. ASHRAE Transactions, Vol. 100(2), pp. 774-786.

BSO. 1991. BLAST Technical Reference Manual. BLAST Support Office, University of Illinois.

Carslaw, H.S. and J.C. Jaeger. 1947. Conduction of Heat in Solids. Oxford, U.K.: Clarendon Press.

Crawley, D.B., L.K. Lawrie, F.C. Winkelmann, W.F. Buhl, A.E. Erdem, C.O. Pedersen, R.J. Liesen and D.E. Fisher. 1997. What's Next for Building Energy Simulation-A Glimpse of the Future. Proceedings of Building Simulation 1997, Vol. II, pp. 395-402.

Eskilson, P. 1987. Thermal Analysis of Heat Extraction Boreholes. Ph.D. Thesis, Department of Mathematical Physics, University of Lund, Lund, Sweden.

EnergyPlus. 2002. EnergyPlus Module Developer's Guide. U.S. Department of Energy.

Fisher, D.E., R.D. Taylor, F. Buhl, R.J. Liesen and R.K. Strand. 1999. A Modular, Loop-Based Approach to HVAC Energy Simulation and its Implementation in EnergyPlus. Proceedings of Building Simulation 1999,   Vol. III, pp. 1245-1252.

Gordon, J.M. and K.C. Ng. 1994. Thermodynamic Modeling of Reciprocating Chillers. Journal of Applied Physics, Vol. 75(6), pp. 2769-74.

Hamilton, J.F., J.L. Miller. 1990. A Simulation Program for Modeling an Air-Conditioning System. ASHRAE Transactions, Vol. 96(1), pp. 213-221.

Hart, D.P. and R. Couvillion. 1986. Earth Coupled Heat Transfer, Publication of the National Water Well Association.

Hellstrom, G. 1989. Duct Ground Heat Storage Model: Manual for Computer Code. Department of Mathematical Physics, University of Lund, Lund, Sweden.

Hellstrom, G. 1991. Ground Heat Storage. Thermal Analysis of Duct Storage Systems: Part I Theory. Department of Mathematical Physics, University of Lund. Lund, Sweden.

Ingersoll, L.R. and H.J. Plass. 1948. Theory of the Ground Pipe Heat Source for the Heat Pump. Heating, Piping & Air Conditioning. July. pp. 119-122.

Ingersoll, L.R., O.J. Zobel, and A.C. Ingersoll. 1954. Heat Conduction with Engineering, Geological, and Other Applications. New York: McGraw-Hill.

Jin, H. 2002. Parameter Estimation Based Models of Water Source Heat Pumps. Ph.D. Thesis, Department of Mechanical and Aerospace Engineering, Oklahoma State University, Stillwater, Oklahoma.

Jin, H. and J.D. Spitler. 2002. A Parameter Estimation Based Model Of Water to Water Heat Pumps for Use in energy Calculation Programs. ASHRAE Transactions, Vol. 108(1), pp. 3-17.

Kavanaugh, S.P. 1985. Simulation and experimental verification of vertical ground coupled heat pump systems. Ph.D. thesis, Oklahoma State University, Stillwater,

Oklahoma.

Kelvin, Sir W. Thomson. 1882. Mathematical and Physical Papers, II.

Klein S.A., W.A. Beckman, J.W. Mitchell, J.A. Duffie, N.A. Duffie, T.L. Freeman, J.C. Mitchell, J.E. Braun, B.L. Evans, J.P. Kummer, R.E. Urban, A. Fiksel, J.W. Thornton, N.J. Blair, P.M. Williams and D.E. Bradley. 1996. TRNSYS – A Transient System Simulation Program. Manual, v15, Solar Energy Laboratory, University of Wisconsin, Madison, Wisconsin.

LBNL. 1980. DOE-2 Reference Manual, Lawrence Berkeley Laboratory and Los Alamos Scientific Laboratory.

Mei, V.C. and C.J Emerson. 1985. New Approach for Analysis of Ground-Coil Design for Applied Heat Pump Systems. ASHRAE Transactions, Vol. 91(2), pp. 1216-1224.

Popovic, P., H.N. Shapiro. 1995. A Semi-empirical Method for Modeling a Reciprocating Compressor in Refrigeration System. ASHRAE Transactions, Vol. 101(2), pp. 367-382.

Rees, S.J. 2002. Personal Communications.

Spitler, J.D., D.E. Fisher and D.C. Zietlow. 1989. A Primer on the use of Influence Coefficients in Building Simulation. Department of Mechanical and Industrial Engineering, University of Illinois at Urbana-Champaign, Urbana, Illinois.

Stefanuk, N.B.M., J.D. Aplevich, M. Renksizbulut. 1992. Modeling and Simulation of a Superheat-controlled Water-to-Water Heat Pump. ASHRAE Transactions, Vol. 98(2), pp. 172-184.

Stoecker, W.F. and J.W. Jones. 1982. Refrigeration and Air Conditioning, 2nd ed. New York: McGraw-Hill.

Thornton, J.W., T.P. McDowell, J.A. Shonder, P.J. Hughes, D. Pahud and G. Hellstrom. 1997. Residential Vertical Geothermal Heat Pump System Models: Calibration to Data. ASHRAE Transactions, Vol. 103(2), pp. 660-674.

Yavuzturk, C. 1999. Modeling of Vertical Ground Loop Heat Exchangers for Ground Source Heat Pump Systems. Ph.D. Thesis, Department of Mechanical and Aerospace Engineering, Oklahoma State University, Stillwater, Oklahoma.

Yavuzturk, C. and J.D. Spitler. 1999. A Short Time Step Response Factor Model for Vertical Ground Loop Heat Exchangers. ASHRAE Transactions, Vol. 105(2), pp. 475-485.

Yavuzturk, C. and J.D. Spitler. 2000. Comparative Study to Investigate Operating and Control Strategies for Hybrid Ground Source Heat Pump Systems Using a Short Time-Step Simulation Model. ASHRAE Transactions, Vol. 106(2), pp. 192-209.

VITA ♌

Murugappan Arunachalam

Candidate for the Degree of

Master of Science

Thesis: IMPLEMENTING GROUND SOURCE HEAT PUMP AND GROUND LOOP
HEAT EXCHANGER MODELS IN THE ENERGYPLUS SIMULATION
ENVIRONMENT

Major Field: Mechanical Engineering

Biographical:

Education: Received Bachelor of engineering from Annamalai University,
Chidambaram, India in June 1998. Completed the requirements for the
Master of Science Degree with a major in Mechanical Engineering at
Oklahoma State University in December 2002.

Experience: Employed as Teaching Assistant by Department of Computer
Science, Oklahoma State University, Stillwater, Oklahoma. Sep 2002 to
present. Employed by Oklahoma State University, Department of
Mechanical Engineering as a graduate Research Assistant from August
1999 to August 2002.

Professional Memberships: American Society of Heating, Refrigerating, and Air
Conditioning Engineers, Inc.